QUANTITATIVE REMOTE SENSING OF ESSENTIAL BIODIVERSITY VARIABLES: UNDERSTANDING THE ROLE OF CANOPY VERTICAL HETEROGENEITY

Tawanda Winmore Gara

QUANTITATIVE REMOTE SENSING OF ESSENTIAL BIODIVERSITY VARIABLES: UNDERSTANDING THE ROLE OF CANOPY VERTICAL HETEROGENEITY

DISSERTATION

to obtain
the degree of doctor at the University of Twente,
on the authority of the rector magnificus,
prof.dr. T.T.M. Palstra,
on account of the decision of the Doctorate Board,
to be publicly defended
on Wednesday 25 September 2019 at 14.45 hrs

by

Tawanda Winmore Gara
born on 01 August 1983
in Kariba Zimbabwe

This thesis has been approved by

Prof.dr. A.K. Skidmore, supervisor
Dr. R Darvishzadeh Varchechi, co-supervisor
Dr. T Wang co-supervisor

ITC dissertation number 364
ITC, P.O. Box 217, 7500 AE Enschede, The Netherlands

ISBN 978-90-365-4854-0
DOI 10.3990/1.9789036548540

Cover designed by Benno Masselink
Printed by ITC Printing Department

Graduation committee:

Chairman/Secretary

Prof.dr.ir. A. Veldkamp	University of Twente

Supervisor

Prof.dr. A.K. Skidmore	University of Twente

Co-supervisors

Dr. R Darvishzadeh Varchehi	University of Twente
Dr. T. Wang	

Members

Prof.dr. F.D. van der Meer	University of Twente
Prof.dr.ing. W. Verhoef	University of Twente
Prof.dr. J.H.C. Cornelissen	Free University Amsterdam
Prof.dr. J. Kattge	Max Planck Institute

To my family and friends

Acknowledgements

This work could not have been in its current form without the contribution of some individuals and organizations. Firstly, I would like to acknowledge the University of Twente, for the financial support to study for my PhD at the Faculty of Geoinformation Science and Earth Observation. Without the financial support, it could not have been possible to complete this PhD trajectory in the Netherlands.

I extend my heartfelt gratitude to my promoter Prof A. K Skidmore, who patiently and tirelessly supervised this study to completion. You challenged me with robust scientific questions ad suggestions. Andrew you were a source of inspiration, guidance and support throughout my 4-year PhD stay in the Netherlands. You were patient with my progress especially during the early stages when I struggled with my studies. I vividly remember the meetings we had in your office and how they shaped my scientific to date. You made me feel comfortable by discussing life in general and the situation back in Zimbabwe.

I also extend my deep appreciation and gratitude to the excellent advisory support of my daily supervisor, Dr Roshanak Darvishzadeh. Your availability, friendship and constant support played a significant role in the completion of this work. Our meetings and discussions on my work widened by scientific thinking. It was a pleasure working with you for the entire period of my PhD. I could come to your office without appointment to discuss my ideas and findings. I also thank you for your logistical support in transporting the potted plants for my greenhouse experiment from Almelo to Enschede. I also thank you for the advice on setting up the greenhouse experiment and detailed considerations in spectral measurements in the laboratory. You will remain an inspiration in my academic life.

I also want to thank Dr Tiejun Wang my second supervisor. I initially worked with Tiejun as my supervisor during my MSc thesis on modelling elephant movement patterns in Amboseli, Kenya. That was the beginning of our close link and friendship. After the completion of my MSc you encouraged me to apply for the *AiO* position at ITC. You encouraged me to work hard especially during the time when switching from wildlife modelling to spectroscopy of vegetation was a huge challenge. I also thank Tiejun for the swift response with regard to feedback on manuscripts and suggestions for journals to consider for submission of my manuscripts. We had a wonderful drive together from Enschede to Sumava (Czech Republic) during which we discussed a lot about life and academic life in general.

Marco Heurich and Joe Premier, my sincere appreciation for the logistical support during my fieldwork visits in Bavaria Forest National Park. I had a long and wonderful field experience that changed the way I see forest ecosystems. My stay in the Park for close to 6 months in total will remain an unforgettable experience. I thank you for providing accommodation and laboratory space to process my leaf samples. I would also like to thank Yifang Shi and Jing Liu for your assistance in part of my fieldwork.

I am also grateful to the staff in ITC. These include Esther Hondebrink, for organizing my meetings with Andrew. Benno Masselink for organizing equipment for fieldwork and for your assistance in designing posters that I presented in Zurich and Brno during the EARSeL SIG Imaging Spectroscopy Workshops. I would like to express my gratitude to Waste Siderius and Kathrin Zweers for assistance in laboratory measurements.

I also thank my friends and colleagues especially my fellow PhDs in the NRS department for sharing our experience and challenges of our PhD journey. Our PhD tutorials made a huge difference. I remember Alby was so active in our tutorials and your contributions made a difference. My fellow PhD colleagues include Jing, Yifang, Yifei, Trini, Alby, Sugandh, Elnaz, Mitra, Parinaz, Festus, Abebe, Zhihui, and Xi. I also thank my close friend and fellow PhD student Haidi for the chats we had during coffee breaks and being a close acquaintance during our short stay in Zurich and Munich for the EARSeL Workshops and EBVs summer school respectively.

To the SADC community in Enschede, I thank you for the light moments we shared especially the SADC dinners and activities. Many thanks goes to Peter, Lekula, Donald, Webster, Simba, Archford, Vincent, Tasi, Tanya and others that I could not mention by their names. Our SADC dinners were refreshing and provided opportunity to discuss African politics. I also thank my fellow Christians for the fellowship time we had most Sundays at the Prince school and the encouragement to keep on working.

I also thank the staff at Fit for Free Schuttersveld, Enschede for the professional hospitality during my gym sessions. My deep gratitude also go to my doctor A van der Lugt and all the staff at the Medisch Spectrum Twente for taking care of my health during my 4-year stay in Enschede. You all made a difference and made me feel at home.

I am also greatly indebted to my wife Chipo, my daughter Zoey and the whole family for their moral support. Chipo you endured a challenging period when I left Zimbabwe for further studies in the Netherlands soon after our wedding. I had little time for you but you understood and encouraged me to work tirelessly. You had a difficult time looking after our little daughter Zoey and travelling with her to the Netherlands on your occasional visits. However, your visits made a huge difference. I am also grateful for our little new baby Zuriel. I also thank my mother for the love and encouragement. You are a mother that any child could wish to have. It is unfortunate that I lost my dad during my PhD studies. I thought you would see the end to this journey mdhara.

Table of Contents

List of figures

List of tables

List of abbreviations and acronyms

ANOVA	Analysis of Variance
ASD	Analytical Spectral Device
C_{ab}	Leaf chlorophyll
Cab_c	Canopy chlorophyll
C_c	Canopy carbon
$CI_{rededge}$	Red-edge Chlorophyll Index
CTVI	Corrected Transformed Vegetation Index
D_w	Dry weight
EBVs	Essential Biodiversity Variables
EWT	Equivalent Water Thickness (Cw)
FOV	Field of View
F_w	Fresh Weight
GEMI	Global Environmental Monitoring Index
GPS	Global Position System
IRECI	Inverted Red-edge Chlorophyll Index
LAI	Leaf area Index
LMA	Leaf mass per area (Cm)
LMA_c	Canopy leaf mass per area
LUT	Look-up-table
MCARI	Modified Chlorophyll Absorption Ratio Index
N	Nitrogen
N_c	Canopy nitrogen
NDVI	Normalised difference vegetation index
NIR	Near infrared
$NRMSE_{cv}$	cross validated Normalised Root Mean Square Error
PAR	Photosynthetically active radiation
PEP	Phenolyenolpyruvate
PLS-DA	Partial Least Squares - Discriminatory Analysis
PLSR	Partial Least Squares Regression
PROSPECT	Leaf Optical PROperties SPECTra model
R^2	Coefficient of determination
R^2_{cv}	cross validated Coefficient of determination
RF	Random Forest
RMSE	Root Mean Square Error
rNDVI	Renormalized NDVI
RTM	Radiative Transfer Models
RuBP	ribulose-1.5-biphosphate

SCCCI	Simplified Canopy Chlorophyll Index
SLA	Specific leaf area
SREP	Sentinel-2 Red-edge Position
SWIR	Shortwave infrared
TCARI/OSAVI	Transformed Chlorophyll Absorption in Reflectance Index/Optimized Soil-Adjusted Vegetation Index
VIP	Variable Importance Projection

Chapter 1

General introduction

1.1 Ecological importance of plants traits

Understanding the spatial and temporal dimensions of plant traits in the face of global environmental change is critical to assessing the health and spatial planning of fragile ecosystems. Plant traits such as foliar nitrogen (N), leaf mass per area (LMA), chlorophyll (C_{ab}), equivalent water thickness (EWT) and specific leaf area (SLA) are essential indicators of the quality and health of vegetation (Knox *et al.*, 2010; Mutanga *et al.*, 2005). Nitrogen is a key element in chlorophyll (0.2 - 6.4 % by dry weight) and in enzymes (i.e. ribulose-1.5-biphosphate (RuBP) carboxylase and phenolyenolpyruvate (PEP)) essential for photosynthesis and subsequently carbon fixation in C3 and C4 plants respectively (Cho *et al.*, 2013; Gibson, 2008; Schlemmer *et al.*, 2013). As a source of protein for herbivores, foliar nitrogen content is known to determine the distribution and foraging behaviour of wildlife (Hassall *et al.*, 2001; Schweiger *et al.*, 2015). LMA and its reciprocal SLA together with leaf carbon content reflect the plant economic spectrum with regard to nutrients uptake, light harvesting and carbon sequestration (Martin and Thomas, 2011; Poorter *et al.*, 2009). C_{ab} is an important bio-indicator for assessing plant physiological status and photosynthetic capacity (Malenovský *et al.*, 2013). EWT, on the other hand, provides information on plant water status (Yao *et al.*, 2014). Temporal changes in plant traits influence ecosystem biogeochemical cycling (Fisher *et al.*, 2012) and ecosystem productivity (Casas *et al.*, 2014). The significance of leaf traits in ecosystem structure, functioning and provision of ecosystem services prompted the realisation that leaf traits are a critical component of essential biodiversity variables (EBVs) (Skidmore *et al.*, 2015). Understanding the spatio-temporal dimension of these leaf traits improves the monitoring and conservation of EBVs towards the Aichi Biodiversity Targets (Pereira *et al.*, 2013).

1.2 Vertical heterogeneity in leaf traits across the canopy

Plant traits do not exclusively exhibit variation over Cartesian space and time but also show changes across the vertical canopy profile. Plant physiology studies have demonstrated that leaf trait content vary relative to the position of the leaf in a plant canopy (Huang *et al.*, 2011; Huang *et al.*, 2014; LÖTscher *et al.*, 2003; Wang *et al.*, 2005). The vertical heterogeneity in leaf traits content across canopy is known to improve plant photosynthetic capacity and light use efficiency (Li *et al.*, 2013). Two complementary theories, i.e. the optimisation (Hirose and Werger, 1987) and coordination (Chen *et al.*, 1993) theories attempt to explain the mechanism responsible for the vertical heterogeneity in leaf traits across the canopy.

1.2.1 Optimisation theory

The optimization theory is hinged on three principles i.e. (1) the irradiance of a leaf at a given canopy depth (2) the distribution of leaf traits especially N relative to the depth of the canopy (3) the photosynthetic activity of a leaf as a function of irradiance and leaf traits concentration (Hirose and Werger, 1987). The theory postulates that plants allocate N based on light distribution pattern within the canopy. Plants allocate more N to the upper illuminated leaves that receive the highest photon flux density compared to lower shaded leaves (Li *et al.*, 2013). This intrinsic mechanism optimizes the total canopy photosynthetic capacity (Field, 1983). Although the optimization theory is widely accepted in plant physiology domain, it has received criticism for oversimplification and lack of realistic underpinning biological mechanism (Chen *et al.*, 1993).

1.2.2 Coordination theory

The coordination theory explains that the vertical heterogeneity in leaf traits distribution is an attempt by plants to maintain a balance between Rubisco-limited rate of carboxylation (W_c) and electron transport-limited rate of carboxylation (W_j) (Chen *et al.*, 1993). The two processes depend on leaf traits content and the rate of photosynthesis (Li *et al.*, 2013). The driving force for the allocation of leaf traits especially N within a canopy is the variation between leaf N content at a given time and the N required to bring W_c and W_j into a balance (Chen *et al.*, 1993). The theory infers that the primary objective of vertical heterogeneity in N distribution is not to maximise canopy photosynthesis but rather an inherent mechanism to enhance internal balance (Dreccer *et al.*, 2000).

Although the two theories improve our understanding of the vertical heterogeneity in leaf traits across the canopy, the impact of vertical canopy position on leaf spectral properties and retrieval of leaf traits across multiple species over the growing season has received little attention.

1.3 Remote sensing plant traits

Conventional methods of leaf traits measurements involve destructive harvesting and transportation of large foliar samples from discrete plots to laboratories for analysis (Ling *et al.*, 2014; van Deventer *et al.*, 2015). These conventional methods are costly as they require huge amounts of laboratory chemicals to extract nutrient constituents in addition to the high human resources required to collect and process the samples (Shengyan *et al.*, 2002). Although these flaws cannot be completely eliminated in remote sensing leaf traits, the remote sensing procedure requires sufficient samples (>30) to calibrate a parsimonious and robust model that can be used to explicitly quantify leaf traits repeatability over large spatial extents.

Based on the knowledge and identification of spectral features that are sensitive to variation in foliar biophysical and biochemical properties a number of studies (Christensen *et al.*, 2004; Ciganda *et al.*, 2012; Curran *et al.*, 2001; Darvishzadeh *et al.*, 2008c; Delegido *et al.*, 2010; Delegido *et al.*, 2014; Dutta *et al.*, 2015; Eitel *et al.*, 2010; Ferwerda and Skidmore, 2007; Haboudane *et al.*, 2004; Haboudane *et al.*, 2002; Main *et al.*, 2011; Malenovsky *et al.*, 2013; Mutanga and Skidmore, 2007; Quanzhou *et al.*, 2014; Ramoelo *et al.*; Ramoelo *et al.*, 2013) have utilized empirical and physical models based on *in-situ,* air- and spaceborne remote sensing measurements to retrieve vegetation properties in different ecosystems with varying level of success. Empirical models explore the parametric and non-parametric statistical relationship between spectral features [reflectance, derivatives (first and second), vegetation indices, depth and width of absorption features] and foliar nutrients. Although statistical models are easy and faster to compute, they are associated with problems of transferability over space and time as in most instances the relationship between spectral data and leaf traits is sensor- site-, time, and biome specific (Clevers and Kooistra, 2012; Darvishzadeh *et al.*, 2008b). Moreover, statistical models characterizing the relationships between spectral data and foliar biophysical and biochemical properties are not grounded in physical theory (Kokaly *et al.*, 2009). Physical models on the other hand rigorously simulate light absorption and scattering inside vegetation canopies accounting for leaf biochemical composition, canopy structural properties and background soil based on radiation transfer theory (Homolová *et al.*, 2013). However, the inversion process of physical models is computationally demanding and associated with 'ill-posed problem' (Weiss *et al.*, 2000) *i.e.* where the inversion solution is not always unique, as various combinations of canopy parameters may yield almost similar spectra (Atzberger and Richter, 2012), resulting in uncertainties in model predictions (Pasolli *et al.*, 2015). Although, a number of studies have successfully retrieved plant biochemical and physical properties in different ecosystems using physical models very little is known on how the heterogeneity in leaf traits across the canopy affect modelling of leaf optical properties and retrieval of leaf traits using physical models such as PROSPECT.

1.4 Upscaling leaf traits to canopy level

There is often a mismatch of spatial scales at which *in-situ* and *in-vitro* traits are measured and the field of observation of remote sensing instruments. This mismatch requires scaling leaf traits from leaf level to canopy scale (Homolová *et al.*, 2013). The mean leaf traits weighted relative to the abundance of dominant species are often multiplied by LAI (m^2 m^2) or foliage biomass (g m^2)

to obtain a canopy-integrated value that corresponds to canopy reflectance observed by the sensor (He and Mui, 2010b). In most instances, the weighted mean traits are determined from samples collected from the sunlit upper canopy (Gara *et al.*, 2019). This approach is centred on the implicit assumption that foliage material dominates canopy reflectance and variability in leaf traits across the vertical canopy profile is 'insignificant'. This assumption is hinged on the theory that the absorption of incoming photosynthetically active radiation (PAR) follow a bell-shaped function positive skewed to the upper canopy (Kropff and Goudriaan, 1994). On this basis, the contribution of leaf traits from the shaded lower canopy is considered 'invalid' in canopy traits modelling (Roelofsen *et al.*, 2013). However, the validity of this approach remains unknown for other leaf traits outside photosynthetic pigments. To this end, there is an imperative need to explore the effect of upscaling approaches and expression methods on canopy traits modelling. This knowledge can provide a baseline of understanding how deep into the canopy do sensors observe.

1.5 Research Objectives

The principal aims of this study were to:

i. Examine the effect of vertical canopy position on leaf spectral properties and traits across multiple species
ii. Examine the effect of leaf position within a canopy on the performance of the PROSPECT model in modelling leaf optical properties and retrieval of leaf traits across the growing season
iii. Evaluate the effect of leaf-to-canopy upscaling approaches on modelling canopy traits using *in-situ* hyperspectral and simulated Sentinel-2 measurements
iv. Examine the effect of canopy traits expression on modelling canopy traits using Sentinel-2 MSI across the growing season.

1.6 Study area

Objectives i and iii (Section 1.5) were addressed based on hyperspectral measurements conducted in a controlled laboratory environment using short plants purchased from the local nursery. In order to understand the validity of results obtained in the laboratory, we collected samples in Bavaria Forest National Park (BFNP), Germany (Fig 1.1) to address objective ii and iv.

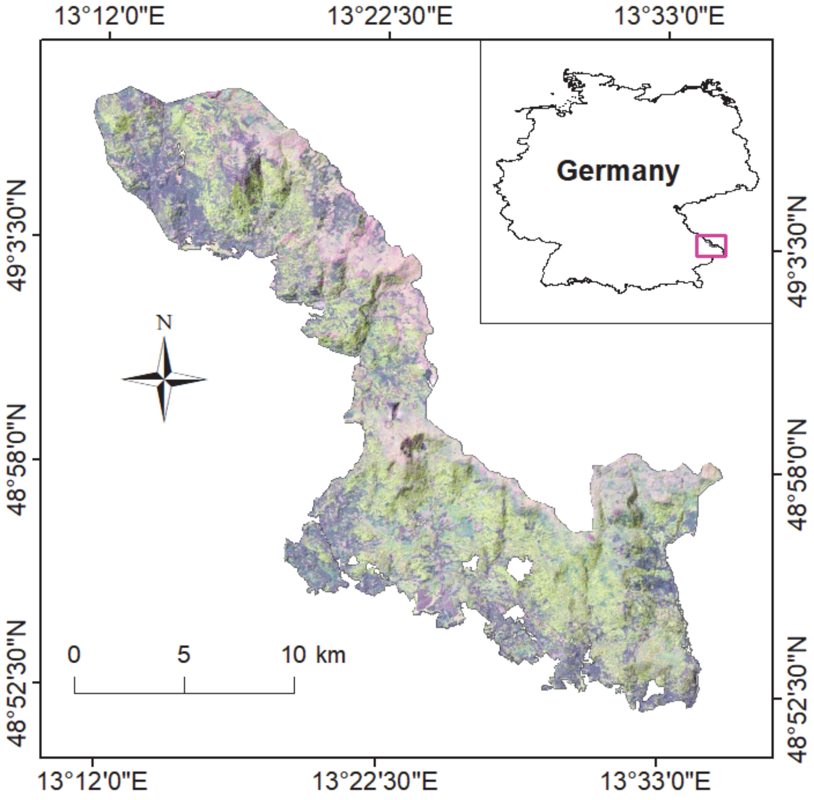

Figure 1.1 The location of Bavaria Forest National Park in Germany. Overlaid on the Park is Sentinel-2 satellite imagery of 13 July 2017.

BNFP is part of the mixed temperate Bohemian forest ecosystem. The Park is approximately 24 218 ha in size, with elevation stretching from 600 to 1453 m (Heurich *et al.*, 2010a). Annual precipitation ranges from 1200 to 1800 mm and the park experience a mean annual temperature of ~5° C. The evergreen Norway spruce (*Picea abies*) and deciduous European beech (*Fagus sylvatica*) are the dominant trees species, while white fir (*Abies abies*), sycamore maple (*Acer pseudoplatanus*), and mountain ash (*Sorbus aucuparia*) are the less dominant species in the park (Heurich *et al.*, 2010b).

1.7 Thesis outline

This thesis consists of six chapters including introduction, four core chapters and a synthesis. Chapter 1 provides a background of the research, objectives and thesis outline. The four core chapters are scientific outputs published (2) or submitted (2) to peer-reviewed international (ISI) journals. The four core chapters were conducted at three different levels of investigation, i.e. leaf level, canopy level and landscape level.

Leaf level

Chapter two and three were conducted at leaf level using leaf hyperspectral data measured using a field spectroradiometer coupled with an Integrating Sphere. Chapter 2 examines the ability of leaf optical properties to track variability in leaf traits across the vertical profile using Partial Least Discriminatory Analysis (PLS-DA). Chapter 3 sought to examine whether the position of a leaf in a canopy affects the performance of PROSPECT in modelling leaf optical properties and the retrieval of leaf C_{ab}, EWT and LMA across the growing season.

Canopy level

Chapter 4 explores the use of *in-situ* canopy hyperspectral measurements and simulated Sentinel-2 data measured in a laboratory using short potted plants. The chapter examined the effect of different approaches of upscaling leaf traits to canopy level on modelling canopy traits (LMA, chlorophyll, nitrogen and carbon).

Landscape-level

Chapter 5 examined the effect of canopy traits expression on modelling canopy traits (LMA, chlorophyll, nitrogen and carbon) using Sentinel-2 multispectral data across the growing season in BFNP. In addition to understanding the effect of canopy traits expression, the chapter explores the capability of Sentinel-2 MSI to map the spatio-temporal variation in canopy traits across the landscape.

Findings of the four core chapters are synthesized in Chapter 6. Finally, Chapter 6 concludes the thesis by discussing the implications of the results obtained in the core chapters and future research avenues.

Chapter 2

Impact of vertical canopy position on leaf spectral properties and traits across multiple species*

---

* This chapter is based on:
Gara, T.W., Darvishzadeh, R., Skidmore, A. K., Wang, T. (*2018*). Impact of Vertical Canopy Position on Leaf Spectral Properties and Traits across Multiple Species. *Remote Sensing, 10, 346*

Gara, T. W., Darvishzadeh, R., Skidmore, A. K., & Wang, T. Leaf spectral properties track variability in leaf traits across the canopy vertical profile: Poster presented at *10th EARSeL SIG Imaging Spectroscopy Workshop* 19-21 April 2017, Zurich, Switzerland

Abstract

Understanding the vertical pattern of leaf traits across plant canopies provide critical information on plant physiology, ecosystem functioning and structure and vegetation response to climate change. However, the impact of vertical canopy position on leaf spectral properties and subsequently leaf traits across the entire spectrum for multiple species is poorly understood. In this study, we examined the ability of leaf optical properties to track variability in leaf traits across the vertical canopy profile using Partial Least Square Discriminatory Analysis (PLS-DA). Leaf spectral measurements together with leaf traits (nitrogen, carbon, chlorophyll, equivalent water thickness and specific leaf area) were studied at three vertical canopy positions along the plant stem: lower, middle and upper. We observed that foliar nitrogen (N), chlorophyll (C_{ab}), carbon (C), and equivalent water thickness (EWT) were higher in the upper canopy leaves compared with lower shaded leaves, while specific leaf area (SLA) increased from upper to lower canopy leaves. We found that leaf spectral reflectance significantly ($P \leq 0.05$) shifted to longer wavelengths in the 'red edge' spectrum (685–701 nm) in the order of lower > middle > upper for the pooled dataset. We report that spectral bands that are influential in the discrimination of leaf samples into the three groups of canopy position, based on the PLS-DA variable importance projection (VIP) score, match with wavelength regions of foliar traits observed to vary across the canopy vertical profile. This observation demonstrated that both leaf traits and leaf reflectance co-vary across the vertical canopy profile in multiple species. We conclude that canopy vertical position has a significant impact on leaf spectral properties of an individual plant's traits, and this finding holds for multiple species. These findings have important implications on field sampling protocols, upscaling leaf traits to canopy level, canopy reflectance modelling, and subsequent leaf trait retrieval, especially for studies that aim to integrate hyperspectral measurements and LiDAR data.

2.1 Introduction

Leaf traits play a key role in ecosystem structure, functioning and resilience (Diaz *et al.*, 2004) and ecophysiology (Reich *et al.*, 2003). They improve our understanding of evolutionary and phylogenetic relationships among different forms of biota (Winemiller *et al.*, 2015) as well as the parameterization of dynamic global biogeochemical models and nutrient budget simulations (Scheiter *et al.*, 2013). Based on the realization that leaf traits are a critical component of essential biodiversity variables (EBVs) (Skidmore *et al.*, 2015), quantifying leaf traits improves our conservation and spectroscopic monitoring efforts of EBVs towards the Aichi Biodiversity Targets (Pereira *et al.*, 2013).

Field spectroscopy provides a cost-effective and practical means to monitor EBVs and ecosystem functioning with a capacity to upscale to airborne and satellite imagery. Multi- and hyper-spectral sensors afford a comprehensive spectral information that has provided a cost effective opportunity to; estimate foliar biochemistry (Ferwerda and Skidmore, 2007; Kokaly, 2001), quantify plant biophysical properties (Darvishzadeh *et al.*, 2008b; Dusseux *et al.*, 2015), identify plant species (Mariey *et al.*, 2001; Schmidt and Skidmore, 2003) and assess plant physiological status over space and time (Rapaport *et al.*, 2015). Basically, two approaches [i.e., empirical (statistical) and physical models (radiative transfer models-RTM)] are often employed to link spectral signatures and field measured leaf traits. Empirical approaches explore parametric and non-parametric statistical relationships between spectral data or features and leaf traits (Verrelst *et al.*, 2015a). Physical models on the other hand, rigorously simulate light absorption and scattering inside vegetation canopies accounting for leaf traits composition, canopy structural properties and soil background based on radiation transfer theory (Homolová *et al.*, 2013). Although these spectroscopic approaches for studying plant traits are promising, many efforts have been placed on the spectra-trait relationship for mature, sunlit leaves at the top-of-canopy. The implicit assumption is that variability in leaf traits content and leaf spectral properties within a canopy are very small and consequently, top-of-canopy foliar samples are representative of the canopy as a whole (Thomas *et al.*, 2008). To this end, the vertical heterogeneity in leaf traits across the canopy is often not accounted for in most modelling approaches. However, the distribution of leaf traits within vegetation canopies is complex and often varies across the canopy vertical profile especially in resource constrained ecosystems (Li *et al.*, 2013).

The distribution of leaf traits content across the canopy vertical profile is indicative of the strategies plants use to optimize critical metabolic processes such as photosynthesis (Coble *et al.*, 2016b). Plants exhibit higher nutrient stoichiometry in the upper illuminated leaves that receive higher photon flux density compared to lower canopy shaded leaves (Hirose and Werger, 1987).

The vertical distribution of leaf traits particularly nitrogen content is an attempt to maintain a balance between the RuBisCO-limited rate of carboxylation and electron transport limited rate of carboxylation (Chen *et al.*, 1993). Plants are also known to absorb foliar nutrients from older leaves located in the lower canopy and translocate the nutrients to the upper canopy leaves for protein repair and maintenance of a metabolic balance (Hikosaka, 2005). These intrinsic mechanisms result in marked effects on leaf morphological, chemical as well as physiological traits across the canopy vertical profile (Weerasinghe *et al.*, 2014) and subsequently influence whole canopy spectral reflectance (He *et al.*, 2016). In light of this background, we hypothesize that leaf spectral properties track variability in leaf traits across the canopy vertical profile.

Although the concept of vertical heterogeneity in leaf morphological, chemical and physiological traits is well documented in plant physiology domain (Coble *et al.*, 2016b; Weerasinghe *et al.*, 2014), to date few studies (Khavaninzadeh *et al.*, 2015; Liu *et al.*, 2015; Ma and Upadhyaya, 2018; Van Wittenberghe *et al.*, 2014) have examined the impact of canopy vertical position on leaf spectral properties in addition to assessing the ability of leaf optical properties (in VNIR, SWIR spectral domain) to track variability in leaf traits across the canopy vertical profile for multiple species across the entire spectrum. One of the possible reasons related to limited or lack of studies thereof is the inadequacy and complexity in collecting field measurements at different canopy positions to characterize the vertical heterogeneity in leaf spectral properties and leaf traits (Li and Wang, 2013a). A few studies that have attempted to understand the leaf traits-spectra interactions across the canopy have not only restricted their work on understanding the effect of canopy position on the empirical relationship between crops' leaf spectra, and their C_{ab} and nitrogen content but also focused on the wavelengths before 1100 nm (Liao *et al.*, 2013; Yu *et al.*, 2015). For example, Ma and Upadhyaya (2018), examined the effects of leaf position on tomato leaf optical properties at only two wavelengths i.e., 660 and 730 nm. To this end, spectral discrepancies across the canopy vertical profiles need to be fully characterized across the whole spectrum and across multiple species outside crops. Simultaneous measurement of leaf optical properties together with a suite of leaf traits across the canopy require attention for improved understanding of the spectra-traits interaction across the canopy vertical profile. Understanding the effect of vertical heterogeneity on leaf spectral properties does not only offer a promising path in canopy reflectance modelling using multi-layer radiative transfer models (RTM) but also has a strong implication on within-canopy sampling and leaf traits upscaling to canopy and subsequently landscape level. For instance, Wang and Li (2013) demonstrated that vertical heterogeneity in leaf dry matter per unit area, C_{ab}, water and dry matter contents have a significant effect on simulated canopy reflectance and subsequently inversion of multiple-layer canopy radiative transfer model. Sprintsin *et al*. (2012) also demonstrated that upscaling leaf traits to canopy scale based on the 'big leaf' (sunlit only) and 'two leaf' (sunlit plus shaded) upscaling models, can have a profound effect on gross primary productivity estimations against flux tower measurements. Their study demonstrated that the exclusion of the photosynthetic contribution of shaded leaves can underestimate the canopy photosynthesis estimations by over 70% in highly clumped forest stands. In this regard, a detailed understanding on the impact of vertical canopy position on leaf traits content and spectral reflectance properties is imperative and has broad implications on leaf traits upscaling to canopy level and their subsequent retrieval or estimation.

This study aims at examining the effect of canopy vertical position on leaf spectral properties across multiple species. We studied the impact of canopy position on leaf spectral properties to assess the capability of leaf optical properties to track variability in leaf traits across the vertical canopy profile. We also aimed at identifying key spectral wavebands that are influential in the discrimination of leaf samples into the three groups of canopy position. We hypothesize that the influential spectral wavebands match wavelength absorption features associated with the measured leaf traits.

2.2 Materials and Methods

2.2.1 Species description

We selected four plant species with different leaf forms and canopy structure to examine the impact of canopy vertical position on leaf spectral properties and traits at leaf level. The selected species were *Camellia japonica* (n = 10, mean height 83.71 ± 4.75 cm), *Ficus benjamina* (n = 10; mean height 82.07 ± 4.27 cm), *Chamaedorea elegans* (n = 10; mean height 88.5 ± 4.75 cm) and *Fatshedera lizei* (n = 10; mean height 88.93 ± 1.53 cm). *C. japonica* is an evergreen broad-leaved woody plant whose flowers are bisexual and disposed in racemes. The leaf blade length for *C. japonica* range between 5 and 10 cm and a mature *C. japonica* can reach a height of 6 m. *F. benjamina* is also an evergreen shrub with pendulous branches bearing glossy, elliptic, slender pointed ovate leaves. A mature *F. benjamina* plant can reach 30m in height while the leaf blades can extend up to 8 cm. *C. elegans* is an evergreen palm with slender, solitary or clustered stems bearing slender stalked, pinnate leaves. The leaf blade length for *C. elegans* range between (six) 6 and 12 cm and the plant can reach 4 m at maturity. *F. lizei* is a hybrid between *Fatsia japonica* and *Hedera helix*. *F. lizei* is characterized by large, leathery, palmately lobed leaves and small flower in globose panicles. The plant can grow up to 4 m in height and its leaf blades range between 7 and 25 cm at maturity. All the plants used in this study were purchased from a local nursery.

2.2.2 Experimental setup

Considering that plants obtained from the nursery were pre-treated with fertilizer, we changed the potted soil to a new homogenized mixture of seven parts of poor-nutrient sand soil to two parts of fertile loamy soil. After changing the potting soil, three soil nitrogen treatments (high, medium and low) were administered to 40 plants. For the high (n = 13) and medium (n = 14) treatment groups, 2.9 g and 0.9 g per pot were supplied per pot respectively, while for the low (n = 13) treatment no fertilizer was supplied. The fertilizer was administered once a week over a four-week period after which plants were left to acclimatize for another four weeks without fertilizer treatment. The three soil nitrogen treatment were administered in order to create variation in leaf traits and subsequently leaf spectral properties among the different potted plants. The potted plants were kept under artificial light and at a normal room temperature of 21 °C. Three overhead halogen lamps of 50 W each were used for illumination. To minimize the effect of a microclimate the pots were randomly placed in the experimental room and rotated after every two days. Care was taken to avoid plants shading one another.

2.2.3 Leaf spectral measurement

For each leaf sample measurement, approximately three (3) gram of fresh leaves (between six to ten leaves - depending on leaf size and weight) were randomly sampled from the upper, middle and lower canopy vertical layers for each plant (Fig 2.1). At each of three canopy layers, leaf samples were picked from both the outer and interior canopy in all directions. The three layers were determined based on the height of a plant along the stem. We divided the canopy into three layers for two reasons. Firstly, the plants used in this study were relatively short (mean height ~85 cm) to identify and characterize more than three canopy layers. Secondly, three canopy layers match forestry and agronomic standards in reporting research in canopy layers (Whitehurst *et al.*, 2013; Wilkes *et al.*, 2016). The leaves picked from the three canopy layers were stored in a portable cooler and all laboratory measurements were performed within two hours of leaf picking. Leaf directional hemispherical reflectance from 350 to 2500 nm for each sample was measured using an ASD FieldSpec-3 Pro FR spectroradiometer coupled with an ASD RTS-3ZC Integrating Sphere. To minimize spectral noise, the spectroradiometer was set to average two hundred scans into a single spectrum per each spectral measurement. The spectra were calibrated for dark current and stray light following the Integrating Sphere User Manual instructions (ASD, 2008). During spectral measurements, care was taken to avoid leaf primary veins. Spectral measurements of leaves constituting a sample were averaged to a single spectrum that represented the spectra of each sample. In total spectral reflectance measurements were performed on 120 samples (40 plants × 3 canopy layers). A moving second order Savitzky-Golay filter (Savitzky and

Golay, 1964) with a frame size of 11 was applied on each sample spectra to minimize instrument noise. Due to the low signal-to-noise ratio for wavelengths after 2200 nm as well as spectral bands before 400 nm, the spectra were cropped to 400–2200 nm range. Therefore, 1801 spectral bands were retained for further analysis

Figure 2.1 The demarcation of the three canopy layers.

2.2.4 Leaf traits measurement

Following measurement of leaf spectral properties, the following leaf traits were measured; leaf chlorophyll content (C_{ab}), leaf nitrogen content (N), leaf carbon content (C), fresh weight, dry weight and leaf area. Consequently, equivalent water thickness (EWT) and specific leaf area (SLA) were then retrieved. For each sample the average leaf chlorophyll content (C_{ab}: μg/cm^2) was determined using a CCM-300 chlorophyll content meter (Opti-Sciences, 2011). After measuring the C_{ab}, fresh weight (Fw g) for each sample was determined using a digital scale at an accuracy of 0.01 g. We also measured the leaf surface area (LA cm^2) of each sample using an AMH 350 area meter (ADC-BioScientific, 2013). The samples were then oven-dried for 72 hours at 65 °C to determine dry weight (Dw g). Specific leaf area (SLA cm^2/g) and equivalent water thickness (EWT cm) were calculated using the following formulas:

$$\text{SLA (cm}^2\text{/g)} = \text{LA/Dw} \tag{2.1}$$

$$\text{EWT (cm)} = \text{Fw} - \text{Dw/LA} \tag{2.2}$$

where: Dw, Fw and LA are sample dry weight, fresh weight and leaf area respectively.

Leaf N and C (% dry weight) were determined by dry combustion using the Perkin Elmer 2400 CHNS/O Elemental Analyzer (Perkin-Elmer, 2005). Prior to determining leaf N and C content using the elemental analyzer leaves representing a sample were shredded and grounded to a fine and homogeneous powder using a mortar and pestle to pass through a 180 µm mesh screen. The sample powder was placed in tin capsules for N and C analysis. We duplicated twenty-five percent of samples and run an acetanilide standard after every ten to fifteen samples to constantly monitor the system calibration and integrity. Results from the elemental analyzer were obtained on a dry mass ash-included basis (Meerdink *et al.*, 2016). We then converted the mass-based N obtained from the elemental analyzer to the area-based N by dividing mass-based N of each sample by dry mass per unit area (Wang *et al.*, 2015a).

2.2.5 Statistical analysis

2.2.5.1 Impact of canopy vertical position on leaf spectral properties and traits

To understand the impact of canopy vertical position on leaf spectral properties, we examined whether there was a statistical difference between mean leaf spectral reflectance of the three canopy positions at each wavelength across the entire electromagnetic spectrum (400–2200 nm). We also examined whether leaf traits vary across the canopy vertical profile. Variability in leaf spectral reflectance and leaf traits were performed for both individual species and for the pooled dataset. Differences in mean leaf spectral reflectance (per wavelength), as well as leaf traits at the three canopy positions, were tested using a one-way analysis of variance (ANOVA) with canopy position as a fixed factor. We tested the null hypothesis that there was no significant difference in leaf spectral reflectance of different canopy positions at every spectral wavelength; H_o: $\mu 1 = \mu 2 = \mu 3$ versus the alternative hypothesis that there was a difference; *vis*: H_o: $\mu 1 \neq \mu 2 \neq \mu 3$. The mean leaf spectral reflectance for the upper, middle and lower layers at every spectral wavelength is denoted by $\mu 1$, $\mu 2$, and $\mu 3$, respectively. Following a significant ANOVA test, *Tukey* Honest significance difference (HSD) *post-hoc* tests (Tukey, 1949) were performed on the leaf spectral reflectance data and leaf traits respectively. *Post-hoc* tests were computed to highlight pairwise differences in both leaf spectral reflectance and leaf traits for all possible pairs (upper vs. lower, middle vs. upper, middle vs. lower) of the three canopy positions. *Tukey* HSD *post hoc* test accounts for type I error by reducing the significant level of each test such that the group-wise type I error rate remains at a selected level, in this case, ɑ = 0.05 (Quinn and Keough, 2002). The multiple comparisons highlights leaf traits and wavelengths that significantly vary between each pair of canopy positions (upper vs. lower, middle vs. upper, middle vs. lower) with minimal error (Carvalho *et al.*, 2013). The ANOVA and *Tukey* HSD *post hoc* tests were performed using R 3.4.1 for Windows.

2.2.5.2 Discriminating leaf samples into respective canopy positions groups

While the ANOVA and *Tukey* HSD *post hoc* test for difference in means between groups, discriminatory analysis can be used to classify and identify key variables that maximize assignment of objects to their defined group. We set out to identify and confirm whether influential spectral wavebands in the discrimination of leaf samples into the three vertical canopy positions matches the wavelength absorption features associated with the measured leaf traits. Identification of influential wavebands that match spectral absorption features of the traits provide an opportunity to assess whether leaf optical properties track variability in leaf traits across the vertical canopy profile. We used a bootstrapped Partial Least Squares-Discriminant Analysis (PLS-DA) to identify key wavebands that influence the spectral separatibility of leaf samples into the three canopy positions groups. Bootstrapping with 1000 replicates was used to train the PLS-DA model. PLS-DA is a classification technique that fuses Partial Least Square regression and the properties of discriminant analysis for identification of the variables that enhance the separation or classification of different groups (Wold *et al.*, 2001). PLS-DA aim to discriminate the response matrix (Y) by means of a predictive matrix (X) utilizing a set of orthogonal components (so-called latent variables) that maximizes the co-variance between matrices (X) and (Y) (Makvandi *et al.*, 2016). The Y matrix in our study represents the three canopy position (upper, middle and lower), while the X represents the spectral reflectance (400–2200 nm). This technique is suitable for high dimensional and collinear datasets such as hyperspectral measurements. Prior to model calibration, we randomly split our dataset into model calibration (70%) and external validation (30%). The model calibration dataset was used to develop the PLS-DA model to discriminate the leaf samples. The model was then applied on the 30% external validation dataset that was never used in the development of the model to determine the performance of the model. The number of latent variables (nlv) were determined by maximizing the accuracy of the PLS-DA model i.e., the model with the maximum accuracy was considered to have the optimum number of latent variables (Pereira *et al.*, 2016). We used the variable importance of projection (VIP) to determine the influence of each waveband on the discrimination of the leaf samples into their defined vertical canopy position group. VIP scores greater than one (1) were regarded as influential in the classification procedure. The PLS-DA analysis was performed using R 3.4.1 for Windows using the classification and regression (caret) package (Kuhn, 2008).

2.3 Results

2.3.1 Characteristics of leaf traits

Table 2.1 summarizes the characteristics of leaf traits across the three canopy levels. N ranged from 3.15×10^{-5} to 4.04×10^{-4} μg/cm^2 whereas C_{ab} varied from 24.86 to 72.85 μg/cm^2. SLA spanned a ten-fold range of values (53.67–530.21 cm^2/g), while the range of C was only limited between 37.96 and 47.55%. EWT ranged from 0.00545 to 0.0275 cm. Generally, N, C_{ab}, C, and EWT increased from the lower to the upper canopy while SLA decreased with increasing canopy depth.

2.3.2 Impact of canopy position on leaf spectral properties

Leaf spectral reflectance significantly ($P \leq 0.05$) shifted to longer wavelengths in the 'red edge' spectrum in the order of lower > middle > upper (Fig 2.2) for the pooled species data. The spectra significantly shifted to longer wavelengths in wavebands 685–701 nm (Fig 2.3). Moreover, mean leaf spectral reflectance displayed a consistent descending pattern in the order of lower > middle > upper canopy layers in the visible spectrum (400–700 nm; Fig 2.2). Spectral variations in the 'red edge' and visible spectrum demonstrated a significant ($P \leq 0.05$) increase in C_{ab} and N observed from the lower to the upper canopy layer (Table 2.1). At longer wavelengths, leaf spectra for the upper canopy leaves consistently exhibited relatively low reflectance values around 1450 and 1940 nm compared to leaf spectra for the middle and lower canopy sections (see inserts Fig 2.2).

Table 2.1: Summary statistics of leaf traits at the three canopy layers

Leaf Trait	Upper (n = 40)				Middle (n = 40)				Lower (n = 40)			
	min	max	mean	SD	Min	max	mean	SD	min	max	mean	SD
N μg/cm^2)	7.31 × 10^{-5}	2.94 × 10^{-4}	1.68 × 10^{-4}	6.29 × 10^{-5}	3.15 × 10^{-5}	4.04 × 10^{-4}	1.46 × 10^{-4}	6.7 × 10^{-5}	5.24 × 10^{-5}	2.36 × 10^{-4}	1.31 × 10^{-4}	5.07 × 10^{-5}
C_{ab} (μg/cm^2)	30.96	72.85	52.82	14.44	27.03	69.54	49.19	13.77	24.86	68.41	46.6	15.7
SLA (cm^2/g)	53.67	380.4	201.94	105.42	57.43	512.21	220.16	140.87	54.3	530.21	234.08	144.92
C (%)	37.96	47.55	45.01	1.63	41.33	46.69	44.58	1.14	38.94	46.4	43.79	1.61
EWT (cm)	6.28 × 10^{-3}	2.56 × 10^{-2}	0.0172	6.77 × 10^{-3}	5.98 × 10^{-3}	2.53 × 10^{-2}	0.0162	6.28 × 10^{-3}	5.46 × 10^{-3}	2.76 × 10^{-2}	0.0163	6.57 × 10^{-3}

Table 2.2 Summary of pairwise variation in leaf traits per species and within pooled data per each canopy position pair. Significant p-value at 0.1 *, 0.05 ** and 0.01 *** are indicated.

Species	Trait	Canopy Position Combination Middle vs. Lower	 Upper vs. Lower	 Middle vs. Upper
F. benjamina	N	0.219	0.000 ***	0.04 **
	C_{ab}	0.68	0.025 **	0.14
	SLA	0.79	0.025 **	0.10 *
	C	0.12	0.002 ***	0.18
	EWT	0.11	0.623	0.49
C. japonica	N	0.92	0.002 ***	0.000 ***
	C_{ab}	0.81	0.12	0.029 **
	SLA	0.72	0.912	0.467
	C	0.96	0.933	0.99
	EWT	0.18	0.984	0.23
C. elegans	N	0.89	0.000 ***	0.000 ***
	C_{ab}	0.28	0.002 ***	0.06 *
	SLA	0.66	0.000 ***	0.000 ***
	C	0.34	0.05 **	0.56
	EWT	0.06 *	0.013 **	0.77
F. lizei	N	0.11	0.6	0.51
	C_{ab}	0.000 ***	0.000 ***	0.94
	SLA	0.05 **	0.67	0.007 ***
	C	0.08 *	0.07 *	0.99
	EWT	0.14	0.006 ***	0.35
Pooled	N	0.516	0.02 **	0.24
	C_{ab}	0.71	0.051 *	0.51
	SLA	0.493	0.075 *	0.63
	C	0.048 **	0.0009 ***	0.39
	EWT	0.93	0.083 *	0.035 **

N = nitrogen, C_{ab} = chlorophyll, SLA = Specific leaf area, C = carbon, EWT equivalent water thickness.

This spectral variation relates to relatively higher EWT observed for the upper leaves for the pooled dataset (Table 2.1). A *Tukey* HSD *post hoc* test revealed significant ($P \leq 0.05$) pairwise difference in leaf spectra only between the upper and lower canopy layers within the 685–701 nm spectral range (Fig 2.3). This pairwise difference in spectra confirmed the significant differences observed for most traits especially between the upper and lower canopy layers (Table 2.2).

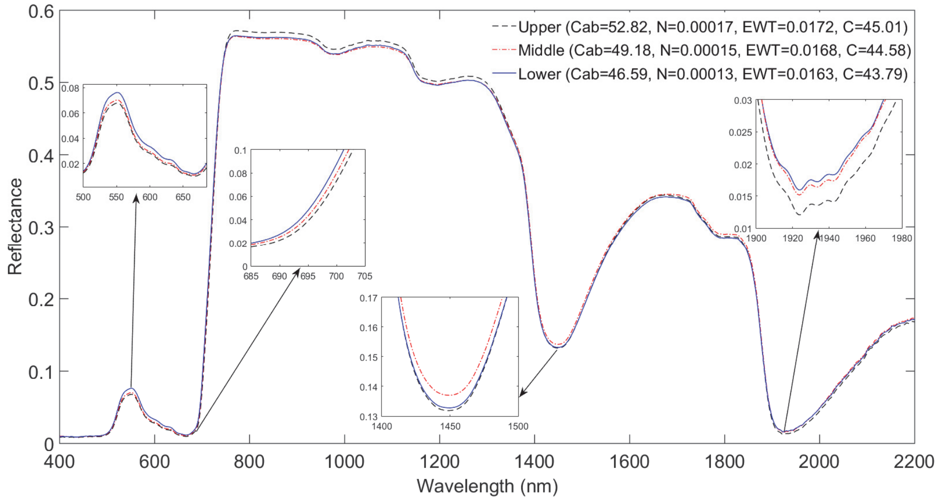

Figure 2.2 Mean leaf spectral reflectance at each canopy position for the pooled dataset. Note that the red-edge shifts to longer wavelengths with increasing C_{ab}.

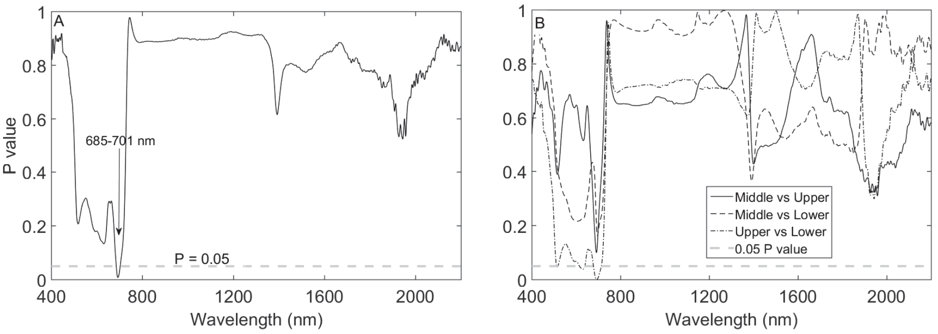

Figure 2.3 Variation in leaf spectral reflectance at different canopy positions for the pooled dataset (ANOVA test) (A); and pairwise variation in leaf spectral reflectance at different canopy positions (B).

An ANOVA test showed that spectral response varied among species, resulting in species-dependent leaf spectral properties across the canopy vertical profile. Generally, for all the species studied leaf spectral reflectance was consistently higher for the lower canopy layer in the visible spectrum (Fig 2.4)—a result confirmed by the ANOVA test (Fig 2.5A) followed by the *Tukey* HSD *post hoc* test (Fig 2.5B–E). The descending spectral reflectance trend in the visible spectrum (lower > middle > upper) was more pronounced for *F lizei*, *F.benjamina* and *C elegans*. This pattern is similar to the one observed for the pooled species data. *C. Japonica* exhibited a small variation in the visible spectrum between canopy layers—reflecting a small variation in C_{ab} observed in Fig 2.6. We found no significant variation in leaf spectra for *C. japonica* in the NIR spectral domain, and this reflects variation in C observed for this species which was not statistically significant (P > 0.05). In the SWIR spectral domain especially in wavebands centered around 1950 nm, leaf spectra for *C. japonica* and *C. elegans* decreased in the order of lower > middle > upper canopy layers (Fig 2.4 C,D). The descending pattern in leaf spectra in these wavebands was statistically significant (P ≤ 0.05) for *C elegans* (Fig 2.5 E), while for *C. japonica* the descend was significant between the upper layer against the middle and lower canopy layers respectively (Fig 2.5 D). The trend observed for *C. japonica* and *C. elegans* conform to the trend observed for the pooled species data. Leaf spectra for the lower canopy layer for *F. lizei* and *F. benjamina* exhibited significantly low reflectance values in the SWIR spectral domain compared to the upper and middle canopy layers (Fig 2.4A, B).

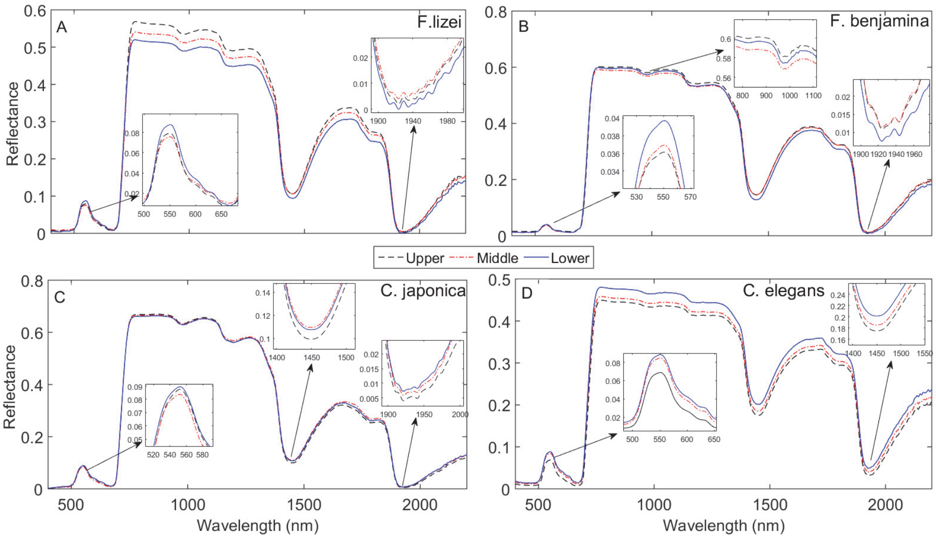

Figure 2.4 Species-specific mean leaf spectral reflectance at each canopy position for *F. lizei* (A), *F. benjamina* (B), *C. japonica* (C) and *C. elegans* (D).

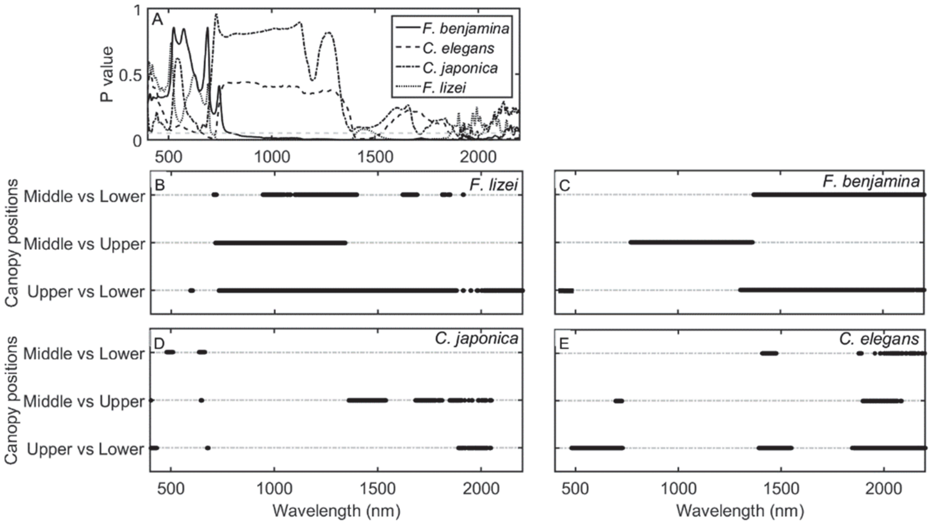

Figure 2.5 Species- specific ANOVA test for mean leaf spectral reflectance at three canopy positions (A) and pairwise t-test of mean leaf spectral reflectance at three canopy positions for *F. lizei* (B), *F. benjamina* (C), *C. japonica* (D) and *C. elegans* (E). Dark circles indicate spectral wavebands that were significantly different ($P \leq 0.05$) for each pairwise comparison.

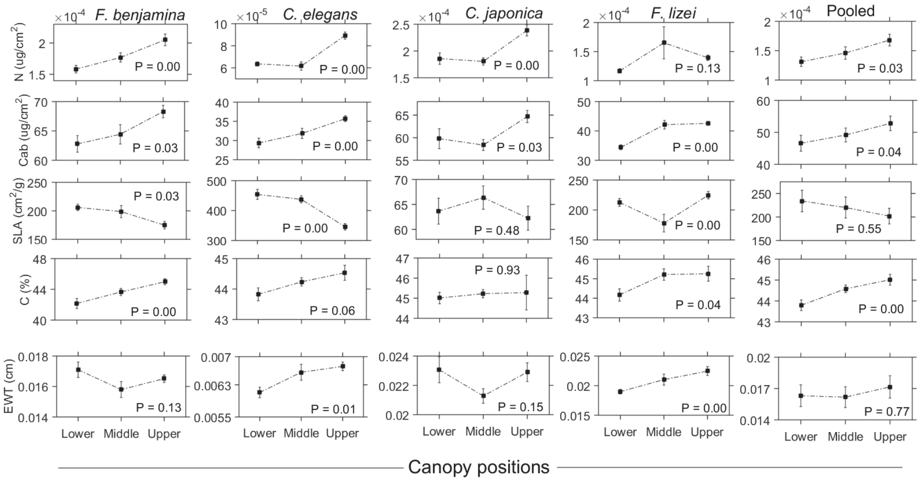

Figure 2.6 Graphical matrix showing variation in leaf functional traits across the vertical canopy profile for the studied species as well as for the pooled dataset (fifth column). Error bars represent standard errors.

2.3.3 Variation in leaf functional trait content across the vertical canopy profile

C_{ab}, N, and C demonstrated a significant ($P \leq 0.05$) ascending pattern in order of lower > middle > upper canopy layers for individual species as well as the pooled dataset (Fig 2.6). This demonstrated that upper canopy leaves contained higher trait content than shaded lower canopy leaves. Among all, it was noted that *F. lizei* demonstrated a contrasting pattern for N, with high foliar N values in the middle layer compared to the bottom and upper layer. SLA was observed to be generally lower in the upper canopy layers compared to middle and lower layers. Again it was noted that *F. lizei* demonstrated significantly ($P \leq 0.05$) low SLA values in the middle layer compared to the upper and lower layers. EWT exhibited contrasting patterns among species. For example, *C. elegans* and *F. lizei* demonstrated a significant ($P \leq 0.05$) increase in EWT values in the order of lower > middle > upper. In contrast, *C. Japonica* and *F. Benjamina* demonstrated low EWT values in the middle layer compared to bottom and upper canopy layers. Details of leaf traits comparison across the canopy at the species level and pooled dataset based on the *Tukey* HSD *post hoc* test are shown in Table 2.2. Prominent variability in leaf traits existed between the upper and lower layers of the canopy than any other canopy layer pair.

2.3.4 Discriminating leaf samples into respective canopy positions groups

Leaf samples were successfully discriminated into their defined vertical canopy position groups with an overall accuracy of 64 % based on nine (9) latent variables (Table 2.3) using PLS-DA.

Table 2.3 PLS-DA model calibration and performance.

Model				Internal Validation	External Validation
N	Ncal	Nval	nlv	Accuracy (%) (S.D)	Accuracy (%)
120	84	36	9	72 (8.3)	64

N is total number of samples, Ncal is number of samples used for calibration, Nval is the number of samples used for validation and nlv is the number of latent variables, accuracy is the overall accuracy (%) while SD is the standard deviation

Key wavebands that were influential in the spectral discrimination of leaf samples into their defined vertical canopy position groups were identified as 400–761, 1372–1407, 1902–1989 and 2106–2170 nm (Fig 2.7). These wavebands had VIP scores greater than the significant threshold of one (1)—demonstrating the strong influence on the classification procedure. Highly influential spectral wavebands (i.e., with VIP score > 2) were identified in the visible spectrum (around 507 nm) and in the red-edge spectrum (around 721 nm). Other influential spectral wavebands matched with wavelength regions of known leaf water (1372–1407) and as well as SLA and N (1902–1989 and 2106–2170 nm) absorption features. The influential wavebands (VIP score >

1) exhibit key wavebands in the discrimination of leaf samples into the three vertical canopy positions.

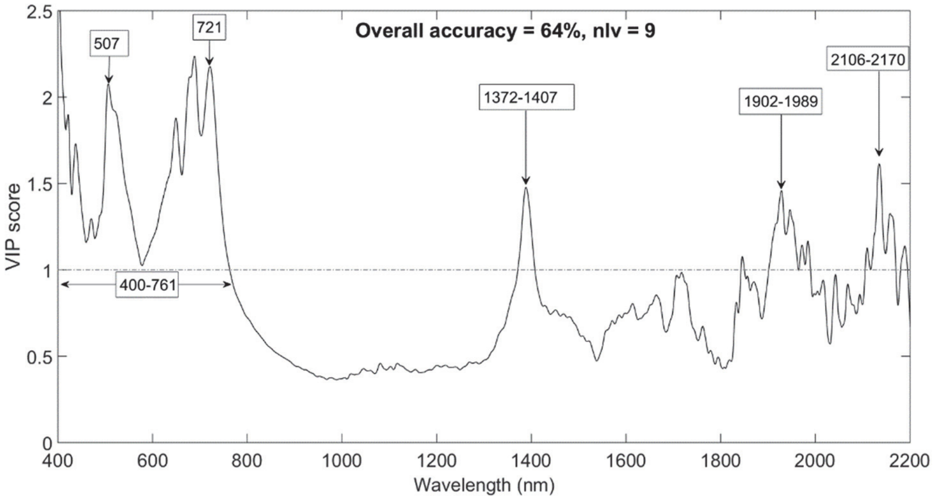

Figure 2.7 Key wavelengths that enhance leaf sample discrimination. Canopy position was used as the discriminant factor.

2.4 Discussion

2.4.1 Effect of canopy position on leaf spectral properties and leaf traits

In this study, we explored the impact of vertical canopy position on leaf spectral properties and subsequently leaf traits on multiple species across the entire spectrum. We report discrepancies in leaf spectral properties across the vertical canopy profile of multiple species indicating that leaf spectral properties reflect variability in leaf traits content within a canopy. Results from this study demonstrated that leaf spectra significantly ($P \leq 0.05$) shifted to longer wavelengths in the 'red edge' spectrum (685–701 nm) when the data from four studied species were pooled (Fig 2.2 and 2.3). Spectral shifts in the 'red edge' spectrum reflected an increase in C_{ab} and N in the order of lower > middle > upper canopy layers observed in Fig 2.6 and Table 2.2 for the pooled dataset. Although earlier studies have also demonstrated that wavelengths in the 'red-edge' spectral region are sensitive to variations in C_{ab} and foliar N content (Clevers and Gitelson, 2013; Li *et al.*, 2014; Mutanga and Skidmore, 2007), however spectral shifts in the red edge across vertical canopy profile were not examined. Results observed in the "red edge' spectrum are related to Ma and Upadhyaya (2018) who demonstrated that reflectance at 730 nm for the upper canopy leaves was significantly lower compared to the lower shaded leaves. However, Ma and Upadhyaya (2018) did not use the full leaf spectrum but focused on optical properties variations at 660 and 730 nm only. In the visible spectrum, mean leaf spectral reflectance decreased in the order of lower > middle > upper canopy layers (Fig 2.2). This ascending pattern in leaf spectral reflectance in the visible spectrum concurred with the significant increase in C_{ab} and N content from the lower to the upper canopy observed in Fig 2.6 for the pooled dataset. The leaf spectral reflectance pattern observed in the visible spectrum concur with results obtained by Yu *et al*. (2015) in a study performed in pepper plants. However, the spectral discrepancies in the visible spectrum of the pepper plants were only related to measured foliar N as a suite of other traits were not measured. Allocating more foliar N and C_{ab} to the upper canopy leaves is known to improve plant photosynthetic capacity and light use efficiency by 20% and 30% respectively (Homolová *et al.*, 2013). Our observation demonstrates the ability of leaf spectral properties to track variation in foliar nutrients particularly C_{ab} and N across the vertical canopy profile.

Leaf spectra for all the studied species were consistently higher for the lower canopy layer compared to the upper and middle canopy layers in the visible spectrum (Fig 2.4). The spectral discrepancy in the visible spectrum reflected a significant increase in C_{ab} and N from the lower to the upper canopy for almost all the species studied (Fig 2.6). However, *C. japonica* exhibited a small change in spectral reflectance in the visible spectrum. This could be explained by the more open canopy characterizing the *C. Japonica* canopy, which allows more light to reach the lower canopy layers. Anten and Ackerly (2001) observed that defoliation in *C. elegans* canopies significantly increased C_{ab} and subsequently light-saturated photosynthesis per unit leaf area for the newly exposed leaves. Contrary to the spectral patterns observed in the visible spectrum in our study, Khavaninzadeh *et al*.(2015), observed that leaf reflectance measured using a three band RGB camera increased significantly from the lower to upper canopy in a study conducted in an area characterized by high levels of air pollution. In this regard, changes in leaf optical patterns as a function of canopy height can be used as a proxy of vegetation strain to stress factors such as air pollution.

Results from our study demonstrated that only *C. elegans* leaf spectral reflectance (Fig 2.4D) increased concomitantly with its SLA (Fig 2.6) which may be explained by the species ability to adjust traits content across their vertical canopy profile (Chazdon, 1986). Generally, spectral analysis at species-specific level revealed significant spectral discrepancies outside the visible and 'red edge' spectral regions (Fig 2.5A). The spectral discrepancies in the NIR and SWIR varied among species, resulting in species-dependent leaf spectral properties across the vertical canopy profile. Variation in spectral response between species can be explained by different growth strategies employed by plants which potentially influence the allocation and immobilization of leaf traits across the canopy profile. However, the trend observed for N and SLA absorption features (centered on 2000 nm) especially between the lower and upper canopy layers was more or less similar across all species (Fig 2.5).

Influential wavebands in the spectral separatibility of leaf samples demonstrated the ability of leaf optical properties to track variation in leaf traits across the vertical canopy profile (Fig 2.7). Spectral wavebands between 400–761 nm, especially the more pronounced peaks (i.e., VIP scores > 2) in the visible spectrum (507 nm) and red edge spectrum (721 nm) are known to be strongly influenced by foliar C_{ab} and N (Curran, 1989; Li *et al.*, 2014). The 1372–1407 nm spectral wavebands are sensitive to leaf water content (EWT), while variation in the SWIR 1902–1989 nm and 2106–2170 nm have been identified to be sensitive to protein, N, dry matter and its reciprocal SLA (Ali *et al.*, 2016). These observations imply that leaf traits do not only vary with the phenological stage of a plant (Meerdink *et al.*, 2016), but also with the light environment (micro climate) within the vertical canopy profile (Coble *et al.*, 2016b). The position of a leaf within the canopy especially between sunlit and shaded leaves is known to influence the concentration of leaf traits such as N, C, and SLA, which are strongly related to the photosynthetic capacity of vegetation (Li *et al.*, 2013). The spectral match observed between key wavebands in leaf samples discrimination and spectral absorption features of leaf traits across the vertical canopy profile demonstrated that leaf spectral reflectance has the ability to explain the impact of vertical canopy profile on leaf traits. High influential wavebands match wavelength regions of C_{ab}, EWT, and N absorption features.

The vertical heterogeneity in leaf traits can be explained by two ecological mechanisms i.e., the optimization and coordination theories. The optimization theory (Hirose and Werger, 1987) explains that plants develop an intrinsic mechanism to allocate more N to the upper illuminated leaves which receive the highest photon flux density compared to lower shaded leaves (Li *et al.*, 2013). This mechanism optimizes total canopy photosynthetic as nitrogen-rich (30–50% N) enzyme i.e., ribulose-1.5-biphosphate (RuBP) carboxylase and phenolyenolpyruvate (PEP) responsible for carbon fixation in C3 and C4 plants respectively are deployed to commensurate light conditions within the canopy. Upper canopy leaves are therefore characterized by a higher density of mitochondria per cell area (Tissue *et al.*, 2002) and increased rates of carbon gain (Weerasinghe *et al.*, 2014) to support increased metabolic demands. The coordination theory further explains that the vertical heterogeneity in leaf traits especially N is an attempt by plants to maintain a balance between the Rubisco-limited rate of carboxylation (Wc) and electron transport-limited rate of carboxylation (W_j) (Chen *et al.*, 1993). The driving force for the allocation of N within a canopy is the variation between leaf N content at a given time and the leaf N content that is required to bring W_c and W_j into a balance (Chen *et al.*, 1993; Li *et al.*, 2013). The ascending pattern in leaf traits content may also be attributed to the interaction between leaf age and light acclimatization. Previous studies demonstrate that in fast-growing and broad-leaf evergreen species newly developing foliage often overshadow older leaves resulting in marked changes in light availability to older leaves and subsequently affecting leaf biochemical properties (Niinemets, 2007). In addition, shading is also known to result in accelerated ageing, senescence and increased leaf turnover (Hikosaka, 2005). Leaf senescence in the lower canopy induces re-mobilization of foliar nutrients particularly N to the upper canopy leaves. Moreover, Hikosaka and Hirose (2000) observed that leaf N and photosynthetic capacity decrease with leaf life span in *C. japonica* canopies. This mechanism results in an increased gradient in leaf traits content across the vertical canopy profile (Kull and Kruijt, 1999). As such, this study demonstrated that leaf spectral properties track dynamics in leaf traits across the vertical canopy profile as observed in Fig 2.7. Significant variations in the spectrum were observed especially in the red edge spectrum for the pooled dataset. This observation is consistent with our understanding of leaf physiology within plant canopies.

2.4.2 Implication to remote sensing of plant traits

Our results have important implications on within-canopy sampling and scaling up strategies of leaf traits to canopy and landscape scales, especially for studies that are conducted in environments where foliage material from the lower canopy influences canopy reflectance. This study put into perspective upscaling methods such as the direct extrapolation (He and Mui, 2010a) that apply leaf traits-spectra relationship observed at leaf level to canopy scale by assuming that all leaves within a plant canopy have the same trait content (Peterson *et al.*, 1988). Our results indicate that leaf samples from different canopy layers exhibit different traits content and are subsequently spectrally distinct. This observation implies that failure to account for the vertical heterogeneity in key traits across the vertical canopy profile can potentially lead to considerable inaccuracies in leaf traits upscaling and subsequently leaf traits estimation especially at canopy scale (Luo *et al.*, 2016). For example, a recent study by Coble *et al*. (2016b) demonstrated that canopy photosynthesis estimated from models that do not account for the vertical variation in leaf traits, particularly N and dry matter content, overestimated the canopy photosynthesis by over 60%. However, before exploring the effect of vertical heterogeneity on the leaf to canopy upscaling approaches, it is imperative to understand the spectra-traits interaction at leaf level. Leaf spectra-traits interaction at leaf level provides an opportunity to understand the mechanism without the influence of canopy structure [i.e., leaf area index (LAI), canopy height, etc.], soil background and viewing geometry on the spectral reflectance (Wang *et al.*, 2017). An improved understanding on the effect of vertical heterogeneity of traits on spectral properties across the vertical canopy profile is also critical in improving our understanding, designing and parameterization of robust multi-layer RTM that is able to simulate canopy reflectance with minimal error (Wang and Li, 2013). Improving the design and performance of such models requires the understanding and ability to disentangle and quantify the relative contribution of each canopy layer to the top of canopy reflectance. This study also has implications for studies that aim to integrate hyperspectral measurements and LiDAR data to understand the three dimensional (3D) variability in leaf traits across vegetation canopies (Zhu *et al.*, 2017).

2.5 Conclusions

The effect of vertical canopy position on leaf spectral properties and leaf traits content across multiple species is not well documented. In this study, we examined the effect of vertical canopy position on leaf traits and leaf spectral properties across multiple species. We also assessed the ability of leaf optical properties to track variability in leaf traits across the vertical canopy profile. Results of this study demonstrate that vertical canopy position is a significant source of variation in leaf spectral properties and traits content. We observed that leaf spectra significantly shifted to longer wavelengths in the 'red edge' spectrum when data from all species were pooled together. The spectral shift reflected an increase in leaf traits content especially C_{ab} and N in the order of lower > middle > upper canopy layers. At species-specific level leaf, spectral responses outside the visible spectrum varied, resulting in species-dependent leaf spectral properties across the vertical canopy profile. Key wavebands that are influential in the discrimination of leaf samples into their defined canopy positions match wavelength regions of C_{ab}, EWT, SLA, and N absorption features-which significantly varied across the vertical canopy profile. This observation demonstrated the capability of leaf optical properties to track variability in leaf traits across the vertical canopy profile. We, therefore, conclude that changes in foliar nutrients translate into changes in vegetation spectral properties across the vertical canopy profile. These findings have implications on within-canopy sampling, leaf traits upscaling, interpretation and use of data in species trait databases. Future studies should aim to understand how the vertical heterogeneity in leaf traits affects the estimation of plant traits from hyperspectral measurements at canopy scale.

Chapter 3

Leaf position within a canopy affects the performance of PROSPECT in retrieval of leaf traits throughout the growing season[*]

---

[*] This chapter is based on Gara, T.W., Darvishzadeh, R., Skidmore, A. K., Wang, T and Huerich, M. (2019) Evaluating the performance of PROSPECT in retrieval of leaf traits throughout the growing season. *International Journal of Applied Earth Observation and Geoinformation 83: 101919.*

Abstract

Leaf traits and subsequently leaf spectral properties depend on leaf phenological stage and light conditions within a canopy. The PROSPECT radiative transfer model has been extensively and successfully used to retrieve leaf traits for mature, sunlit leaves at peak vegetation growth, i.e. summer. However, research on the quantification of leaf traits using PROSPECT across the canopy vertical profile throughout the growing season is still lacking. Therefore, this study aims at examining the effect of leaf position on the performance of the PROSPECT model in modelling leaf optical properties and retrieving leaf chlorophyll content (C_{ab}), equivalent water thickness (EWT), and leaf mass per area (LMA) throughout the growing season. To achieve this objective, we collected 588 leaf samples from the upper and lower canopies of deciduous stands over three seasons (i.e., spring, summer and autumn) in Bavaria Forest National Park, Germany. Leaf traits including C_{ab}, EWT and LMA, were measured for all the samples, and their reflectance spectra were obtained using an ASD FieldSpec-3 Pro FR spectroradiometer coupled with an Integrating Sphere. We subsequently inverted the PROSPECT model to retrieved C_{ab}, EWT and LMA using the look-up-table (LUT) approach. Our results consistently demonstrated that leaf samples collected from the lower canopy achieved a stronger match between measured and PROSPECT simulated reflectance spectra, especially in the NIR spectrum compared to leaf samples collected from the upper canopy throughout the growing season. This observation concurred with the pattern of C_{ab} and EWT retrieval accuracies across the canopy i.e. the retrieval accuracy for the lower canopy was consistently higher (NRMSE = 0.1-0.2 for C_{ab}; NRMSE = 0.125-0.16 for EWT) when compared to the upper canopy (NRMSE = 0.122 - 0.269 for C_{ab}; NRMSE = 0.162 -0.0.258 for EWT) across all seasons. In contrast, LMA retrieval accuracies for the upper canopy (NRMSE = 0.146 - 0.184) were higher compared to the lower canopy (NRMSE = 0.162 - 0.239) for all seasons except for the spring season. For all the leaf traits examined in this study, the range in retrieval accuracy between the upper and lower canopy was greater in summer (compared to other seasons). We report for the first time that although the PROSPECT model provides reasonable retrieval accuracy of C_{ab}, EWT and LMA, variations in leaf biochemistry and morphology through the vertical canopy profile affects the performance of the model over the growing season. Findings of this study have important implications on field sampling protocols and upscaling leaf traits to canopy and landscape level using multi-layered physical models coupled with PROSPECT.

3.1 Introduction

Plants traits, such as leaf chlorophyll content (C_{ab}), leaf mass per area (LMA) and equivalent water thickness (EWT) play a key role in understanding ecosystem functional processes, such as primary productivity and nutrient cycling. Specifically, C_{ab} is a key bio-indicator of plant health and photosynthetic capacity (Evans and Poorter, 2001; Lichtenthaler *et al.*, 1996), while LMA reflects the plant economic spectrum strategy with regard to nutrients uptake, light harvesting and carbon sequestration (Poorter *et al.*, 2009). EWT, on the other hand, provides information on plant water status (Yao *et al.*, 2014). Consequently, routine measurement of leaf traits is valuable to assess progress towards the Aichi Biodiversity Targets set by the Convention on Biological Diversity (CBD) (Pereira *et al.*, 2013; Skidmore *et al.*, 2015).

Leaf traits and their leaf spectral properties are strongly controlled by leaf phenological stage and light conditions within a canopy (Yang *et al.*, 2016). Leaf traits are known to change as a function of time during the growing season within a year (Behrman *et al.*, 2015). Moreover, changes in abiotic factors, such as temperature, rainfall and photo-period result in changes in the leaf physiological, biochemical and morphological traits (Coble *et al.*, 2016a). However, leaf traits do not only exhibit seasonal changes but also changes as a result of different light conditions such as between the sunlit, upper and shaded lower canopy (Gara *et al.*, 2018a). Illuminated upper canopy leaves display higher nutrient stoichiometry when compared to shaded lower canopy leaves (Weerasinghe *et al.*, 2014). For example, Yang *et al*. (2016) demonstrated that shaded leaves display lower C_{ab}, nitrogen and LMA when compared to sunlit leaves. The variation in leaf traits across the canopy vertical profile is important in maintaining an equilibrium between the ribulose-1.5-bisphosphate (RuBP) - limited rate of carboxylation and the electron transport - limited rate of carboxylation (Chen *et al.*, 1993). These intrinsic mechanisms result in marked effects on leaf morphological, chemical as well as physiological traits across the canopy vertical profile and subsequently result in variations in leaf optical properties (Qiu *et al.*, 2018). Plants are also known to translocate foliar nutrients as leaves age, moving nutrients from lower canopy leaves to the upper canopy leaves for protein repair and maintenance of a metabolic balance (Hikosaka, 2005). In this regard, capturing seasonal variations in leaf traits throughout the vertical canopy profile is critical for understanding dynamics in terrestrial ecosystem structure and functioning.

Several leaf traits databases aimed at understanding forest structure and functioning have been established based on *in situ* and *in vivo* trait measurements (Kattge *et al.*, 2011; Poschlod *et al.*, 2003). Although these conventional methods provide accurate measurements, they are expensive, time-consuming and particularly challenging for quick and repeated measurements. Field spectroscopy, on the other hand, has a capacity to augment conventional methods by indirectly retrieving leaf traits from spectral measurements (Carvalho *et al.*, 2013). This approach is cost-effective and allows repeated assessments over time with a capacity to upscale to airborne and satellite imagery. Essentially two approaches, empirical (statistical) and physical models (radiative transfer models-RTM) are employed to establish a relationship between leaf traits and spectral measurements (Verrelst *et al.*, 2015a). Empirical models explore parametric and non-parametric statistical relationship between leaf traits and vegetation spectra or derivatives such as vegetation indices (Darvishzadeh *et al.*, 2012). Although statistical models are relatively easy to calibrate, they are associated with challenges of transferability because in most instances the relationship between spectral data and leaf traits is sensor, site, time, and biome dependent (Verrelst *et al.*, 2014). Moreover the performance of statistical models can be affected by the representativeness of the set of reference samples used for calibration (Pasolli *et al.*, 2015). The development of physical models or radiative transfer models (RTMs) on the other hand has improved our understanding of the interaction between radiation and foliage material. Physical models, rigorously simulate light absorption and scattering based on radiation transfer theory and are thus transferable across sites and biomes (Homolová *et al.*, 2013). However, the main challenge of physical models is that they often require a number of inputs for parameterization, which subsequently result in computation and model inversion sophistication (Zhang and Wang, 2015).

A number of RTMs have been developed to model leaf spectral properties and subsequently retrieve leaf traits through inversion. These models include PROSPECT (PROpriétés SPECTrales) (Feret *et al.*, 2008; Jacquemoud and Baret, 1990; Jacquemoud *et al.*, 1996), LIBERTY (Leaf Incorporating Biochemistry Exhibiting Reflectance and Transmittance Yields) (Dawson *et al.*, 1998), N flux models (Allen and Richardson, 1968), ray tracing models (Govaerts and Verstraete, 1998) and stochastic models (Maier *et al.*, 1999). Most of these physical models except PROSPECT have received relatively limited use within the vegetation spectroscopy community. This is mainly because they require a large number of input variables that are laborious and time consuming to measure and subsequently pose a challenge in model inversion. The PROSPECT model has been widely used to retrieve leaf traits from simulated hemispherical reflectance and transmittance spectra in different vegetation communities (Barry *et al.*, 2009; Malenovský *et al.*, 2006; Renzullo *et al.*, 2006; Zhang *et al.*, 2007). One advantage of the PROSPECT model is that it can be intricately coupled with canopy radiative models, such as SAILH to retrieve leaf traits at canopy and landscape level (Si *et al.*, 2012; Tripathi *et al.*, 2012; Verhoef, 1984). In spite of its popularity, robustness and transferability, studies that have examined the effect of leaf position on the performance of PROSPECT in modelling leaf spectral properties and retrieval of leaf traits throughout the growing season are lacking. Although an attempt to retrieve C_{ab} through the vertical canopy profile using the PROSPECT model was demonstrated by Demarez (1999) and Zhang *et al*. (2007), very little is known on how the PROSPECT model perform with regard to retrieval of other key radiation absorbers, i.e. LMA and EWT across the canopy and throughout the growing season. More specifically, no study has attempted to evaluate the effect of leaf position within a canopy on the modelling of leaf spectral properties across a growing season using PROSPECT. Previous studies have mainly focused on the retrieval of leaf traits for mature, sunlit leaves at peak vegetation growth, i.e. summer (Ali *et al.*, 2016; Wang *et al.*, 2015b). Therefore, this study sought to examine the effect of leaf position within a canopy on the performance of the PROSPECT model in modelling leaf optical properties and retrieval of leaf traits, specifically chlorophyll content (C_{ab}), equivalent water thickness (EWT) and leaf mass per area (LMA) across throughout the growing season.

3.2 Materials and methods

3.2.1 Study area and field data collection

To examine the effect of leaf position within a canopy on the performance of PROSPECT for modelling leaf spectral properties and retrieving leaf traits across the canopy throughout the growing season, we collected leaf samples from Bavarian Forest National Park (Fig 3.1). The Park is part of the Bohemian forest ecosystem and is located in south-eastern Germany ($49^{o}31'19"$N and $13^{o}12'9"$N). The Park covers a total area of approximately 24 218 ha. Elevation stretches from 600 to 1453 m (Heurich *et al.*, 2010a). The climate is temperate with annual precipitation ranging from 1200 to 1800 mm (of which approximately 50% is snow), and a mean annual temperature of between three (3) and 6^{o} C. The Park is characterized by acidic and poor nutrient soil. The dominated tree species in the park are mainly the evergreen Norway spruce (*Picea abies*) (67%) and deciduous European beech (Fagus sylvatica) (24.5%). Other less dominant species include white fir (*Abies abies*) (2.6%), sycamore maple (*Acer pseudoplatanus*) (1.2%), and mountain ash (*Sorbus aucuparia*) (3.1%) (Cailleret *et al.*, 2014).

Field data were collected for three seasons, i.e. spring, summer and autumn of 2017. Spring data were collected between mid-May and mid-June, while summer field data were collected from mid-July to mid-August, and the autumn field data were collected between mid-September and mid-October. Sampling sites were randomly generated in deciduous and mixed vegetation stands based on the vegetation map provided by the Department of Conservation and Research, Bavarian Forest National Park (Silveyra Gonzalez *et al.*, 2018). Most of the sample plots were located along the permanent transects designed for

Biodiversity Research (Fig 3.1). In the field, we used a hand-held Global Positioning System with an error of ±5m to navigate to the sampling sites. At each sampling site, a north-oriented plot of 30 m × 30 m was demarcated using a tape measure. We also recorded the centre location of each plot, using a Leica GPS 1200 (at an accuracy of less than 1 m after post-processing).

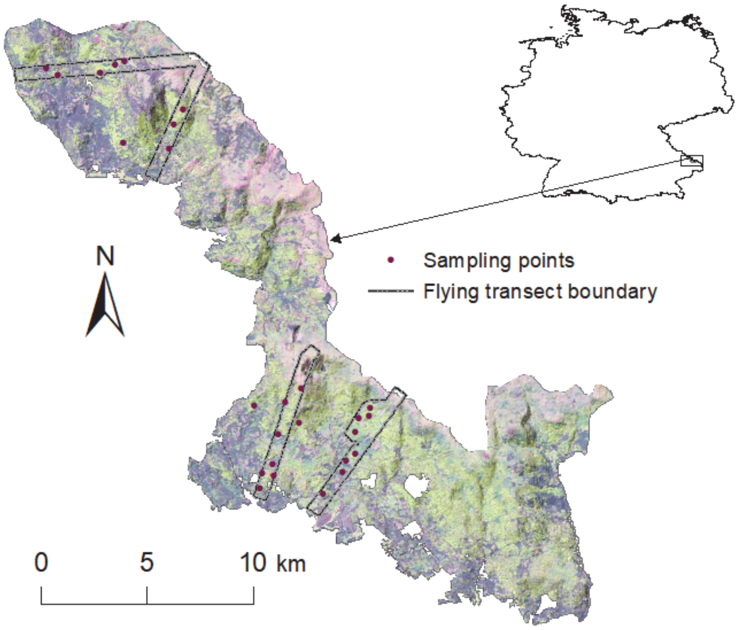

Figure 3.1 Map of the Bavaria Forest National park and the location of the park in Germany. Sampling points are overlaid on a natural colour composite of Sentinel-2 satellite imagery of 13 July 2017. Black lines are the permanent flying transects boundaries designed for biodiversity research.

In total 588 leaf samples were collected from twenty-six deciduous and mixed vegetation sample plots across the three seasons. Species name and sample sizes for each season are shown in Table 3.1. Leaf samples were separately collected from the upper (n = 294) and lower canopy (n = 294) of each sampled tree. The average height of sampled trees was 24.4±7.52 m (measured using a Nikon Forestry 550 hypsometer). Leaf samples from the sunlit, upper canopy were shot from the top one meter canopy using a crossbow, whilst leaf samples from the lower canopy were collected from the shaded, lowest living branch of the canopy using an extendable pair of secateurs (Arellano *et al.*, 2017; Atherton *et al.*, 2017). Sampling was performed on three to five trees with a diameter at breast height greater than 10 cm. A marker was placed on each sampled tree to facilitate tree identification for subsequent seasonal field measurements. Collected leaf samples were immediately measured for C_{ab} using CCM-300 chlorophyll content meter (Opti-Sciences, 2011). The leaf samples were then wrapped with moist paper towels and zip-locked in polythene bags. The leaf samples were then transported in a cooler with ice packs within 6 hours to the laboratory for further measurements (Atherton *et al.*, 2017). Although the composition of our samples were heavily skewed to the European beech (92.86%), analysis with or without the other collected species (constituting 7.14%) did not alter the pattern in leaf traits retrieval accuracy across the canopy throughout the growing season (Appendix: Table A1). Therefore, all analyses were performed including all the species.

Table 3.1 Distribution of collected samples by species across the three seasons

Species	Scientific name	Spring	Summer	Autumn	Total
European beech	*Fagus sylvatica*	156	194	196	546
Sycamore maple	*Acer pseudoplatanus*	6	12	12	30
Elm *spp*	*Ulmus minor*	2	2	2	6
Common rowan	*Sorbus aucuparia*	2	2	2	6
Total		**166**	**210**	**212**	**588**

3.2.2 Laboratory measurement

3.2.3 Leaf trait measurements

The following leaf traits were measured in the laboratory; fresh weight (Fw g), dry weight (Dw g) and leaf surface area (LA). Fresh weight for each sample was determined, using a high precision digital scale at an accuracy of 0.01g. The leaf samples were then scanned, using AMH 350 area meter to determine the leaf surface area (ADC-BioScientific, 2013). The leaf samples were oven dried at 65°C until a constant weight was attained after approximately 72 hours and then their dry weight was measured (Gara *et al.*, 2018b). Subsequently, EWT and LMA were calculated using the following formula:

$$\text{EWT (cm)} = \text{Fw} - \text{Dw}/\text{LA} \tag{3.1}$$

$$\text{LMA (g/cm}^2\text{)} = \text{Fw}/\text{LA} \tag{3.2}$$

where: Dw, Fw and LA are the dry weight, fresh weight and leaf area of each sample, respectively. The summary and variation of measured traits are shown in Fig 3.2.

3.2.4 Leaf reflectance spectra measurement

Leaf directional hemispherical reflectance from 350 to 2500 nm for each sample was measured, using an ASD FieldSpec-3 Pro FR spectroradiometer coupled with an ASD RTS-3ZC Integrating Sphere. To minimize spectral noise, the spectroradiometer was set to average two hundred scans into a single spectrum per each spectral measurement (Ali *et al.*, 2016). Radiance measurements were converted to reflectance against scans of a calibrated white spectralon panel (with approximately 99% reflectance). During spectral measurements, care was taken to avoid leaf primary veins. The spectral reflectance measurements were corrected for dark current and stray light following the Integrating Sphere User Manual instructions (ASD, 2008). Spectral measurements of 5-10 leaves (depending on leaf size and weight) constituting a sample were averaged to a single spectrum to represent the sample. A moving second order Savitzky-Golay filter with a frame size of 11 was applied to each sample reflectance spectra to minimize instrument noise (Savitzky and Golay, 1964). Due to the low signal-to-noise ratio for wavelengths beyond 2200 nm as well as spectral bands before 400 nm, the reflectance spectra were cropped to 400–2200 nm range. Therefore, 1801 spectral bands were retained for further analysis. All required laboratory measurements were completed on the same day of sample collection.

3.2.5 Calibration of the PROSPECT model

The PROSPECT leaf optical properties model is a radiative transfer plate model for simulating leaf directional-hemispherical reflectance over the optical domain of 400-2500 nm (Jacquemoud and Baret, 1990). The PROSPECT model idealizes a leaf as elementary layers characterized by absorbing and scattering properties (Feret *et al.*, 2008). The model requires four input parameters including leaf structure index (N_{struc}), leaf chlorophyll content (C_{ab}, µg/cm^2), leaf water content (EWT, cm) and leaf dry matter content (LMA, g/cm^2). PROSPECT has been widely validated for the retrieval of leaf traits across a variety of species especially for mature, sunlit leaf samples at peak vegetation growth, i.e. summer (Ali *et al.*, 2016; Li and Wang, 2013b; Malenovský *et al.*, 2006; Wang *et al.*, 2015a). However, in this study we assess the effect of leaf position in the vertical canopy profile on the performance of PROSPECT for modelling leaf spectral properties and retrieval of leaf traits across canopy positions through a growing season. To achieved a higher accuracy in the retrieval of inputs parameters the dimension of the LUT has to be sufficiently large (Combal *et al.*, 2003; Tang *et al.*, 2007).

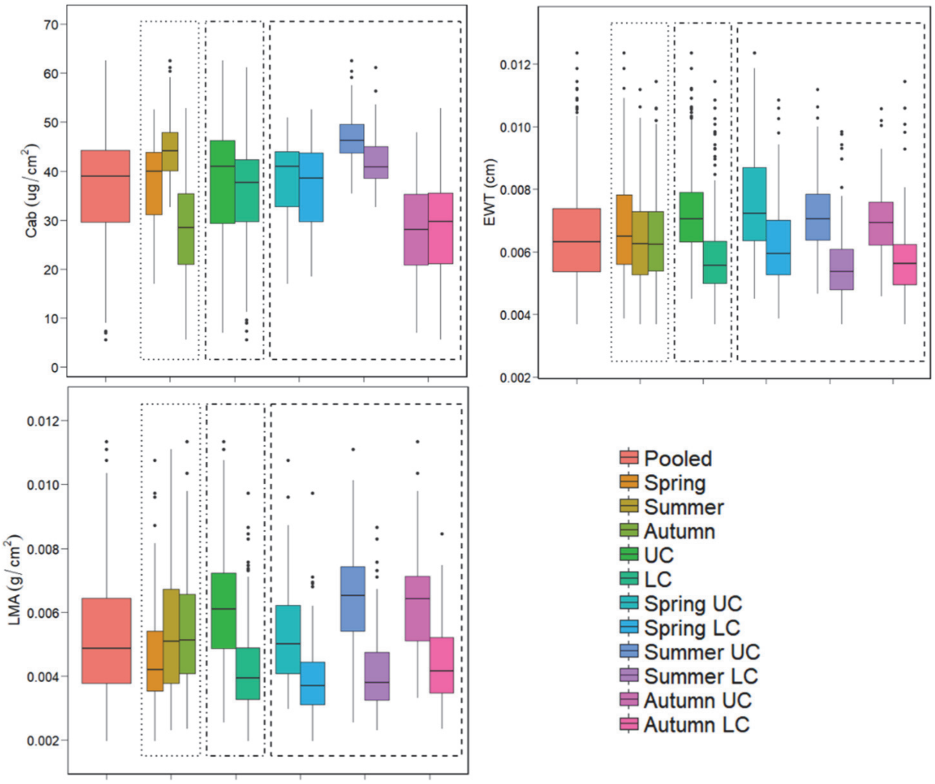

Figure 3.2 Seasonal variation in measured C_{ab}, LMA and EWT across canopy positions (UC and LC represent upper and lower canopy respectively)

We therefore used the improved (1 nm) and recalibrated PROSPECT 4 model (Feret *et al.*, 2008) in forward mode to generate a LUT with 250 000 leaf spectral reflectance simulations. We used PROSPECT 4 instead of later versions because we did not measure leaf carotenoid and anthocyanins content, which are input parameters in PROSPECT 5 and PROSPECT D (Feret *et al.*, 2008; Féret *et al.*, 2017). The ranges of the PROSPECT input variables (Table 3.2) were selected guided by prior information gathered from field-collected data. Specifically, the range of input parameters used for PROSPECT calibration were based on field collected data widened by 10% of their respective means. In order to preserve a relationship that existed between field-measured LMA and EWT ($r = 0.66$, $p = 0.00$, Fig 3.3), the PROSPECT model was run by generating input variables (LMA and EWT) using a multivariate normal distribution function based on the mean and covariance matrix of their field measured values. For the N structure index, we used the same range presented by Ali *et al*. (2016) who retrieved N for similar species in the same study area. It is often a prerequisite to calibrate the physical and optical constants, such as refractive index and absorption coefficients of the PROSPECT model to the target experimental data. However, in this study, we validated the suitability of the original PROSPECT model to simulate field measured reflectance spectra by computing the RMSE between measured and simulated reflectance spectra. The generated RMSE (Fig 3.5a) was generally lower than reported in the literature (Feret *et al.*, 2008; Sun *et al.*, 2018). Therefore, we used the PROSPECT model without re-calibrating the physical and optical constants (Ali *et al.*, 2016).

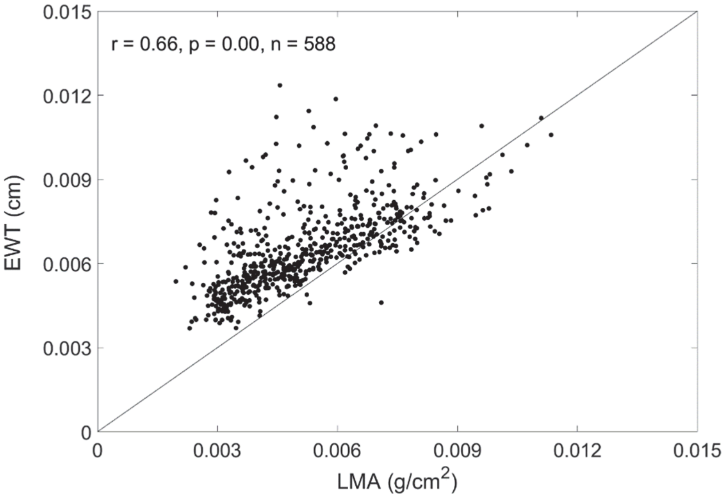

Figure 3.3 Correlation between EWT and LMA for field-collected data

Table 3.2: Ranges of the leaf variables used to build the LUT with the size of 250 000-reflectance spectra

Parameter	unit	min	max	mean	SD
Leaf structure parameter (N)	---	1	2.22	1.52	0.15
Total leaf chlorophyll content (C_{ab})	μg/cm^2	2	67	36.57	10.6
Equivalent water thickness (Cw)	cm	0.0025	0.015	0.0015	0.0066
Leaf mass per area (Cm)	g/cm^2	0.0015	0.014	0.0016	0.0053

3.3.1 Inversion of the PROSPECT model

There are a number of inversion approaches that can be used to assess the performance of RTMs in modelling leaf spectral reflectance and retrieving leaf traits. The main inversion methods are iterative optimization, neural networks and look-up table (LUT) (Sun *et al.*, 2018; Wang *et al.*, 2015a). Optimization algorithms and neural networks search for the 'best fit' between measured and simulated spectra by successive input variable iteration (Verrelst *et al.*, 2015a). The overall performance of optimization algorithms depends on the initial guess (Preidl and Doktor, 2011). The main challenge with optimization algorithms is that they computationally demanding and time-consuming when inverting large look-up tables. The LUT inversion approach on other hand is based on querying the LUT using a merit function (Liang, 2007). The function essentially minimize the summed difference between measured and simulated spectra across the selected wavelength. The LUT approach has an advantage over other inversion methods because it is computationally efficient and guarantee finding global minima (Rivera *et al.*, 2013; Sehgal *et al.*, 2016). Previous studies have also demonstrated that the inversion technique has a minor influence on the inversion results (Buddenbaum and Hill, 2015; Kimes *et al.*, 2000). The main factors that influence the performance of model inversion are the spectral range considered for target constituent and the signal to noise ratio of the spectra (Feret *et al.*, 2008). In this study, we therefore used the widely used LUT approach to assess the performance of the PROSPECT model in modelling leaf spectral properties and retrieval of leaf traits. The best match between simulated spectra to each measured reflectance spectra is determined by calculating and finding the lowest root mean square error (Eqn 3.3) of the unconstrained non-linear multivariate function (Darvishzadeh *et al.*, 2012). In practice, model inversion involves finding the parameter vector θ = [N, C_{ab}, LMA, EWT] that minimizes the merit function $J(\theta)$.

$$J(\theta) = \sqrt{\frac{\sum_{\lambda} \rho mes - \rho sim^2}{n}} \tag{3.3}$$

Where ρmes and ρsim are measured and simulated spectral reflectance respectively, n is the number of wavelengths (λ) i.e. 1801 used in this study. The selection of single best fitting spectra may not be the optimal strategy of inverting the LUT as this is prone to ill-poseness (Darvishzadeh *et al.*, 2012). In this study, we observed that using a single best fitting spectral or multiple solutions (i.e. mean of the best 10, 50 and 100 solutions) did not affect the pattern of leaf traits retrieval accuracy (Appendix: Fig A1-A3).

3.3.2 Model Performance Assessment

To assess the performance of the PROSPECT model inversion in simulating leaf spectral reflectance of leaf samples collected at different canopy positions, we examined the agreement between the measured and the best-match reflectance spectra simulated by the PROSPECT model using the root mean square error (RMSE). We also compared leaf traits retrieved from the PROSPECT model against the field-measured ones using the coefficient of determination (R^2), RMSE and normalized root mean square error (NRMSE = RMSE/range).

3.3 Results

3.3.1 PROSPECT performance in reflectance spectra simulation across canopy positions throughout the growing season

The effect of leaf position on the performance of LUT inversion was initially evaluated based on the agreement between simulated and measured reflectance spectra. Generally, the PROSPECT model inversion yielded reflectance spectra that closely matched the measured spectra for both the upper and lower canopy across all seasons and throughout the entire spectrum (Fig 3.4). However, some variation were observed, for example, there were relatively higher peaks of spectra mismatch in wavelengths 490-530, 700-789 and 1500-1680 and 1880-1895 nm for the pooled dataset (Fig 3.5a). Across seasons and canopy positions, the peak in the 490-530 nm spectrum was observed for the autumn dataset. The RMSE peak in the ‘red-edge’ spectrum remains prominent for all the three seasons, with the highest RMSE observed for spring followed by summer and then autumn seasons. High errors in the 1500-1680 nm wavelengths were observed across all seasons. The RMSE in the NIR were lowest in autumn and highest in spring (Fig 3.5b). The lower canopy demonstrated a better match between simulated and measured reflectance spectra compared to the upper canopy, especially in the NIR (800-1300; Fig 3.4, 3.5c) and SWIR across all seasons (Fig 3.5d-f). Spectral disagreement in the ‘red edge’ between the upper and lower canopy was higher in the spring (Fig 3.5d) and summer (Fig 3.5e) when compared to autumn (Fig 3.5f). A prominent spectral mismatch was observed in wavelengths centred at 515 nm for the autumn season, which is absent in spring and summer, respectively.

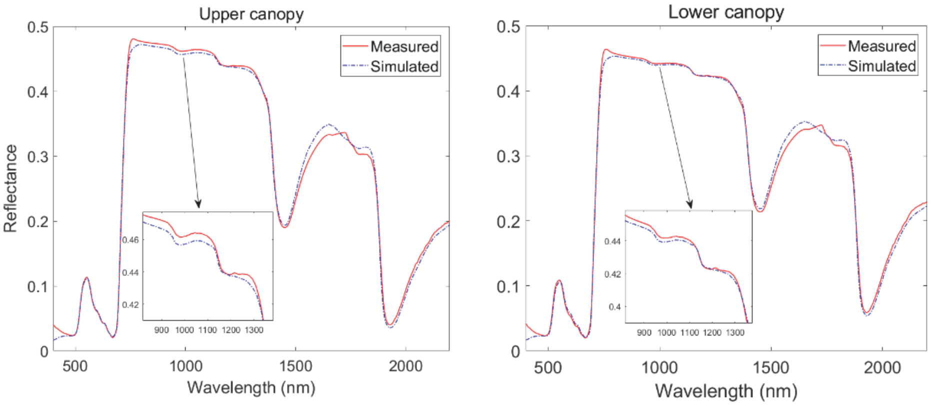

Figure 3.4 Mean measured and simulated leaf reflectance spectra for the upper and lower canopy for all samples used in the study. The spectral mismatch between measured and simulated reflectance is greater for the upper canopy compared to the lower canopy leaf samples (see inserts).

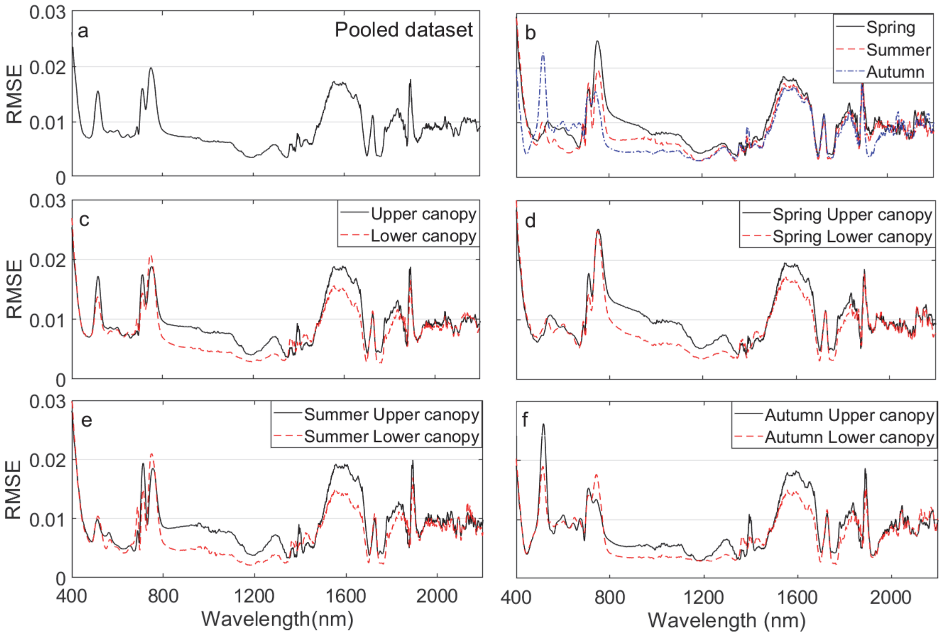

Figure 3.5 Variation in RMSE between measured and simulated leaf reflectance for pooled dataset (a), seasons (b), leaf position (c); and leaf position for spring (d), summer (e) and autumn (f).

3.3.2 PROSPECT performance in leaf traits retrieval across canopy positions throughout the growing season

Leaf traits retrieved via the PROSPECT model inversion were compared to leaf traits measured in the field. Results show that the retrieval accuracy for C_{ab} was higher for the lower canopy (NRMSE= 0.103) when compared to the upper canopy (NRMSE = 0.122) across all seasons (Fig 3.6). The retrieval accuracy of C_{ab} for the lower canopy consistently outperformed that of the upper canopy for each season. The difference in C_{ab} retrieval accuracy between upper canopy and lower canopy was small in spring (NRMSE = 0.209 and NRMSE = 0.2 for lower and upper canopy respectively) when compared to summer (NRMSE = 0.269 and NRMSE = 0.199 for lower and upper canopy respectively) and autumn (NRMSE = 0.1 and NRMSE = 0.14 for lower and upper canopy respectively respectively). Across seasons, C_{ab} was retrieved with higher accuracy in autumn (NRMSE = 0.112) when compared to spring (NRMSE = 0.195) and summer (NRMSE = 0.219).

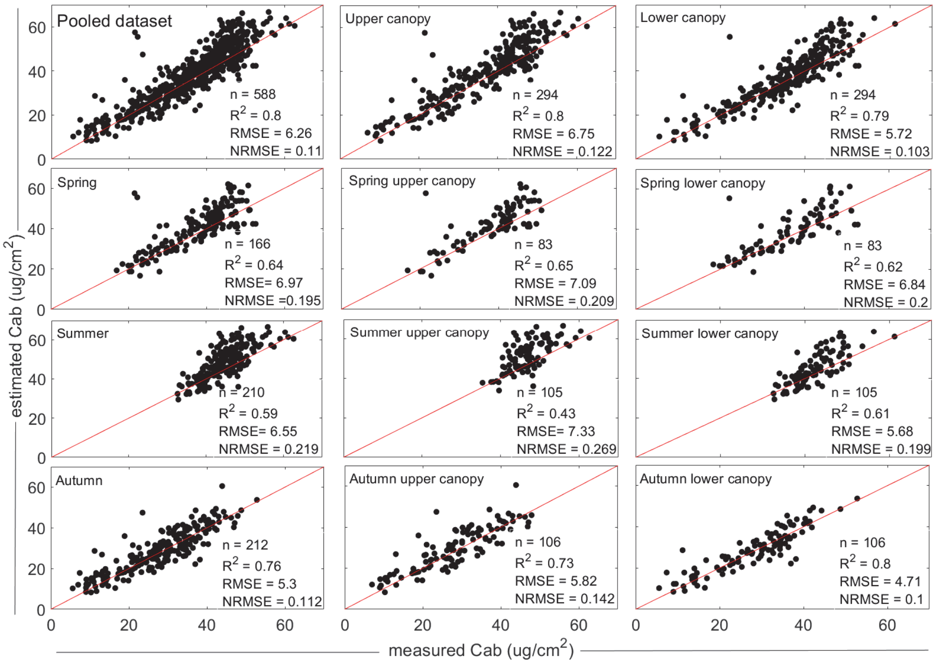

Figure 3.6 Retrieval accuracies of the leaf chlorophyll content (C_{ab}) across canopy positions throughout the growing season.

Results of the study show that EWT for the lower canopy was retrieved with higher accuracy (NRMSE = 0.125) when compared to the upper canopy (NRMSE = 0.188) across all seasons (Fig 3.7). Upper canopy EWT was retrieved with low accuracy (NRMSE = 0.162 for spring, NRMSE = 0.24 for summer and NRMSE = 0.258 for autumn) when compared to low canopy (NRMSE = 0.128 spring, NRMSE 0.16 = summer and NRMSE = 0.129 autumn) across all seasons. The difference in EWT retrieval accuracy between the upper and lower canopy widened as the season progressed with a huge difference observed in summer. Generally the retrieval accuracy of EWT was high in spring (NRMSE = 0.13), compared to summer (NRMSE = 0.172) and autumn (NRMSE = 0.168). The pattern of EWT retrieval accuracy between the upper and lower canopy follow a similar trend observed for C_{ab}.

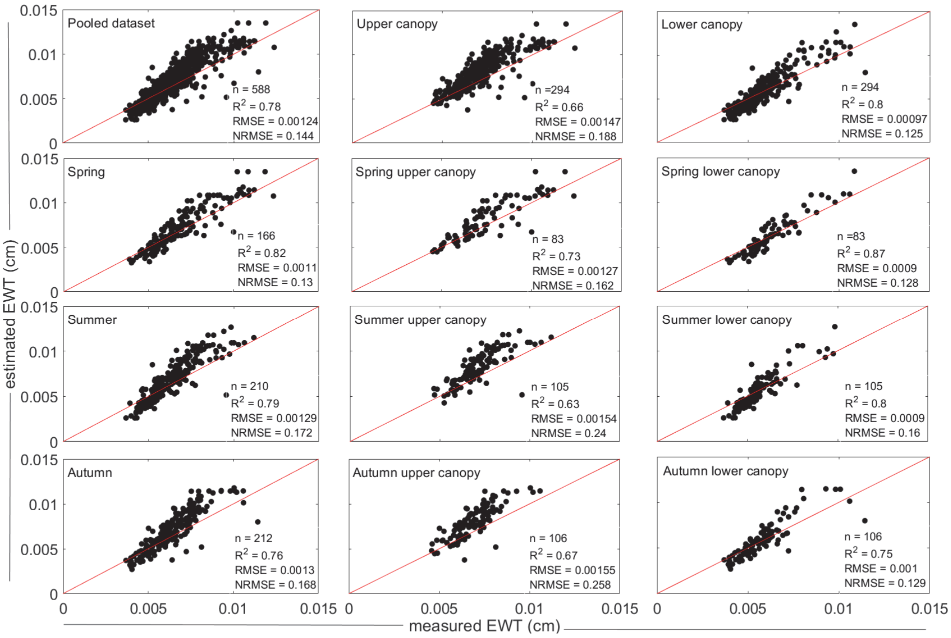

Figure 3.7 Retrieval accuracies of EWT across canopy positions throughout the growing season.

The retrieval accuracy for LMA was higher for the upper canopy (NRMSE = 0.154) compared to lower canopy (NRMSE = 0.176) across all seasons (Fig 3.8). A similar trend was also observed for summer (NRMSE = 0.146 and NRMSE= 0.213) and autumn (NRMSE = 0.174 and NRMSE = 0.239). In contrast, lower canopy LMA for spring was retrieved with higher accuracy (NRMSE = 0.162) when compared to the upper canopy (NRMSE = 0.184) for the same season. The difference in LMA retrieval accuracy between the upper canopy and the lower canopy was wide in summer and autumn compared to spring. Generally, LMA was retrieved with higher accuracy in summer (NRMSE = 0.148) when compared to spring (NRMSE = 0.154) and autumn (NRMSE = 0.158). The difference in retrieval accuracy of LMA across seasons was small however the summer season exhibited a better fit (R^2 = 0.82).

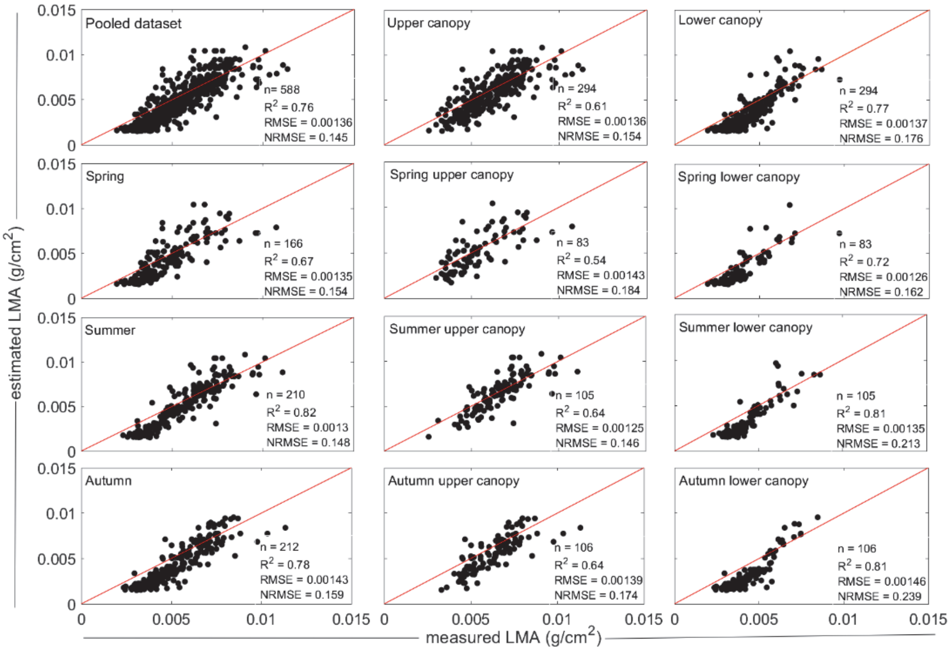

Figure 3.8 Retrieval accuracies of the leaf mass per area (LMA) across canopy positions throughout the three growing seasons.

3.4 Discussion

3.4.1 Does the position of a leaf within a vertical canopy profile affects modelling leaf spectral reflectance throughout the growing season?

The PROSPECT model exhibited the capability to reconstruct leaf reflectance spectra across the canopy throughout the growing season. The stronger agreement between measured and simulated reflectance spectra observed for the lower canopy leaves compared to the upper canopy leaves (Fig 3.4 and 3.5) can be attributed to difference in leaf morphological traits, such as specific leaf area (SLA) and LMA between leaf samples collected from the two canopy layers. These morphological differences have been reported to complicate the modelling of leaf optical properties and subsequently retrieval of leaf traits (Qiu *et al.*, 2018). Field data used in this study evidently demonstrated high SLA values for leaf samples collected from the lower canopy when compared to the upper canopy leaf samples throughout the growing season (Fig 3.9), implying that generally upper canopy leaves are thicker compared to lower canopy leaves. Leaf reflectance decreases when a leaf thickens due to the increase in the quantity of light intercepting tissue (Demarez, 1999).

The relatively high RMSE between measured and simulated leaf reflectance in wavebands centred around 510, 740 and 1590 and 1885 nm across seasons and canopy positions, imply that these wavebands are either not well measured or modelled by the PROSPECT model. The spectral mismatch in these wavebands has been observed even for re-calibrated PROSPECT models. For example, Li and Wang (2011) observed RMSE of up to 0.06 in the 'red edge' and SWIR spectral regions after recalibrating the PROSPECT 4 model. The lower RMSEs between measured and simulated leaf reflectance in the 'red edge' spectrum for autumn in comparison to spring and summer can be ascribed to the sensitivity of the 'red edge' spectrum when the distribution of foliar nutrients within the leaf volume become uniform during senescence in the autumn season (Maillard *et al.*, 2015). This observation reflects the subtle sensitivity of the PROSPECT model to variation in chlorophyll content at peak vegetation growth, which potentially has an effect on retrieval accuracy of C_{ab} during the summer season. To the best of our knowledge, our study provides the first preliminary understanding on the effect of leaf position within a vertical canopy profile on the performance of PROSPECT model by inspecting the spectral match between measured and simulated leaf reflectance spectra throughout the growing season.

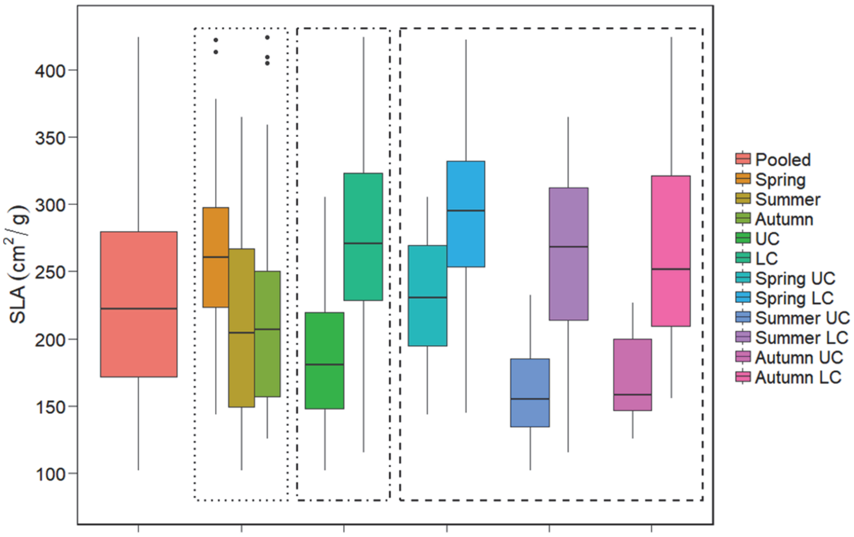

Figure 3.9 Variation in SLA across canopy positions throughout the growing season. (UC and LC represent upper and lower canopy respectively).

3.4.2 Effect of leaf position on the retrieval accuracy of leaf traits throughout the growing season

The higher accuracy of retrieval of C_{ab} obtained for leaf samples collected from the lower canopy compared to the upper canopy throughout the growing season (Fig 3.6) can be attributed to the distribution of chloroplasts within a leaf that affects absorption and transmittance of radiation by leaf chlorophyll pigments. Most of the chloroplasts for upper sunlit leaves are clumped in the palisade layer whilst for shaded leaves, the chloroplasts are evenly distributed between the palisade and spongy mesophyll layer (Adds *et al.*, 1997). We speculate that the evenly distributed chloroplast in shaded lower canopy leaves improves the sensitivity and interaction of radiation and chlorophyll pigments. The widest differences in C_{ab} retrieval accuracy between upper and lower canopy coincided with the period of maximum leaf chlorophyll content (Fig 3.2). This observation can be attributed to the manifestation of the shadow effect on the lower canopy resulting in a reduction in photosynthetically active radiation (PAR) reaching to the lower canopy. The position of a leaf across the canopy vertical profile is a key determinant of its pigment content and subsequently photosynthetic capacity (Arellano *et al.*, 2017). The illuminated upper canopies are known to display high pigment content to commensurate the high relative irradiance received. The least retrieval accuracy of C_{ab} across all seasons (i.e. summer (NRMSE = 0.219) coincided with the season of high leaf chlorophyll content (Fig 3.2). This observation is in agreement with the findings of Zhang *et al*. (2007) who obtained the lowest accuracy in the retrieval of C_{ab} in summer, using the PROSPECT model in sugar maple stands. The seasonal distribution of chlorophyll pigments within a leaf can be linked to poor leaf chlorophyll retrievals obtained in summer. During peak vegetation growth, chlorophyll and other nutrients are confined in chloroplast cells, and these cells are organized in a clumped manner. As leaves senescence, chloroplast degrades, and the chlorophyll pigments together with other nutrients like leaf protein are released in remobilizable form and become uniformly distributed across the leaf volume (Carrión *et al.*, 2014). This phenomenon, therefore, improves the interaction between radiation and leaf nutrients that are freely and uniformly distributed across the leaf volume.

Results of our study demonstrate contrasting patterns in seasonal retrieval accuracies of LMA and EWT across canopy positions. We expected LMA and EWT to display similar seasonal retrieval patterns across the canopy, mainly because these two traits co-vary on the leaf economic spectrum, i.e. EWT facilitates transportation of nutrients and is a key regulator of photosynthesis and subsequently the amount of dry matter content accumulated in a leaf (Asbjornsen *et al.*, 2011; Waring and Landsberg, 2011). Statistically, LMA and EWT demonstrated a positive co-variance and strong correlation (r = 0.66, p = 0.00, Fig 3.3). Previous studies reported that EWT is probably easier to retrieve via PROSPECT inversion due to its dominance and well-elaborated specific absorption features compared to LMA (Feret *et al.*, 2008; Jiang *et al.*, 2018; Wang *et al.*, 2011). The high EWT retrieval accuracies obtained for the lower canopy in comparison to the upper canopy throughout the growing season conform to the variation in spectral matching between measured and simulated reflectance spectra for the two canopy layers especially in key water absorption wavebands [970, 1200 and 1400 nm (Curran, 1989)]. The pattern in EWT retrieval accuracy across canopy positions and seasons can be explained by the high wax-cuticle load that characterize upper canopy leaves in a bid to prevent photo-damage, especially at peak vegetative growing season that is characterized by increased radiation amounts (Bouzoubaâ *et al.*, 2006; Jacoby *et al.*, 1990). High wax-cuticle load conceal the interaction between radiation and leaf biochemical constituents especially in the NIR/SWIR optical domain resulting in complex relationship with reflected light (Barry *et al.*, 2009; Féret *et al.*, 2018).

Contrary to EWT retrieval accuracy patterns across seasons and canopy positions, we observed that the retrieval accuracy of LMA for the upper canopy outperformed that of the lower canopy for all the seasons except the spring. This observation does not reflect the discrepancies in spectral matching between measured and PROSPECT simulated reflectance spectra observed in Fig 3.4 and 3.5 especially for wavelengths in the NIR and SWIR reported to be sensitive to LMA variations (Baret and Fourty, 1997; Feret *et al.*, 2008). Several reasons can be ascribed to the contrasting pattern in LMA retrieval accuracies across the canopy throughout the growing season. Firstly, LMA is often retrieved with relatively low accuracy because the high specific absorption coefficients of water which conceal the effect of LMA spectral response (Jacquemoud *et al.*, 1996; Riano *et al.*, 2005). Secondly, LMA consists of a wide range of constituents, such as protein, lignin, cellulose, starch, sugar and lipids (Qiu *et al.*, 2018). The specific absorption coefficient spectrum used in the PROSPECT model is considered a weighted average of the molecular absorption spectra of these constitutes (Jacquemoud *et al.*, 1996). This approach is likely to induce uncertainties, especially in wavelengths of high LMA absorption as different components of these constituents can yield different specific absorption coefficients of LMA. Thirdly, thicker leaves or leaves of higher LMA values tend to have denser tissues and less air space, which results in diverse leaf internal structure and complex light scattering (Demarez, 1999). Finally, although it has been demonstrated earlier that the SWIR (especially between 2100-2300 nm) is more sensitive to LMA (Wang *et al.*, 2011), our spectral reflectance data had low signal to noise ratio in this spectrum. Retrieval of LMA did not show similar patterns to C_{ab} and EWT retrieval across the canopy, it was generally retrieved with higher accuracy (NRMSE = 0.145 for the pooled dataset) compared to previous studies that used the PROSPECT model in the same ecosystem. For example, Ali *et al*. (2016) reported an NRMSE of 0.23 while Wang *et al*. (2015a) reported an NRMSE of 0.22 for LMA retrieved using the PROSPECT inversion based on 53 sunlit leaf samples collected in summer. The relatively lower accuracy reported in these studies could be ascribed to a small sample size (n = 53 compared to 588 samples in this study) used for model validation. To our knowledge, our work provides the first attempt to examine the effect of leaf position within a vertical canopy profile on the performance of the PROSPECT model when retrieving leaf traits throughout a growing season.

3.4.3 Implications on plant traits spectroscopy

Results presented in this study have implications on modelling leaf optical properties and retrieval of foliar traits especially using multi-layer canopy radiative models (Kuusk, 2001). The conventional approach of sampling foliar material exclusively from the sunlit upper canopy has recently become a contentious approach in remote sensing vegetation canopies. Recent studies demonstrate that the vertical heterogeneity in leaf chlorophyll, water and dry matter content have a significant effect on canopy reflectance measured by remote sensing instruments (Wang and Li, 2013; Yang *et al.*, 2017; Zhao *et al.*, 2017). The vertical heterogeneity in leaf traits is known to affect re-absorption and scattering of radiation within vegetation canopies, and subsequently, the top of canopy reflectance measured by remote sensing instruments (Verhoef and Bach, 2007). Our previous study (Gara *et al.*, 2018b) also demonstrated that incorporating leaf traits from the shaded lower canopy improve the modelling accuracy of dry matter related canopy traits such as canopy LMA, nitrogen and carbon using *in-situ* hyperspectral measurements. Results presented in the current study demonstrate that the position of a leaf affects the performance of the PROSPECT model and the retrieval of its input parameters. This observation implies that failure to account for the vertical heterogeneity in leaf traits between sunlit upper and shaded lower leaves together with their optical properties might introduce significant uncertainties in modelling canopy reflectance and retrieval of canopy traits (Li *et al.*, 2018b; Yang *et al.*, 2017). These results are particularly relevant to the vegetation spectroscopy community considering that the PROSPECT model is coupled with widely used canopy RTMs such as INFORM (Schlerf and Atzberger, 2006) and SAILH (Jacquemoud *et al.*, 2009).

3.5 Conclusion

Our results demonstrated a strong agreement between the measured and PROSPECT simulated reflectance spectra for leaves from the lower canopy compared to the upper canopy, especially in the NIR spectral region, throughout the growing season. This pattern concurred with the higher retrieval accuracy of C_{ab} and EWT for the lower canopy compared to the upper canopy throughout the growing. Variations in C_{ab} and EWT retrieval accuracy across the canopy vertical profile can be linked to seasonal changes in leaf biochemistry and morphology especially SLA. On the contrary, the LMA retrieval accuracy pattern did not reflect the spectral match observed between the upper and lower canopy. This implies that there is further need to separate and model respective constituents of LMA to improve PROSPECT stability and credibility. We conclude that the PROSPECT model provides reasonable retrieval accuracies for C_{ab}, EWT and LMA from reflectance spectra across canopy position throughout the growing season. However, our results for the first time demonstrated seasonal variation in retrieval accuracy of leaf traits via PROSPECT model inversion through a vertical canopy profile. Our results points out the potential source of uncertainties in the retrieval of leaf traits using the widely used PROSPECT model.

Chapter 4

Leaf to canopy upscaling approach affects the estimation of canopy traits[*]

---

[*] This chapter is based on Gara, T.W., Skidmore, A. K., Darvishzadeh, R., Wang, T. (2019) Leaf to canopy upscaling approach affects the estimation of canopy traits. GIScience & Remote Sensing, 56, 554-575.

Abstract

Leaf traits are often upscaled to canopy level using sunlit leaf samples collected from the upper canopy. The implicit assumption is that the top of canopy foliage material dominates canopy reflectance and the variability in leaf traits across the canopy is very small. However, the effect of different approaches of upscaling leaf traits to canopy level on model performance and estimation accuracy remains poorly understood. The principal aim of this study is to examine the effect of different approaches when upscaling leaf traits to canopy level on model performance and estimation accuracy using spectral measurements (*in-situ* canopy hyperspectral and simulated Sentinel-2 data) in short woody vegetation. To achieve this, we measured foliar nitrogen (N), leaf mass per area (LMA), foliar chlorophyll and carbon together with leaf area index (LAI) at three vertical canopy layers (lower, middle and upper) along the plant stem in a controlled laboratory environment. We then upscaled the leaf traits to canopy level by multiplying leaf traits by LAI based on different combinations of the three canopy layers. Concurrently, *in-situ* canopy reflectance was measured using an ASD FieldSpec-3 Pro FR spectrometer, and the canopy traits were related to *in-situ* spectral measurements using partial least square regression (PLSR). The PLSR models were cross-validated based on repeated *k-fold*, and the normalized root mean square errors ($NRMSE_{cv}$) obtained from each upscaling approach were compared using one-way analysis of variance (ANOVA) followed by *Tukey's post hoc* test. Results of the study showed that leaf-to-canopy upscaling approaches that consider the contribution of leaf traits from the exposed upper canopy layer together with the shaded middle canopy layer yield significantly ($p < 0.05$) lower error ($NRMSE_{cv} < 0.2$ for canopy N, LMA and carbon) as well as high explained variance ($R^2 > 0.71$) for both *in-situ* hyperspectral and simulated Sentinel-2 data. The widely-used upscaling approach that considers only leaf traits from the upper illuminated canopy layer yielded a relatively high error ($NRMSE_{cv} > 0.2$) and lower explained variance ($R^2 < 0.71$) for canopy N , LMA and carbon. In contrast, canopy chlorophyll upscaled based on leaf samples collected from the upper canopy and total canopy LAI exhibited a more accurate relationship with spectral measurements compared with other upscaling approaches. Results of this study demonstrate that leaf to canopy upscaling approaches have a profound effect on canopy traits estimation for both *in-situ* hyperspectral measurements and simulated Sentinel-2 data in short woody vegetation. These findings have implications for field sampling protocols of leaf traits measurement as well as upscaling leaf traits to canopy level especially in short and less foliated vegetation where leaves from the lower canopy contribute to the canopy reflectance.

4.1 Introduction

Essential biodiversity variables (EBVs) such as leaf traits play a key role in ecosystem structure, functioning and parameterization of dynamic biogeochemical models and nutrient budget simulations (Scheiter *et al.*, 2013). For example, leaf chlorophyll content is a critical leaf trait in assessing plant physiological status (plant health and/or phenological stage) as well as a plant's photosynthetic capacity (Malenovský *et al.*, 2013). Foliar nitrogen (N) is a key element in chlorophyll (~6% by weight) (Kokaly *et al.*, 2009) and in enzymes responsible for carbon fixation i.e. ribulose-1.5-biphosphate (RuBP) carboxylase and phenolyenolpyruvate (PEP) essential for photosynthesis in C3 and C4 plants, respectively (Cho *et al.*, 2013; Gibson, 2008; Schlemmer *et al.*, 2013). In addition, leaf mass per area (LMA) and carbon content mirror the plant economic spectrum with regard to nutrients uptake, light harvesting and carbon sequestration (Martin and Thomas, 2011; Poorter *et al.*, 2009). An improved understanding of leaf traits is critical in characterizing, monitoring and simulating ecosystem biogeochemical fluxes over space and time. In this regard, leaf traits are a critical component of ecosystem functional and structural diversity - proxies of essential biodiversity variables (EBVs) (Skidmore *et al.*, 2015). Therefore, estimating leaf traits improves the conservation and monitoring efforts of EBVs fluxes towards the Aichi Biodiversity Targets (Pereira *et al.*, 2013).

Remote sensing provides a cost-effective and practical means of estimating and monitoring leaf traits for biodiversity conservation (Kissling *et al.*, 2017). Field spectroscopy and satellite multispectral data such as Sentinel-2 are critical primary data sources that can improve quantitative estimation and monitoring of foliar traits (Chemura *et al.*, 2018). Essentially, two modelling approaches [i.e. empirical (statistical) and physical models (radiative transfer models-RTM)] are employed to estimate field measured leaf traits from spectral data. Empirical models explore parametric and non-parametric statistical relationships between spectral data or indices and field measured leaf traits using statistical techniques such as stepwise regression and partial least squares regression (Verrelst *et al.*, 2015a). Physical models, on the other hand, apply radiation transfer laws to explicitly simulate light absorption, transmittance and scattering inside vegetation canopies by accounting for leaf traits content, canopy structural properties and soil background (Croft *et al.*, 2015; Yi *et al.*, 2014). Quantitative leaf traits that are related or matched to spectral measurements based on these modelling approaches are often determined from leaf samples collected from dominant and co-dominant species within sampling units (Homolová *et al.*, 2013). The leaf traits expressed either in mass (concentration) or area (content) based units are then upscaled to the canopy level using two techniques, i.e. the direct extrapolation and canopy integrated approaches (He and Mui, 2010a). The direct extrapolation approach applies the relationship between leaf traits and reflectance or vegetation indices observed at leaf level directly to the canopy level (Yoder and Pettigrew-Crosby, 1995). The basic assumption of the direct extrapolation method is that trait content or concentration of leaves across the vertical canopy profile is homogeneous (Peterson *et al.*, 1988). However, the direct extrapolation approach is not commonly used because it does not account for canopy structure - a key variable that drives canopy reflectance (Knyazikhin *et al.*, 2013). The canopy integrated method on the other hand upscale leaf traits to canopy level by accounting for LAI or foliage biomass. The plant traits at canopy level are then regressed against canopy reflectance measured using a field spectroradiometer or airborne and satellite multispectral sensors. In both upscaling approaches, leaf samples for determining traits are often collected from the sunlit top-of-the canopy layer, especially in highly foliated forest canopies. The assumption underlying this widely used approach is that the vertical variation in leaf traits across the canopy is small and leaves at the top of the canopy dominate canopy reflectance and thus represents the whole canopy (Thomas *et al.*, 2008). However, in short woody vegetation the foliage material across the vertical profile significantly contributes to the canopy spectral signal (Roelofsen *et al.*, 2013). This phenomenon complicates leaf sampling protocols because 'top of canopy' sampling becomes less valid. To this end, establishing an ecologically meaningful canopy trait value that corresponds to the overall canopy spectral signal is critical when estimating and mapping canopy traits.

The distribution of leaf trait content across vegetation canopies is complex and often varies across the vertical canopy profile (Gara *et al.*, 2018a; Hirose *et al.*, 1989). Plants often exhibit higher nutrient content in the upper canopy and on illuminated leaves that receive increased radiation amounts (Chen *et al.*, 1993; Weerasinghe *et al.*, 2014). The variation in leaf traits across the canopy vertical profile is an established plant physiological mechanism designed to maintain an equilibrium between the RuBisCo-limited rate of carboxylation and electron transport limited rate of carboxylation (Chen *et al.*, 1993). Recent research on multiple-layer radiative transfer models (MRTM) have shown that the vertical heterogeneity in foliar traits (LMA, chlorophyll and water) have a significant influence on simulated canopy reflectance and subsequent retrieval of canopy traits especially in low to moderately foliated canopies (Li and Wang, 2013a; Wang and Li, 2013). Moreover, previous studies demonstrated that canopies of similar foliage material (e.g., LAI or biomass) can yield significantly different canopy reflectance across the whole spectrum (Darvishzadeh *et al.*, 2008a). This observation has been linked to variation in confounding factors such as leaf trait heterogeneity within a canopy (Li *et al.*, 2013; Luo *et al.*, 2016). Related studies have also demonstrated that the "big leaf" (sunlit leaves only) upscaling approach underestimates canopy gross primary production by up to 70 % in highly clumped forest stands compared to the "two leaf" (sunlit plus shaded leaves) approach (Sprintsin *et al.*, 2012). The "big leaf" approach does not account for the vertical variability in leaf traits and assumes that a sunlit leaf in the upper canopy represent the whole canopy, while the "two leaf" approach requires information on the vertical variability in leaf traits based on both sunlit and shaded leaves (Mercado *et al.*, 2006). Within the framework of the "big leaf" and "two leaf" upscaling approaches, we explored different combinations of leaf trait-LAI upscaling scenarios from three vertical (upper, middle and bottom) canopy layers in short woody vegetation in a laboratory setup. To the best of our knowledge, the effect of these upscaling conceptualizations are poorly understood and remain untested in canopy traits estimation using *in-situ* hyperspectral measurements or simulated satellite data. To this end, we, therefore hypothesize that leaf to canopy upscaling approaches have a significant effect on the relationship between canopy traits and spectral measurements and subsequently estimation accuracy of canopy traits.

The principal aim of this study is to evaluate the effect of different approaches of upscaling leaf traits (foliar N, LMA, chlorophyll, and carbon) from leaf to canopy level on model performance and estimation accuracy using spectral measurements (*in-situ* canopy hyperspectral and simulated Sentinel-2 multispectral data) and partial least squares regression. A number of upscaling approaches based on different LAI and leaf trait mathematical combinations were computed and used to calibrate a PLSR model, with the intention of assessing the accuracy of canopy traits estimation. Prior to ascertaining the effect of upscaling approaches, we tested whether leaf traits significantly vary across the canopy vertical profile.

4.2 Materials and methods

4.2.1 Species description

Four plant species of different leaf form and canopy structure, representing tropical and temperate biomes, were used to evaluate the effect of leaf to canopy upscaling approaches on model performance and estimation accuracy using *in-situ* hyperspectral and simulated Sentinel-2 multispectral data. We selected the following plant species; *Camellia japonica* (n = 24, mean height 83.71±4.75 cm), *Ficus benjamina* (n = 24; mean height 82.07±4.27 cm), *Chamaedorea elegans* (n = 24; mean height 88.5±4.75 cm) and *Fatshedera lizei* (n = 24; mean height 88.93±1.53 cm). Further description of the plant species used in this study can be found in Gara *et al*, (2018a). All the plants used in this study were purchased from a local nursery.

4.2.2 Experimental setup

Since the plants purchased from the nursery were assumed to be pre-treated with fertilizer, we changed the pot-soil to a new homogenized mixture of seven parts of nutrient-poor sand soil to two parts of fertile loamy soil. After changing the potting mix, we administered three soil nitrogen treatments (high, medium and low) to the ninety-six (96) plants used in this study. For the high (n = 32) and medium (n = 32) treatment groups, 2.9 g and 0.9 g per pot were supplied respectively, while no fertilizer was applied to the low treatment (n = 32). Further details on the experimental setup is provided in Gara *et al* (2018a).

4.2.3 Canopy spectral measurements

Canopy spectral reflectance from 350 to 2500 nm were measured in a controlled remote sensing laboratory using an ASD FieldSpec-3 Pro FR spectrometer. The walls and ceiling of the laboratory were coated with black material in order to minimize any ambient light or reflection, thus minimizing the effect of diffuse radiation and lateral flux (Darvishzadeh *et al.*, 2009). Three pots of the same species and soil treatment were used to form a canopy as shown in a schematic presentation in Fig 4.1A. In order to create a canopy, the three pots were placed in fixed positions within a 60 cm by 60 cm soil bed. A fiber optic probe with a field of view of 25° was mounted on a tripod at nadir and positioned 90 cm above the soil bed, thus creating a field of view (FOV) with a diameter of 40 cm on the soil surface. A halogen light bulb (235 W) positioned 1.2 m from the canopy was used to supply illumination on the canopy. All canopy spectral measurements were calibrated with a Spectralon white reference panel. The sensor's FOV was completely covered with foliage material; hence the effect of the background soil was minimized. After each canopy spectral measurement, the soil bed was rotated 45° in order to average out the differences in canopy orientation and to minimize the possible bidirectional reflectance distribution function (BRDF) effects (Darvishzadeh *et al*. 2008; 2009). Consequently, the spectral reflectance of 32 canopies were measured. To minimize noise in the canopy reflectance spectra, a moving second order Savitzky-Golay filter (Savitzky and Golay, 1964) with a frame size of 11 was applied to each sample reflectance spectra. Wavelengths before 400 nm and after 2200 nm were too noisy and were thus removed from the dataset. Therefore, 1801 spectral bands were retained for subsequent analysis.

The canopy reflectance spectra measured using the ASD spectroradiometer were convolved to the spectral band configurations of Sentinel-2 multispectral instrument based on the sensor spectral response function. To account for environmental and instrument uncertainties in natural satellite operating system, we added a random Gaussian (white) noise component of 20% to the convolved spectra (Richter *et al.*, 2009; Verrelst *et al.*, 2014). Sentinel-2 is a Multi-Spectral Instrument (MSI) operated by the European Space Agency

(ESA). The Multi-Spectral Instrument (MSI) on board Sentinel-2 is composed of 13 spectral bands ranging from 400 to 2400 nm with a grain size ranging from 10-60 m and a swath width of 290 km (European Space Agency, 2010; Hill, 2013). The mission has two identical multispectral sensors (Sentinel 2A and 2B) in orbit delivering a revisit time of three to five days (Aschbacher and Milagro-Pérez, 2012).

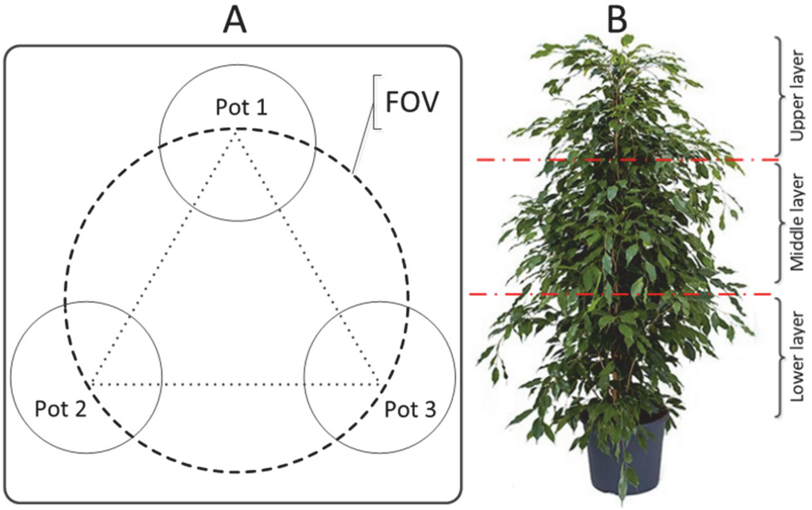

Figure 4.1 Positioning of plant vessels in the field of view (A) and the demarcation of the three canopy layers considered in the experiment (B).

4.2.4 Determining LAI and leaf traits

After measuring canopy reflectance spectra, the canopy was divided into three vertical layers, i.e. upper, middle and lower, as shown in Fig 4.1B. The three layers were determined based on the height of a canopy along the stem. We divided the canopy into three layers for three reasons. First, the plants used in this study were relatively short (mean height ~85 cm) in order to clearly identify more than three canopy layers. Second, identifying less than three canopy layers could have been insufficient to understand the effect of leaf traits vertical heterogeneity on canopy traits estimation. Finally, three canopy layers match forestry and agronomic standards in reporting research in canopy layers (Whitehurst *et al.*, 2013; Wilkes *et al.*, 2016). Foliage material belonging to each canopy layer were harvested. The LAI for each canopy layer was measured as the cumulative leaf surface area of leaves making up a canopy layer divided by the field of view. Care was taken to eliminate leaves outside the field of view. The total surface area of the leaves were measured using a LI-3100C area meter. The calibration of the LI-3100C area meter was routinely checked against a metal surface of known surface area. Representative leaves (approximately 3 g) from foliage material of each canopy layer were randomly sampled for leaf traits measurement. Leaf chlorophyll content (C_{ab} μg/cm^2)

was measured using a CCM-300 chlorophyll content meter (Opti-Sciences, 2011). After measuring chlorophyll, a digital scale at an accuracy of ~0.01 g was used to determine the fresh weight for each sample. We also scanned the leaf surface area (LA cm^2) of each sample using an AMH 350 area meter (ADC-BioScientific, 2013). The samples were then oven-dried at 65 °C until at constant weight was attained after approximately 72 hours after which dry weight was measured. The leaf mass per area (LMA, g/cm^2) was determined by dividing dry weight by fresh leaf area.

After determining LMA, leaf samples were prepared for nitrogen and carbon analysis by grinding them to a fine and homogeneous powder using a mortar and pestle to pass through a 180 µm sieving and mesh screen. Approximately 2 mg of each sample powder was placed in aluminium capsules for nitrogen and carbon analysis using the Perkin Elmer 2400 CHNS/O Elemental Analyzer (Perkin-Elmer, 2005). We duplicated 25% of samples and ran an acetanilide standard after every ten to fifteen samples to constantly monitor the system calibration and reliability. The nitrogen and carbon results from the elemental analyzer were obtained on a dry mass ash-included basis (Meerdink *et al.*, 2016). We therefore multiplied the mass-based nitrogen and carbon by LMA of each sample to obtain area based nitrogen and carbon content (Wang *et al.*, 2015a).

4.2.5 Upscaling leaf traits to canopy level

Using the LAI of each canopy layer, we explored different approaches for upscaling foliar nitrogen, LMA, chlorophyll and carbon to canopy level as described in Table 1. It is important to note that although the study aimed to assess five primary upscaling approaches (i.e., A-E, Table 4.1), we also used several secondary upscaling approaches (F-L) to explore the relative effect of each layer on the spectral signal observed at the top of the canopy, even if these secondary approaches are not necessarily practical in terms of field sampling. For example, upscaling option F requires measuring LAI of the top and bottom canopy layers, which is a challenge especially in environments characterized by tall trees. However, such an upscaling approach assists in assessing the contribution of the middle layer.

4.2.6 Statistical analysis

The effect of different leaf to canopy upscaling approaches on canopy traits estimation were assessed using partial least squares regression (PLSR) and validated using repeated *k-fold* cross validation. In this study we used PLSR for the following reasons; 1) it is more stable and suitable for high dimensional and collinear datasets such as a hyperspectral dataset (Wold *et al.*, 2001); 2) it reduces model overfitting by decomposing spectral data into non-collinear latent variables especially when the number of predictor variables is more than the number of observations (Carrascal *et al.*, 2009); 3) it provides an opportunity to generate an error matrix for the internal validation subset (Kuhn, 2008; Wakeling and Morris, 1993); 4) it is computationally fast and statistically efficient and is widely used in leaf traits estimation using spectral data (Neinavaz *et al.*, 2016; Ramoelo *et al.*, 2011; Roelofsen *et al.*, 2013; Serbin *et al.*, 2014; Shiklomanov *et al.*, 2016; Ullah *et al.*, 2014).

PLSR projects the explanatory variables (canopy reflectance spectra) into new orthogonal latent variables that explain the most variance in the original predictors (Geladi and Kowalski, 1986). The dependent variable (canopy traits) is then regressed against the optimal number of latent variables (Wold *et al.*, 2001). The number of latent factors selected for the PLSR model was determined by minimizing the cross validated root mean square error ($RMSE_{CV}$) generated from the repeated *k-fold* cross validation. In order to avoid overfitting and maintain model parsimony, we restricted the number of latent factors to a maximum of 10% (three) of the sample size i.e. 32 canopies (Bian *et al.*, 2010; Marcoulides and Saunders, 2006; Wold *et al.*, 2001). Repeated *k-fold* cross validation was used to proficiently exploit on our small dataset (n = 32). Five folds repeated 20 times (100 iterations) were used in the cross validation procedure. The repeated *k-fold* cross validation procedure iteratively splits the data set (n=32) into five semi-equal partitions or blocks randomly. At each iteration, *k-1* partitions were used to train the PLSR model while the left out partition were used for validation.

Table 4.1: Leaf to canopy upscaling approaches

Upscaling approach ID	Description	Formula
A	mean leaf traits across the three canopy layers × total canopy LAI	$\left(\frac{1}{n} * \sum_{i=1,2,3} \text{trait}\right) * \sum_{1,2,3} \text{LAI}$
B	mean leaf traits of the top two canopy layers × total canopy LAI	$\left(\frac{1}{n} * \sum_{i=1,2} \text{trait}\right) * \sum_{1,2,3} \text{LAI}$
C	leaf traits of the top canopy layer × total canopy LAI	$\text{trait}_1 * \sum_{1,2,3} \text{LAI}$
D	canopy traits weighted by LAI of each of the three canopy layers	$\sum_{i=1,2,3} \text{LAI}_i * \text{trait}_i$
E	canopy traits weighted by LAI of the top two layers	$\sum_{i=1,2} \text{LAI}_i * \text{trait}_i$
F	canopy traits weighted by the LAI of the top and bottom canopy layers	$\sum_{i=1,3} \text{LAI}_i * \text{trait}_i$
G	canopy traits weighted by LAI of the middle and bottom canopy layer	$\sum_{i=2,3} \text{LAI}_i * \text{trait}_i$
H	leaf traits for the top canopy layer × LAI of the top canopy layer	$\text{LAI}_1 * \text{trait}_1$
I	leaf traits for the middle canopy layer × LAI of the middle canopy layer	$\text{LAI}_2 * \text{trait}_2$
J	leaf traits of the bottom canopy layer × LAI of the bottom layer	$\text{LAI}_3 * \text{trait}_3$
K	mean leaf traits of the top and bottom layers × total canopy LAI	$\left(\frac{1}{n} * \sum_{i=1,3} \text{trait}\right) * \sum_{1,2,3} \text{LAI}$
L	mean leaf traits of the middle and bottom canopy layers × total canopy LAI	$\left(\frac{1}{n} * \sum_{i=2,3} \text{trait}\right) * \sum_{1,2,3} \text{LAI}$

1, 2, and 3 represents upper, middle and lower canopy layers respectively, trait = leaf traits

Table 4.2 Summary statistics of the leaf to canopy upscaling approaches

		Leaf to canopy upscaling approach											
		A	B	C	D	E	F	G	H	I	J	K	L
Canopy N (g/m^2)	min	0.79	0.97	**1.04**	0.69	0.48	0.5	0.29	0.28	0.12	0.09	0.8	0.49
	max	20.24	21.9	**16.92**	22.88	19.53	9.23	19.2	5.75	15.88	6.47	16.61	22.21
	mean	6.95	7.55	6.95	7.33	5.69	3.65	5.31	2.01	3.68	1.63	6.3	6.95
	SD	5.6	6.2	5.16	6.06	5.21	2.63	4.8	1.59	3.93	1.53	4.74	6.12
Canopy LMA (g/m^2)	min	9.62	10.77	**12.25**	9.83	6.13	6.88	5.14	3.36	2.18	2.11	9.41	8.3
	max	78.47	79.24	**71.41**	81.53	66.33	37.39	65.41	19.86	50.21	17.53	74.17	82
	mean	30.23	30.89	30.31	30.69	22.77	16.85	21.75	8.93	13.83	7.92	26.61	30.19
	SD	19.13	19.85	17.83	19.7	16.54	8.59	15.4	5.26	12	4.95	17.8	30.11
Canopy Cab (g/m^2)	min	1.14	1.15	**1.13**	1.14	0.71	0.77	0.65	0.26	0.33	0.14	1.13	1.15
	max	5.13	5.17	**5.31**	5.12	4.04	2.66	3.53	1.59	2.56	1.11	5.18	5.03
	mean	2.18	2.19	2.17	2.19	1.58	1.24	1.56	0.63	0.95	0.61	2.17	2.19
	SD	1.08	1.10	1.13	1.08	0.91	0.45	0.87	0.28	0.69	0.26	1.08	1.05
Canopy Carbon (g/m^2)	min	1.21	1.58	**1.68**	1.11	0.77	0.8	0.46	0.46	0.2	0.14	1.28	0.74
	max	79.21	83.87	**61.17**	89.07	75.26	32.05	75.26	18.13	61.45	14.19	65.54	88.23
	mean	18.64	20.09	17	19.76	15.69	9.1	14.72	5.03	10.65	4.07	16.36	19.45
	SD	22.63	24.73	18.53	24.45	20.71	9.5	19.37	5.77	15.55	4.64	18.46	25.16

This process was repeated iteratively *k* times (100 times in our case) until all the partitions were used for validation as well for calibration. In order to minimize bias on the estimate based on the composition of samples making up each partition the resampling procedure of the dataset was repeated twenty times. In the end, a total of 100 model runs were performed for each canopy trait.

The cross validated R^2_{cv}, and normalized RMSE ($NRMSE_{cv}= RMSE_{cv}/range$) between the predicted and measured canopy trait values were used to evaluate the performance of each PLSR model for each leaf to canopy upscaling approach. For canopy chlorophyll content modelling we used canopy reflectance spectra within the visible and red edge region (400-790 nm) as this spectral region is sensitive to variation in chlorophyll content (Kumar *et al.*, 2001). However, for the other canopy traits (N, LMA and carbon) we used the whole spectrum (400-2200 nm) as these traits do not have a defined spectral feature and are related to other compounds distributed across the whole spectrum (Curran, 1989).

To evaluate the effect of different leaf to canopy upscaling approaches on canopy traits estimation, we compared the mean $NRMSE_{cv}$ of the 100 model runs for each upscaling approach using one-way ANOVA with the upscaling approach as a fixed factor. We then used *Tukey's HSD post hoc* test to perform a pairwise comparison of the upscaling approaches. Prior to the PLSR modelling process, independent variables (spectra) and dependent (leaf traits) variables were mean-centered. All PLSR analyses were performed in R 3.3.3 for Windows using the classification and regression (caret) package (Kuhn, 2008).

4.3 Results

4.3.1 Exploratory data analysis of foliar traits and *in-situ* hyperspectral data across the canopy vertical profile

Foliar N, chlorophyll and carbon content significantly ($p < 0.05$) increased from the lower to the upper canopy layer, while the LAI of the middle canopy layer was significantly ($p < 0.05$) higher compared to LAI of the lower and upper canopy layers (Fig 4.2). LMA generally increased from lower to upper layers. However, LMA did not significantly ($p > 0.05$) vary across the three canopy layers.

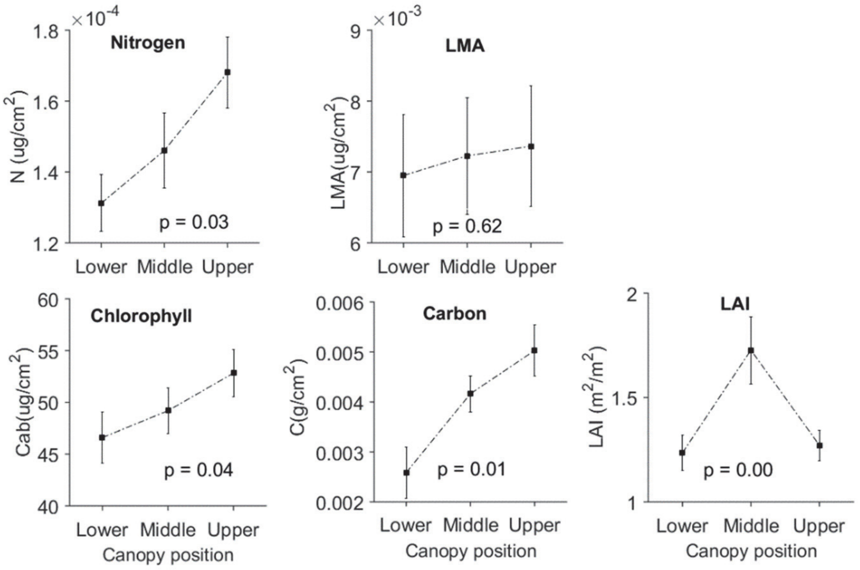

Figure 4.2 Variation in leaf traits and LAI across the canopy vertical profile.

Table 4.2 shows the descriptive statistics of the four canopy traits based on the different leaf to canopy upscaling approaches described in Table 1. Canopy N ($F = 6.21$, $p = 0.00$), canopy LMA ($F = 10.24$, $p = 0.00$), canopy chlorophyll ($F = 16.5$, $p = 0.00$), canopy carbon ($F = 13.48$, $p = 0.00$) significantly varied across the upscaling approaches based on a one-way ANOVA test. Moreover, the range of canopy traits computed from each of the upscaling approaches were different (Table 4.2). For example, the canopy traits based on top of canopy trait content (upscaling approach C – in bold, Table 4.2) had a limited range compared to the range of the other primary upscaling approaches especially for canopy N, LMA and carbon. The range of canopy traits could potentially affect the strength of the relationship between canopy spectral measurements and canopy traits. The mean canopy spectral reflectance flanked by the standard deviation for the thirty-two canopies is shown in Fig

4.3. Increased variations in the canopy spectral reflectance can be observed in the NIR (750 -1350 nm) and SWIR (1400-1850 nm)

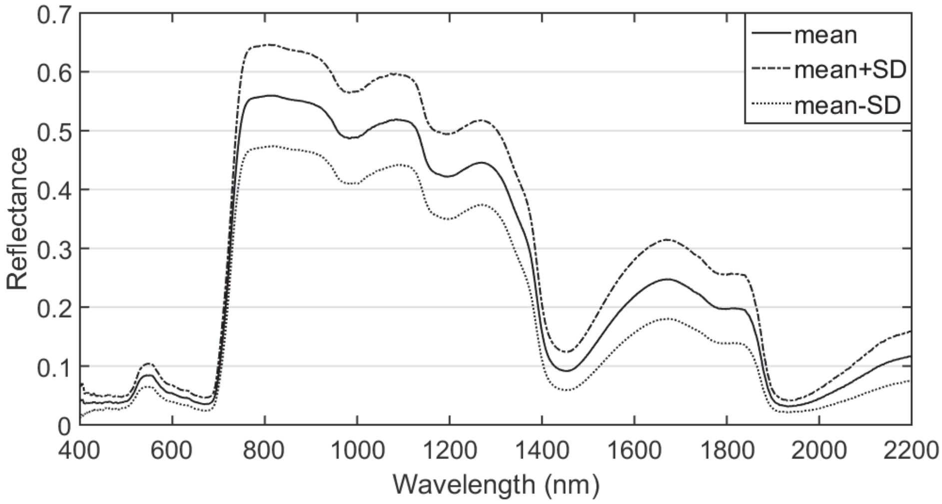

Figure 4.3 The mean and standard deviation of canopy spectral reflectance for the thirty-two canopies used for analysis.

4.3.2 Effect of upscaling approach on model prediction using *in-situ* canopy hyperspectral measurements

Fig 4.4 shows prediction accuracies ($NRMSE_{cv}$) of the twelve upscaling approaches for canopy N, LMA, chlorophyll and carbon based on the repeated *k-fold* PLSR modelling for both *in-situ* hyperspectral measurements and simulated Sentinel-2 multispectral data. An analysis of the primary upscaling approaches indicate that upscaling approach A (mean leaf traits across the three canopy layers × total canopy LAI), B (mean traits of the top two canopy layers × total canopy LAI), D (leaf traits weighted by the LAI of each canopy layer) and E (leaf traits weighted by the LAI of the top two canopy layers) consistently yielded higher retrieval accuracy ($NRMSE_{cv} < 0.2$) and higher explained variance (Table 4.3) compared to upscaling approach C (upper of the canopy traits × total canopy LAI; $NRMSE_{cv} = 0.23$, 0.22, and 0.22 for canopy N, LMA and carbon, respectively). It is worthwhile to note that upscaling approach A exhibited relatively higher model stability based on the limited range of the yielded $NRMSE_{cv}$. A *Tukey* HSD *post hoc* test demonstrated that the $NRMSE_{cv}$ distribution obtained from upscaling approach C (leaf traits of the upper canopy layer × total canopy LAI) was significantly ($p < 0.05$) higher compared to the $NRMSE_{cv}$ obtained from the other primary upscaling approaches especially for canopy N, LMA and canopy carbon (Fig 4.5). The $NRMSE_{cv}$ generated from upscaling approaches A, B, D and E for canopy N, LMA and carbon were not significantly ($p > 0.05$) different from each other demonstrating that they yield comparable retrieval accuracies and ultimately outperformed upscaling approach C.

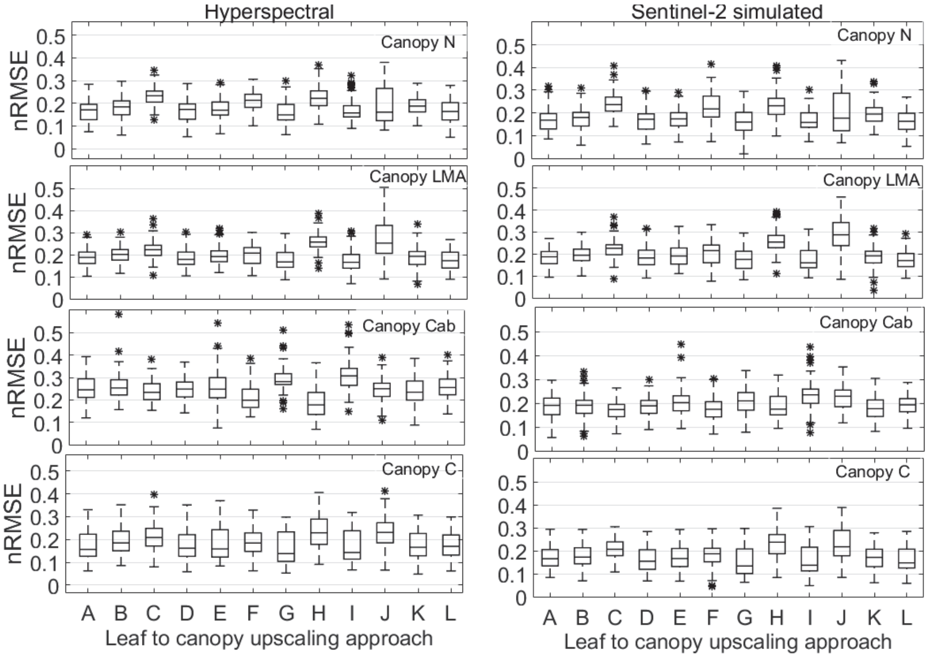

Figure 4.4 Prediction accuracies ($NRMSE_{cv}$) of each upscaling approach for the four traits. The boxplots are based on the repeated *k-fold* cross validation PLSR 100 iterations.

By contrast, canopy chlorophyll content exhibited a different pattern compared to the other canopy traits estimation models. Canopy chlorophyll content upscaled based on leaf samples collected from the upper canopy and total canopy LAI (upscaling approach C) exhibited a better relationship (R^2_{CV} = 0.68, $NRMSE_{cv}$= 0.24) against *in-situ* canopy hyperspectral measurements compared to other canopy chlorophyll upscaling approaches (Fig 4.4, Table 4.3). It is important to note that although upscaling approach C produced a higher retrieval accuracy in canopy chlorophyll estimation; it yielded comparable prediction errors to other primary upscaling approaches i.e. the generated ($NRMSE_{cv}$) were not statistically different ($p > 0.05$, Fig 4.5). Although there were no statistical differences in the generated $NRMSE_{cv}$ among the canopy chlorophyll estimations, it is worthwhile to note that all leaf to canopy upscaling approaches generated high errors ($NRMSE_{cv} > 0.23$) compared to canopy N, LMA and carbon using *in-situ* hyperspectral measurements.

Upscaling approaches that included both LAI and traits of the middle layer (i.e. A, B, D, E, G, I and L) yielded low $NRMSE_{cv}$ especially for canopy N, LMA and carbon. Although the middle canopy layer demonstrated a strong influence on retrieval accuracy of canopy traits, a combination of the middle and upper canopy layers (upscaling approach R^2_{cv}: A = 0.78, B = 0.76, D = 0.79 and E = 0.73) generally outperforms the combination of middle and bottom canopy layer (R^2_{cv}: G = 0.74, L = 0.7) for canopy N estimations (Table 4.3) using hyperspectral measurements. However, upscaling approaches that excludes the middle canopy layer yielded lower explained variance e.g. (R^2_{cv}: F = 0.64, K = 0.62). We observed that upscaling approach B (mean traits of the top two layers × total canopy LAI), K (mean traits of the top and bottom layers × total canopy LAI) and L (mean traits of the middle and bottom layers × total canopy LAI), - all computed based on total canopy LAI, yielded different explained variance (R^2_{cv}: B= 0.65, K= 0.64 and L= 0.7) and prediction errors ($NRMSE_{cv}$: B = 0.2, K = 0.19 and L = 0.17) for canopy LMA estimations. A similar pattern can also be observed regarding the relationship between canopy N or carbon and *in-situ* hyperspectral measurements. For practical purposes, this implies that leaf traits and LAI of the top two canopy layers are key and contribute significantly to canopy spectral reflectance.

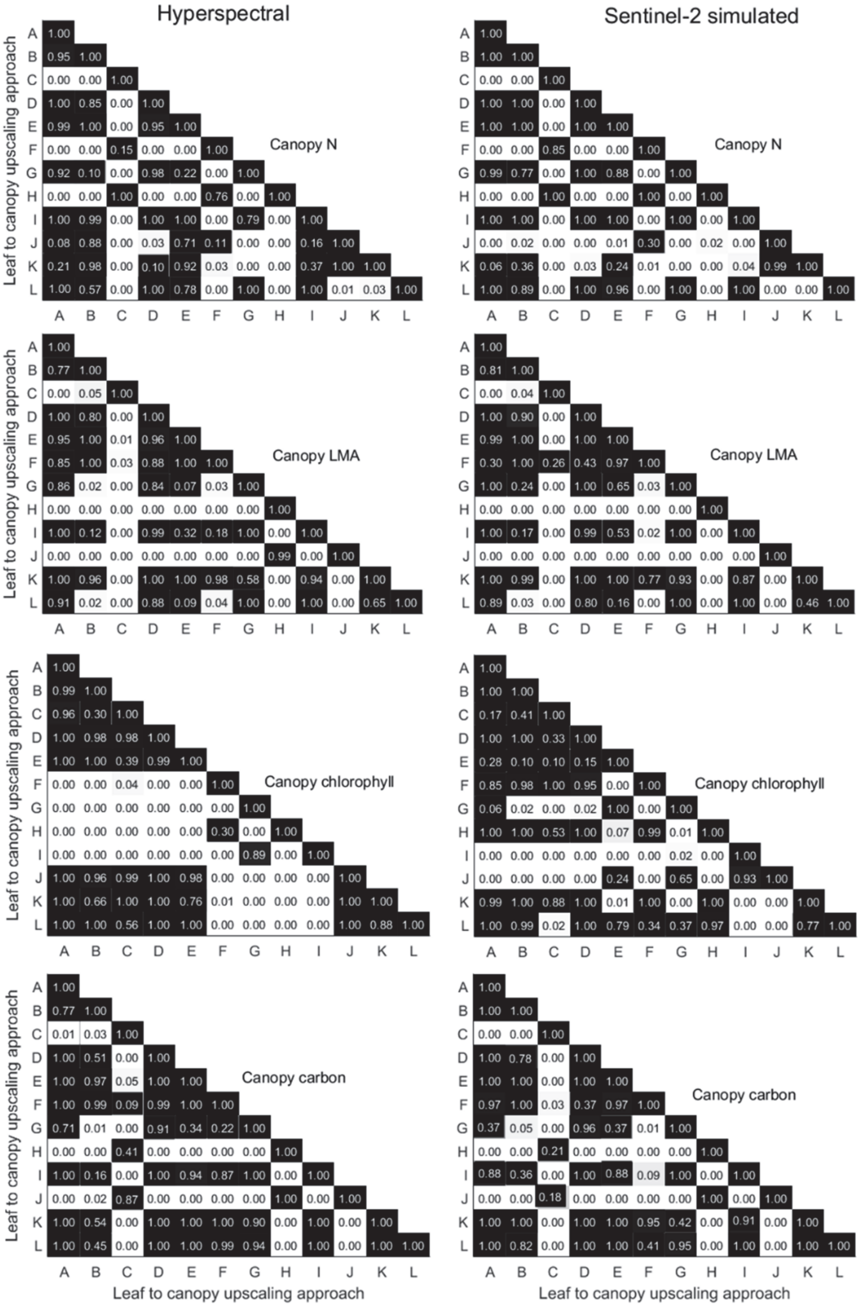

Hyperspectral – Canopy N

	A	B	C	D	E	F	G	H	I	J	K	L
A	1.00											
B	0.95	1.00										
C	0.00	0.00	1.00									
D	1.00	0.85	0.00	1.00								
E	0.99	1.00	0.00	0.95	1.00							
F	0.00	0.00	0.15	0.00	0.00	1.00						
G	0.92	0.10	0.00	0.98	0.22	0.00	1.00					
H	0.00	0.00	1.00	0.00	0.00	0.76	0.00	1.00				
I	1.00	0.99	0.00	1.00	1.00	0.00	0.79	0.00	1.00			
J	0.08	0.88	0.00	0.03	0.71	0.11	0.00	0.00	0.16	1.00		
K	0.21	0.98	0.00	0.10	0.92	0.03	0.00	0.00	0.37	1.00	1.00	
L	1.00	0.57	0.00	1.00	0.78	0.00	1.00	0.00	1.00	0.01	0.03	1.00

Sentinel-2 simulated – Canopy N

	A	B	C	D	E	F	G	H	I	J	K	L
A	1.00											
B	1.00	1.00										
C	0.00	0.00	1.00									
D	1.00	1.00	0.00	1.00								
E	1.00	1.00	0.00	1.00	1.00							
F	0.00	0.00	0.85	0.00	0.00	1.00						
G	0.99	0.77	0.00	1.00	0.88	0.00	1.00					
H	0.00	0.00	1.00	0.00	0.00	1.00	0.00	1.00				
I	1.00	1.00	0.00	1.00	1.00	0.00	1.00	0.00	1.00			
J	0.00	0.02	0.00	0.00	0.01	0.30	0.00	0.02	0.00	1.00		
K	0.06	0.36	0.00	0.03	0.24	0.01	0.00	0.00	0.04	0.99	1.00	
L	1.00	0.89	0.00	1.00	0.96	0.00	1.00	0.00	1.00	0.00	0.00	1.00

Hyperspectral – Canopy LMA

	A	B	C	D	E	F	G	H	I	J	K	L
A	1.00											
B	0.77	1.00										
C	0.00	0.05	1.00									
D	1.00	0.80	0.00	1.00								
E	0.95	1.00	0.01	0.96	1.00							
F	0.85	1.00	0.03	0.88	1.00	1.00						
G	0.86	0.02	0.00	0.84	0.07	0.03	1.00					
H	0.00	0.00	0.00	0.00	0.00	0.00	0.00	1.00				
I	1.00	0.12	0.00	0.99	0.32	0.18	1.00	0.00	1.00			
J	0.00	0.00	0.00	0.00	0.00	0.00	0.00	0.99	0.00	1.00		
K	1.00	0.96	0.00	1.00	1.00	0.98	0.58	0.00	0.94	0.00	1.00	
L	0.91	0.02	0.00	0.88	0.09	0.04	1.00	0.00	1.00	0.00	0.65	1.00

Sentinel-2 simulated – Canopy LMA

	A	B	C	D	E	F	G	H	I	J	K	L
A	1.00											
B	0.81	1.00										
C	0.00	0.04	1.00									
D	1.00	0.90	0.00	1.00								
E	0.99	1.00	0.00	1.00	1.00							
F	0.30	1.00	0.26	0.43	0.97	1.00						
G	1.00	0.24	0.00	1.00	0.65	0.03	1.00					
H	0.00	0.00	0.00	0.00	0.00	0.00	0.00	1.00				
I	1.00	0.17	0.00	0.99	0.53	0.02	1.00	0.00	1.00			
J	0.00	0.00	0.00	0.00	0.00	0.00	0.00	0.00	0.00	1.00		
K	1.00	0.99	0.00	1.00	1.00	0.77	0.93	0.00	0.87	0.00	1.00	
L	0.89	0.03	0.00	0.80	0.16	0.00	1.00	0.00	1.00	0.00	0.46	1.00

Hyperspectral – Canopy chlorophyll

	A	B	C	D	E	F	G	H	I	J	K	L
A	1.00											
B	0.99	1.00										
C	0.96	0.30	1.00									
D	1.00	0.98	0.98	1.00								
E	1.00	1.00	0.39	0.99	1.00							
F	0.00	0.00	0.04	0.00	0.00	1.00						
G	0.00	0.00	0.00	0.00	0.00	0.00	1.00					
H	0.00	0.00	0.00	0.00	0.00	0.30	0.00	1.00				
I	0.00	0.00	0.00	0.00	0.00	0.00	0.89	0.00	1.00			
J	1.00	0.96	0.99	1.00	0.98	0.00	0.00	0.00	0.00	1.00		
K	1.00	0.66	1.00	1.00	0.76	0.01	0.00	0.00	0.00	1.00	1.00	
L	1.00	1.00	0.56	1.00	1.00	0.00	0.00	0.00	0.00	1.00	0.88	1.00

Sentinel-2 simulated – Canopy chlorophyll

	A	B	C	D	E	F	G	H	I	J	K	L
A	1.00											
B	1.00	1.00										
C	0.17	0.41	1.00									
D	1.00	1.00	0.33	1.00								
E	0.28	0.10	0.10	0.15	1.00							
F	0.85	0.98	1.00	0.95	0.00	1.00						
G	0.06	0.02	0.00	0.02	1.00	0.00	1.00					
H	1.00	1.00	0.53	1.00	0.07	0.99	0.01	1.00				
I	0.00	0.00	0.00	0.00	0.00	0.00	0.02	0.00	1.00			
J	0.00	0.00	0.00	0.00	0.24	0.00	0.65	0.00	0.93	1.00		
K	0.99	1.00	0.88	1.00	0.01	1.00	0.00	1.00	0.00	0.00	1.00	
L	1.00	0.99	0.02	1.00	0.79	0.34	0.37	0.97	0.00	0.00	0.77	1.00

Hyperspectral – Canopy carbon

	A	B	C	D	E	F	G	H	I	J	K	L
A	1.00											
B	0.77	1.00										
C	0.01	0.03	1.00									
D	1.00	0.51	0.00	1.00								
E	1.00	0.97	0.05	1.00	1.00							
F	1.00	0.99	0.09	0.99	1.00	1.00						
G	0.71	0.01	0.00	0.91	0.34	0.22	1.00					
H	0.00	0.00	0.41	0.00	0.00	0.00	0.00	1.00				
I	1.00	0.16	0.00	1.00	0.94	0.87	1.00	0.00	1.00			
J	0.00	0.02	0.87	0.00	0.00	0.00	0.00	1.00	0.00	1.00		
K	1.00	0.54	0.00	1.00	1.00	1.00	0.90	0.00	1.00	0.00	1.00	
L	1.00	0.45	0.00	1.00	1.00	0.99	0.94	0.00	1.00	0.00	1.00	1.00

Sentinel-2 simulated – Canopy carbon

	A	B	C	D	E	F	G	H	I	J	K	L
A	1.00											
B	1.00	1.00										
C	0.00	0.00	1.00									
D	1.00	0.78	0.00	1.00								
E	1.00	1.00	0.00	1.00	1.00							
F	0.97	1.00	0.03	0.37	0.97	1.00						
G	0.37	0.05	0.00	0.96	0.37	0.01	1.00					
H	0.00	0.00	0.21	0.00	0.00	0.00	0.00	1.00				
I	0.88	0.36	0.00	1.00	0.88	0.09	1.00	0.00	1.00			
J	0.00	0.00	0.18	0.00	0.00	0.00	0.00	1.00	0.00	1.00		
K	1.00	1.00	0.00	1.00	1.00	0.95	0.42	0.00	0.91	0.00	1.00	
L	1.00	0.82	0.00	1.00	1.00	0.41	0.95	0.00	1.00	0.00	1.00	1.00

Figure 4.5 Pairwise comparison of the upscaling approaches based on the *Tukey's* HSD *post hoc* test. Values in each cell indicate the p-value of each pairwise comparison. White and black cells represent significant and non-significant pairwise comparison, respectively (α = 0.05).

4.3.3 Effect of upscaling approach on model prediction using simulated Sentinel-2 data

Generally, upscaling option C yielded the lowest retrieval accuracy for canopy N ($NRMSE_{cv}$ = 0.23), LMA ($NRMSE_{cv}$ = 0.22) and C ($NRMSE_{cv}$ = 0.21) compared to the other primary upscaling approaches (A, B, D and E) (see Fig 4.4) using simulated Sentinel-2 dataset. The $NRMSE_{cv}$ generated from upscaling approach C were significantly ($p < 0.05$) different from $NRMSE_{cv}$ generated the other primary upscaling approaches (A, B, D and E) in canopy N, LMA and carbon estimations (Fig 4.5). No significant difference ($p > 0.05$) in $NRMSE_{cv}$ were observed between upscaling options A, B, D and E implying they yield comparable results for canopy N, LMA and carbon estimations. The generated R^2_{cv}, confirmed that upscaling approaches A, B, D and E outperformed upscaling approach C for canopy N, LMA and carbon estimations (Table 4.4). In contrast, upscaling approach C yielded the highest retrieval accuracy for canopy chlorophyll estimation compared to upscaling approaches A, B, D and E. On average, upscaling approach C yielded the lowest NRMSE ($NRMSE_{cv}$ = 0.17; Fig 4.4) and highest R^2 (R^2_{cv} = 0.62; Table 4.4) compared to other upscaling options for canopy chlorophyll estimation. However, the generated $NRMSE_{cv}$ were not statistically significantly different ($p > 0.05$) between upscaling approach C and the other primary upscaling approaches i.e. A, B, D and E (Fig 4.5).

Similar to the results observed for canopy trait estimation using *in-situ* hyperspectral measurements, functional attributes (leaf traits and LAI) of the top two canopy layers imposed a strong influence on canopy N, LMA and carbon estimations using simulated Sentinel-2 data. For example, upscaling approach I (leaf traits and LAI of the middle canopy layer) outperformed upscaling approaches H (leaf traits and LAI of the top canopy layer) and J (leaf traits of the bottom canopy layer and × LAI of the bottom canopy layer) for canopy N, LMA and carbon estimation (Fig 4.4). For canopy chlorophyll estimation upscaling approach H ($NRMSE_{cv}$ = 0.18) outperformed upscaling approach I (NRMSEcv = 0.23) demonstrating that the top layer imposes a strong influence on canopy chlorophyll estimation from simulated Sentinel-2 data (Fig 4.4).

Table 4.3 Performance of PLSR reflectance models based on in-situ hyperspectral measurements

UA	Canopy N		Canopy LMA		Canopy C_{ab}		Canopy Carbon	
	nlv	R^2cv±SD	nlv	R^2cv±SD	nlv	R^2cv±SD	nlv	R^2cv±SD
A	2	0.78±0.15	2	0.66±0.18	2	0.65±0.27	3	0.76±0.11
B	2	0.76±0.16	2	0.65±0.19	2	0.64±0.28	3	0.77±0.12
C	2	0.60±0.22	2	0.58±0.17	2	0.68±0.25	2	0.71±0.14
D	2	0.79±0.15	2	0.67±0.17	2	0.64±0.27	3	0.79±0.14
E	2	0.73±0.14	2	0.63±0.16	3	0.57±0.28	3	0.74±0.1
F	2	0.64±0.18	2	0.6±0.21	2	0.61±0.3	3	0.76±0.17
G	2	0.74±0.2	2	0.65±0.22	2	0.64±0.26	3	0.78±0.18
H	2	0.57±0.24	2	0.48±0.2	2	0.38±0.27	2	0.64±0.2
I	2	0.68±0.16	2	0.63±0.24	2	0.56±0.25	3	0.74±0.16
J	2	0.49±0.23	1	0.51±0.29	2	0.5±0.26	3	0.66±0.24
K	2	0.62±0.19	2	0.54±0.16	2	0.64±0.23	3	0.62±0.11
L	2	0.7±0.16	2	0.6±0.16	2	0.6±0.27	3	0.72±0.15

UA: Upscaling approach, nlv: number of latent variables, SD: standard deviation

Table 4.4 Performance of PLSR reflectance models calibrated based simulated Sentinel-2

UA	Canopy N		Canopy LMA		Canopy C_{ab}		Canopy Carbon	
	nlv	R^2_{cv}±SD	nlv	R^2_{cv}±SD	nlv	R^2_{cv}±SD	nlv	R^2_{cv}±SD
A	3	0.73±0.15	3	0.62±0.17	3	0.59±0.24	2	0.73±0.19
B	3	0.73±0.16	3	0.62±0.19	3	0.56±0.28	2	0.73±0.15
C	3	0.53±0.2	3	0.53±0.21	3	0.62±0.2	2	0.67±0.17
D	3	0.71±0.18	3	0.59±0.23	3	0.57±0.23	2	0.75±0.18
E	3	0.68±0.16	2	0.57±0.21	3	0.5±0.24	2	0.70±0.15
F	2	0.52±0.27	3	0.51±0.27	3	0.55±0.24	2	0.7±0.18
G	3	0.67±0.24	3	0.59±0.25	3	0.57±0.24	2	0.75±0.16
H	3	0.49±0.22	2	0.43±0.25	3	0.35±0.26	2	0.6±0.19
I	3	0.64±0.17	3	0.57±0.21	3	0.5±0.27	2	0.71±0.18
J	2	0.39±0.32	2	0.36±0.26	3	0.42±0.25	2	0.61±0.25
K	3	0.6±0.17	3	0.5±0.2	3	0.57±0.25	2	0.52±0.18
L	3	0.70±0.15	3	0.56±0.19	3	0.53±0.27	3	0.66±0.15

UA: Upscaling approach, nlv: number of latent variables, SD: standard deviation

4.4 Discussion

This study set out to examine the effect of different approaches of upscaling foliar N, LMA, chlorophyll and carbon from leaf to canopy level on model performance and estimation accuracy using *in-situ* canopy hyperspectral measurements and simulated Sentinel-2 data. Results of this study demonstrate that leaf to canopy upscaling approaches have a profound effect on the estimation of canopy traits. In comparison to other upscaling approaches the widely-used product of top of canopy traits and total canopy LAI (upscaling approach C) consistently underperformed ($NRMSE_{cv} > 0.2$) compared to other primary upscaling approaches ($NRMSE_{cv} < 0.2$) that consider the contribution of leaf traits content from the shaded middle and lower canopy layers (Fig 4.4). This demonstrates that functional attributes (LAI and leaf traits) of the top canopy layer did not completely control the spectral reflectance observed by the sensor. Upscaling approaches that include functional attributes of the top and middle canopy layers (upscaling approaches B, E) significantly, ($p < 0.05$) improved the estimation accuracies of the canopy traits (Fig 4.5). However, upscaling approaches that considered functional attributes of the three layers (upscaling approach A and D) yielded comparable results to upscaling approaches that considered traits of the top two layers (upscaling B and E; Fig 4.4 and 4.5). The inclusion of functional attributes (leaf traits and LAI) of the lower canopy layer did not significantly improve the estimation accuracy of canopy traits. This demonstrates that canopy reflectance observed by a sensor is not necessarily generated by the entire canopy. The obscured foliage material of the lower canopy contributed less to the canopy spectral signal (Roelofsen *et al.*, 2013). This observation can be linked to the problem of saturation in reflectance and vegetation indices with increasing amount of vegetation (Mutanga and Skidmore, 2004; Prabhakara *et al.*, 2015). Saturation occurs when spectral reflectance or indices reach an asymptotic level beyond which any further increase in vegetation biomass or LAI does not result in a significant change on the spectral signal or index (Liang *et al.*, 2015). This problem may lead to inaccurate and underestimation of canopy traits in high LAI or biomass environments (Thenkabail *et al.*, 2000).

In contrast to observations made on canopy N, LMA and carbon, canopy chlorophyll estimations exhibited an improved relationship with upscaling approach C (leaf traits of the top canopy layer and total LAI) (Fig 4.4). Upscaling approach C yielded the highest R2cv and lowest $NRMSE_{cv}$ in canopy chlorophyll estimations for both *in-situ* hyperspectral measurements (R^2_{cv} = 0.68 and $NRMSE_{cv}$ = 0.24) and simulated Sentinel-2 data (R^2_{cv} = 0.62 and $NRMSE_{cv}$ =0.17). The top layer proved to have a strong influence on canopy chlorophyll estimation for both spectral datasets. This observation concurs with previous studies (Gitelson *et al.*, 2005a; Verrelst *et al.*, 2010) that demonstrate that canopy reflectance (especially in the visible spectrum) is strongly influenced by chlorophyll content of the upper canopy layer due to strong chlorophyll sensitivity within the visible spectrum. However, the explained variance and model accuracy generated from upscaling approach C for canopy chlorophyll estimations for both spectral datasets were not significantly different ($p > 0.05$) from the other primary upscaling approaches that consider the contribution of the exposed top canopy layer together with the shaded middle and bottom layers (Fig 4.5). In this regard, estimation of both dry matter related traits (i.e. N, LMA and carbon) and leaf pigments such as chlorophyll need to consider the vertical variation in leaf traits for improved prediction and mapping of these traits at landscape and regional landscapes. It is important to note that a number of studies report a wide range of explained variances in leaf traits estimation ranging from as low as 46% for canopy N (Ramoelo *et al.*, 2015a) to as high as 92% for canopy chlorophyll (Clevers and Gitelson, 2013) using *in-situ* hyperspectral measurements and simulated Sentinel-2 multispectral data. Most of these studies do not generally provide detailed description of how the leaf traits were upscaled to canopy level. Our results suggest that the approach used to upscale foliar traits from leaf-to-canopy level is a potential source of uncertainty in canopy trait estimation especially in less foliated vegetation biomes where foliage material from the lower canopy contributes to the canopy reflectance.

To understand the relative influence of leaf traits and LAI for each canopy layer on model performance and estimation accuracy, different upscaling combinations of foliar traits and LAI were explored (Table 4.1). Our results indicate that the middle layer had a key effect on the estimation of N, LMA and carbon from *in-situ* canopy hyperspectral measurements and simulated Sentinel-2 data. Leaf-to-canopy upscaling approaches that excluded functional attributes of the middle layer (e.g. upscaling approaches F, H and J) resulted in low explained variance (R^2_{cv} = 0.6, 0.48 and 0.51) and estimation accuracy ($NRMSE_{cv}$ = 0.2, 0.21 and 0.27), compared to upscaling approaches such as G and I (R^2_{cv} = 0.65 and 0.63 and $NRMSE_{cv}$ = 0.15, 0.16 respectively) that included functional attributes of the middle layer in canopy LMA estimation using *in-situ* hyperspectral measurements (Fig 4.4, Table 4.3 and 4.4). A similar pattern was also observed in canopy N; carbon model estimations using either *in-situ* hyperspectral measurements or simulated Sentinel-2 data (Fig 4.4). This observation can be ascribed to the high LAI values of the middle layer (Fig 4.2), which ultimately controlled canopy radiation dynamics (Wang and Li, 2013).

Results of this study also indicated the effect of leaf traits vertical heterogeneity on canopy traits estimation from spectral data. This was shown when different combination of leaf traits from the three canopy layers were explored whilst LAI remained invariant. For example, upscaling approach B (mean traits of the top two layers × total canopy LAI), K (mean traits of the top and bottom layers × total canopy LAI) and L (mean traits of the middle and bottom layers × total canopy LAI) were all computed based on total canopy LAI, however they generated different explained variances and $NRMSE_{cv}$ for N, LMA and carbon. For instance, upscaling approaches B, K and L yielded R^2_{cv} of 0.76, 0.62 and 0.7 for *in-situ* hyperspectral measurements and 0.73, 0.6 and 0.7 for a simulated Sentinel-2 dataset for canopy N prediction models. The average of leaf traits of the top and middle canopy layers (B) resulted in a higher R^2_{cv} (0.76 and 0.73 for *in-situ* hyperspectral and simulated Sentinel-2 data), while the combination of the middle and bottom (upscaling approach L) resulted in explained variance dropping by 6% and 3% respectively for *in-situ* hyperspectral and simulated Sentinel-2 respectively. However, the exclusion of the leaf traits content of the middle layer (upscaling approach K) resulted in a further decrease in explained variance by 8 and 10% for *in-situ* hyperspectral and simulated Sentinel-2, respectively. A similar pattern can also be observed for canopy LMA or carbon for both *in-situ* hyperspectral measurements and simulated Sentinel-2 data. This result indicate that leaf traits of the top and middle canopy layers together with their respective LAI drive canopy reflectance observed by the sensor. This result conforms to Wang and Li's (2013) observation that the vertical heterogeneity in leaf chlorophyll, water and dry matter content variation have a significant effect on simulated canopy reflectance. This observation is also in agreement with Luo *et al*. (2016) who demonstrated that the top three layers of ~ 2 meters high wetland reeds were key in canopy N prediction using vegetation indices computed from *in-situ* hyperspectral measurements. In this regard, the vertical variation in both LAI and leaf traits have an effect on the relationship between canopy reflectance and the canopy traits. This imply that large uncertainties can be presented in canopy parameter estimations if information on the vertical variation of key traits is not incorporated in the modelling approach. However, as LAI is often measured as total canopy LAI (Peng *et al.*, 2017), significant consideration should, therefore be placed on leaf traits that vary across the canopy.

Results obtained in this study are similar to observations of earlier studies (Coble *et al.*, 2016b; Mercado *et al.*, 2006; Sprintsin *et al.*, 2012) that reported that the "big leaf" approach underestimates quantification of total canopy processes such as total canopy photosynthesis and gross primary productivity compared to the "two leaf" approach. The "big leaf" approach assumes that unshaded, sunlit leaves in the upper canopy represents the whole canopy metabolic processes, while the 'two leaf' approach accounts for canopy metabolic processes based on both sunlit and shaded leaves. Sprintsin *et al*. (2012) observed that gross primary production models calibrated based on the big leaf upscaling approach consistently yielded low explained variance and accuracy in gross primary productivity modelling across different vegetation biomes against flux tower measurements. Their study demonstrated that the exclusion of the photosynthetic contribution of the shaded leaves could underestimate canopy gross photosynthesis productivity by over 70% in highly clumped vegetation stands. In light of this background, the "big leaf" is closely related to upscaling approach C that only considered leaf traits of the upper layer. The "two leaf" approach closely resemble the other primary upscaling approaches (A, B, D and E) that factor in the contribution of foliage material from both the exposed upper layers and the shaded lower layers. This observation demonstrate that canopy reflectance observed by a sensor constitutes contribution of all foliage material within the canopy.

Importantly, our study examines the effect of upscaling leaf traits from the leaf to canopy level using *in-situ* canopy hyperspectral and simulated Sentinel-2 data. Results obtained in this study can be tested in forests or woodlands where foliage from the lower canopy contributes to canopy reflectance. Partitioning the total canopy LAI into sunlit and shaded layers following methods such as those proposed by Chen *et al*. (1999) and subsequently collecting leaf samples from both sunlit and shaded layers are critical in examining the contribution of each canopy layer in canopy trait estimations. Hence, the effect of separating LAI and leaf samples into sunlit and shaded on canopy traits estimation using airborne or satellite data need further investigation.

4.5 Conclusion

In this study, we evaluated the effect of different approaches of upscaling leaf traits to the canopy level on the accuracy of estimation of canopy N, LMA, chlorophyll and carbon from *in-situ* hyperspectral measurements and simulated Sentinel-2 reflectance data. Through a robust sampling procedure, we determined leaf traits from different vertical canopy positions and applied various weighted averages to examine how various canopy components affects the estimation of canopy traits from *in-situ* canopy hyperspectral and simulated Sentinel-2 data. Based on the results we conclude that:

i. Leaf-to-canopy upscaling approaches yield significantly different canopy traits values. The range (max-min) of the canopy traits varies depending on the upscaling approach used.

ii. Leaf-to-canopy upscaling approaches that consider the contribution of both the exposed upper canopy leaves together with the shaded lower canopy leaves results in improved prediction of canopy nitrogen, LMA and carbon from both *in-situ* canopy hyperspectral measurements and simulated Sentinel-2 data. However, the same pattern does not hold true for canopy chlorophyll.

iii. The widely used upscaling approach that considers leaf traits from the exposed top of the canopy yields a better accuracy for canopy chlorophyll estimation from *in-situ* canopy hyperspectral measurements. However, the prediction errors obtained among the canopy chlorophyll upscaling approaches were not significantly different ($p > 0.05$).

We therefore, conclude that sampling methods that intend to use remote sensing measurements to upscale leaf traits, especially dry matter related leaf traits, need to account for the vertical heterogeneity in leaf traits across plant canopies for improved canopy traits estimation and mapping. As this study was conducted in the laboratory setup with relatively short shrubs, it is important to ascertain whether similar results can be obtained in high-foliated forests using airborne or satellite spectral measurements.

Chapter 5

Knowledge on the vertical heterogeneity in leaf traits is essential for accurate modelling of canopy trait content using seasonal Sentinel-2 imagery[*]

---

[*] This chapter is based on Gara, T.W., Skidmore, A. K., Darvishzadeh, R., Wang, T. and Heurich Marco (*Under review after first revision*) Knowledge on the vertical heterogeneity in leaf traits is essential for accurate modelling of canopy trait content using seasonal Sentinel-2 imagery**.** *ISPRS Journal of Photogrammetry and Remote Sensing*

Abstract

Leaf traits at canopy level (*hereinafter* canopy traits) are conventionally expressed as a product of total canopy leaf area index (LAI) and leaf trait content based on samples collected from the exposed upper canopy. This traditional expression is centered on the theory that absorption of incident photosynthetically active radiation (PAR) follow a bell-shaped function skewed to the upper canopy. However, the validity of this theory has remained untested for a suite of canopy traits in a temperate forest ecosystem across multiple seasons using multispectral imagery. In this study, we examined the effect of canopy traits expression on modelling canopy traits using Sentinel-2 multispectral data across the growing season in Bavaria Forest National Park (BFNP), Germany. To achieve this, we measured leaf mass per area (LMA), chlorophyll (C_{ab}), nitrogen (N) and carbon content and LAI from the exposed upper and shaded lower canopy respectively over three seasons (spring, summer and autumn). Subsequently, we estimated canopy traits using two expressions i.e. the traditional expression-based on the product of LAI and leaf traits content of samples collected from the sunlit upper canopy (*hereinafter* top-of-canopy expression) and the weighted expression - established on the proportion between the shaded lower and sunlit upper canopy LAI and their respective leaf traits content. Using a Random Forest machine-learning algorithm, we separately modelled canopy traits estimated from the two expressions using Sentinel-2 spectral bands and vegetation indices. Our results showed that dry matter related canopy traits (LMA, N and carbon) estimated based on the weighted canopy expression yield stronger correlations and higher prediction accuracy (generally $NRMSE_{CV} < 0.19$) compared to the top-of-canopy traits expression across all seasons. In contrast, canopy chlorophyll estimated from the top-of-canopy expression demonstrated strong fidelity with Sentinel-2 bands and vegetation indices ($RMSE < 0.48$ μg/cm^2) compared to weighted canopy chlorophyll ($RMSE > 0.48$ μg/cm^2) across all seasons. We also developed a generalized model that explained 52.57 - 67.82% variation in canopy traits across the three seasons. Using the most accurate Random Forest model for each season, we demonstrated the capability of Sentinel-2 data to map seasonal dynamics of canopy traits across the park. Results presented in this study revealed that canopy trait expression can have a profound effect on the modelling the accuracy of canopy traits using satellite imagery throughout the growing seasons. These findings have implications on model accuracy when monitoring the dynamics of ecosystem functions, processes and services.

5.1 Introduction

Effects of land use change; climate change and variability on terrestrial ecosystems are critical to the accurate characterization and quantification of essential biodiversity variable (EBVs). Knowledge on ecosystem functions such as primary productivity and nutrient cycling provide an opportunity to assess the health and adaptation capacity of vegetation ecosystems in face of global environmental change (Pettorelli *et al.*, 2016). Plant traits such as leaf mass per area (LMA), chlorophyll content (C_{ab}), leaf nitrogen (N) and leaf carbon are important in understanding ecosystem processes, functions and services over space and time. For instance, C_{ab} is a critical indicator of plant vigour, phenological stage and photosynthetic capacity (Kalacska *et al.*, 2015; Lichtenthaler and Buschmann, 2001). Leaf dry matter and carbon content quantitatively express the plant economic spectrum strategy in terms of nutrients uptake and use, light harvesting and carbon sequestration (Niinemets *et al.*, 1999). Foliar N is an important element in C_{ab} and a constituent in enzymes responsible for atmospheric carbon fixation (Archontoulis *et al.*, 2011; Clevers and Gitelson, 2013).

Variations in leaf physiological, biochemical and morphological properties strongly rely on the phenological stage of vegetation. Leaf traits change over time through the growing season due to shifts in diurnal temperature and rainfall (Behrman *et al.*, 2015; Workie and Debella, 2018). In addition, leaf traits also exhibit change due to variation in light environments within a canopy such as moving from the sunlit upper to shaded lower canopy (Coble *et al.*, 2016b). Irradiated leaves from the upper canopy display higher nutrient content compared to leaves from the shaded lower canopy. For example, Gara *et al.*(2018a) observed that sunlit upper canopy leaves display higher content of chlorophyll, nitrogen, LMA, EWT and carbon compared to shaded leaves of the lower canopy. The vertical heterogeneity in leaf traits across the canopy can be as much as the phenological variation. The vertical heterogeneity in leaf traits assists in maintaining an equilibrium between the limited rate of carboxylation and the electron transport - limited rate of carboxylation (Chen *et al.*, 1993). These key metabolic processes result in marked differences in morphological, chemical as well as physiological traits between leaves across the vertical canopy domain (Weerasinghe *et al.*, 2014). Plants translocate foliar nutrients during senescence from lower canopy leaves to the upper canopy leaves. The translocation of foliar nutrients to the upper canopy is essential for protein repair and subsequently increase the density of mitochondria per cell area to commensurate the increasing amount of incoming PAR and optimize the photosynthetic capacity of the whole plant (Hikosaka, 2005). As such, accounting for the effect of vertical heterogeneity on foliar traits in spatio-temporal modelling of canopy traits is important for improved understanding of terrestrial ecosystem structure and functioning.

Remote sensing increasingly play a pivotal role in monitoring dynamics of foliar traits over space and time (Moreno-Martínez *et al.*, 2018). *In-situ* plant traits measured from the leaf samples of dominant and co-dominant species within sampling plots can be retrieved from air- or space borne spectral measurements (Homolová *et al.*, 2013). Considering that the traits are determined at leaf level, there is often a need to match spatial scales of *in-situ* measured leaf traits and remote sensing data via upscaling approaches. There are two approaches of upscaling leaf traits to canopy scale i.e. the direct approach and the canopy integrated approach (He and Mui, 2010b). The direct approach relates leaf trait content measured at the leaf level to satellite data without integrating any canopy structural parameter. The direct approach procedure is based on the premise that exposed foliage material controls variation in canopy reflectance and thus sunlit leaves from the upper canopy resemble the entire canopy (Peterson *et al.*, 1988). The canopy integrated approach on the other hand upscales leaf traits to canopy level by accounting for canopy structural parameters such as LAI or crown biomass. The widely used canopy integration approach expresses canopy traits as a product of total canopy LAI and leaf traits content based on leaf samples collected from the sunlit upper canopy (top-of-canopy expression). This approach is centered on the theory that the absorption of incident photosynthetically active radiation (PAR) follows a bell-shaped function sharply skewed to the upper canopy (Kropff and Goudriaan, 1994). This infers that the upper canopy controls canopy radiation dynamics especially with regard to the amount of reflected radiation measured by multispectral sensors. On this basis, the contribution of leaf trait content of shaded leaves from the lower canopy to above canopy reflectance is considered 'insignificant'. However, this theory provides no information on the contribution of the shaded canopy on estimation of canopy traits especially in temperate forests throughout the growing season. A question therefore arises on whether the theory is valid for other leaf traits that control variation in other portions of the electromagnetic spectrum outside the visible spectrum remains unanswered. We hypothesize that leaf traits content from the shaded lower canopy plays a significant contribution to canopy reflectance. Establishing an ecologically meaningful canopy trait value that corresponds to the signal measured by the multispectral instrument is critical in estimating and mapping foliar nutrients at both canopy and landscape scale (Roelofsen *et al.*, 2013). To this end, we hypothesize that canopy traits estimated based on a weighted average between the sunlit upper and shaded lower canopy layers (weighted canopy expression) may improve the accuracy of canopy trait models.

This study therefore seeks to examine the effect of canopy traits expression on modelling canopy traits using Sentinel-2 multispectral data across the growing season in a temperate forest. Firstly, we examined the correlation between Sentinel-2 spectral data and canopy traits estimated from the two canopy expressions. Secondly, we examined variation in estimation accuracy of canopy traits estimated from the two canopy expressions using Sentinel-2 data. Thirdly, we explored the development of a generalized model that captures variation in canopy traits across the growing seasons. Finally, we mapped the variation in canopy traits using the best performing model for each season.

5.2 Materials and methods

5.2.1 Study area

Field measurements were conducted over three seasons of 2017 in Bavarian Forest National Park (BNFP) (Fig 5.1). BNFP is part of the Bohemian Forest Ecosystem. The Park is approximately 24 218 ha in size, with elevation stretching from 600 to 1453 m (Heurich *et al.*, 2010a). Annual precipitation ranges from 1200 to 1800 mm and the park experience a mean annual temperature of ~5^{0} C. The evergreen Norway spruce (*Picea abies*) (67%) and deciduous European beech (*Fagus sylvatica*) (24.5%) are the dominant trees species, while white fir (*Abies abies*) (2.6%), sycamore maple (*Acer pseudoplatanus*) (1.2%), and mountain ash (*Sorbus aucuparia*) (3.1%) are the less dominant species in the park (Cailleret *et al.*, 2014)

5.2.2 Field data collection and laboratory measurements

Field campaigns were conducted during three seasons, i.e. spring, summer and autumn of 2017. Spring data (32 plots) were collected from mid-May to mid-June, while summer field data (40 plots) were collected between mid-July and mid-August, and the autumn field data (40 plots) were collected from mid-September to mid-October. We randomly generated sampling sites in broadleaf, conifer and mixed vegetation stands based on a vegetation map provided by the Department of Visitor Management and National Park Monitoring, Bavarian Forest National Park (Silveyra Gonzalez *et al.*, 2018). Our sample plots were mainly located within the belt transects designed for biodiversity research (Bässler *et al.*, 2009) (Fig 1). In the field, we navigated to the sampling sites using a hand-held Global Positioning System (GPS). At each sampling site, a north-oriented plot of 900 m^2 (30 m × 30 m) was demarcated. We then used a Leica GPS 1200 to measure the precise centre location of each plot (at sub-meter accuracy after post-processing).

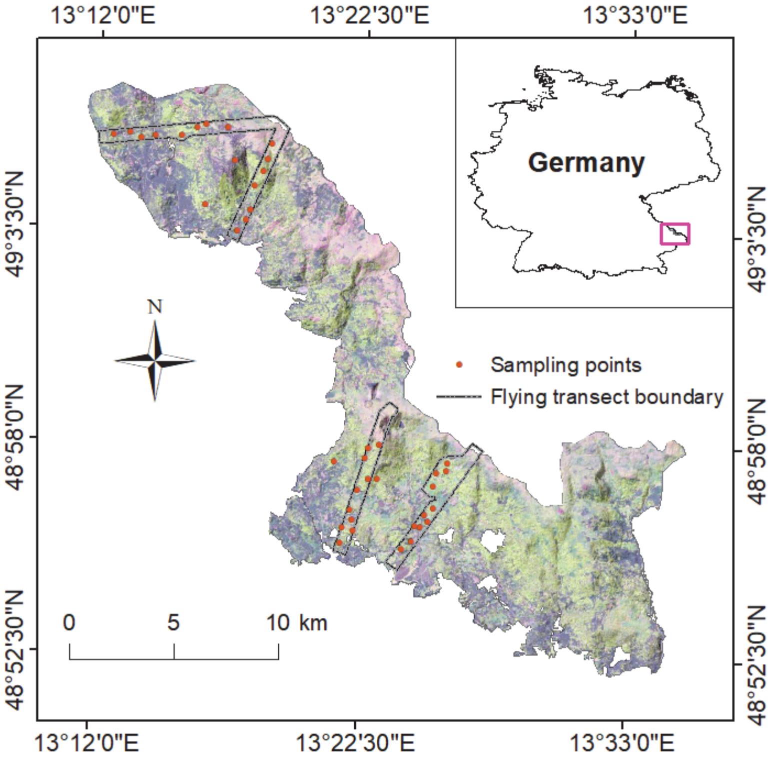

Figure 5.1: The location of Bavaria Forest National Park in Germany and the spatial distribution of sample plots overlaid on a Sentinel-2 satellite imagery of 13 July 2017. Black dotted lines demarcate the boundary of the biodiversity research transects.

Within each plot the following forest structural variables were measured: leaf area index (LAI), stem density, crown diameter, canopy closure and stand height. LAI was measured using a Li-Cor LAI- 2200 plant canopy analyzer. Each plot level LAI was computed based on three reference samples of above canopy radiation (above canopy readings) measured in a nearby open area and five below canopy readings were measured within the plot. Stem density per hectare was determined based on the number of trees with each plot. The height of each tree was estimated using a Nikon Forestry 550 hypsometer.

We then separately collected foliar samples from the exposed upper and shaded lower canopy of each sampled tree. In total, we collected 1 104 leaf samples across the three seasons. A cross bow was used to shoot leaf samples from the sunlit, upper canopy (Ali *et al.*, 2016), whilst an extendable pair of secateurs was used to clip leaf samples from the lowest living branch (Arellano *et al.*, 2017; Atherton *et al.*, 2017). Within each plot, sampling was performed on five trees with a diameter at breast height greater than 10 cm. We labelled the trees to enable identification during subsequent seasonal field measurements. Immediately after collecting the samples we measured leaf chlorophyll using CCM -300 chlorophyll content meter (Opti-Sciences, 2011). We then wrapped the leaf and needle samples with moist paper towels and zip-locked them in polythene bags. The samples were then transported to the laboratory in a cooler with ice packs within 6 hours of collection (Atherton *et al.*, 2017).

Leaf mass per area (LMA, g/cm^2), leaf carbon (Carbon, g/cm^2), nitrogen (N, g/cm^2) and SLA (cm^2/g) were measured in the laboratory. LMA and SLA were retrieved from fresh weight and leaf area as outlined in Gara *et al* (2018b). Leaf nitrogen and carbon were determined using the Perkin Elmer 2400 elemental analyzer. Mass based carbon and nitrogen obtained from elemental analysis were converted to area based by multiplying by LMA (Wang *et al.*, 2015a). Further details on the laboratory procedure and analysis are provided in Gara *et al* (2018a).

5.2.3 Determining plot-level leaf trait

Determining mean leaf trait per plot for a mono-species stand is relatively straightforward compared to a multi-species stand. The mean leaf traits of a mono-species plot is determined by merely averaging leaf trait content of collected samples. However, for a multi-species plot there is need to determine a weighted mean leaf trait content relative to the abundance or foliage biomass of each species within a plot (Homolová *et al.*, 2013). This approach caters for the wide variation in leaf traits content between species within stands. In this study, we computed the plot-level mean trait for the multi-species plots following a procedure described by Wang *et al.*, 2018. The procedure was executed to determine the mean leaf traits content for both sunlit and shaded leaf traits. Essentially, we calculated foliage biomass of each tree species within each plot using established allometric equations (Widlowski *et al.*, 2003). The mean leaf trait content for each plot (LT_{plot}) was weighted relative to fraction of foliage biomass of each species (Eqn 5.1).

$$\mathrm{LT_{plot}} = \sum_{i=1}^{n} \mathrm{LT_i} * \mathrm{fFB_i} \qquad (5.1)$$

Where LT_i is the average leaf trait for species *i* within a plot, fFB is the foliage biomass fraction of species *i* and *n* is the number of species.
The foliage biomass fraction was computed using the following formula (Eqn 5.2)

$$\mathrm{fFB_i} = \frac{\mathrm{fBio_i SLA_i}}{\sum_{i=1}^{n} \mathrm{fBio_i SLA_i}} \qquad (5.2)$$

*ƒ*Bio the foliage biomass fraction of species *i* and SLA is the average specific leaf area for species *i*

5.2.4 Canopy traits expression

In this study, we explored two canopy trait expressions i.e. top-of-canopy and weighted canopy trait. Top-of-canopy expression multiplies leaf trait content of samples collected from the sunlit upper canopy with total canopy LAI. The weighted canopy trait expression computes canopy trait value for each field plot as the weighted sum of LAI and leaf traits for the sunlit and shaded canopy (Eqn 5.3).

$$\sum_{i=1,2} \mathrm{LAI_i} * \mathrm{trait_i} \tag{5.3}$$

where 1 and 2 represents sunlit and shaded canopy layers respectively and trait is leaf traits for each canopy layer

To execute the weighted canopy trait expression we partitioned the total canopy LAI into sunlit fraction and shaded fraction using mathematical formulae (Eqn 5.4 and 5.5) following previous studies (Chen Jing *et al.*, 2012; Sprintsin *et al.*, 2012; Wu *et al.*, 2017).

$$\mathrm{LAI_{sun}} = \frac{1-\exp\left(-\frac{\mathrm{k}*\Omega*\mathrm{LAI_{tot}}}{\cos(\mathrm{SZA})}\right)}{k/\cos(SZA)} \tag{5.4}$$

$$\mathrm{LAI_{shade}} = \mathrm{LAI_{tot}} - \mathrm{LAI_{sun}} \tag{5.5}$$

Where k = extinction coefficient, Ω is clumping index, SZA is solar zenith angle, $\mathrm{LAI_{tot}}$ is canopy total LAI, $\mathrm{LAI_{sun}}$ is sunlit fraction, $\mathrm{LAI_{shade}}$ is shaded fraction. We used an extinction coefficient of 0.7, 0.5 and 0.6 for broadleaf, conifer and mixed plots respectively following Chen *et al.*,(2012). The clumping index for each plot was measured using a LAI 2200 canopy analyzer (Fang *et al.*, 2018). The solar zenith angle was extracted from the Sentinel-2 MSI metadata.

5.2.5 Satellite imagery data and preprocessing

Geometrically corrected top of atmosphere reflectance data of Sentinel-2 Multi-spectral Instrument (MSI, Level 1C) were downloaded from Copernicus Open Access Hub (https://scihub.copernicus.eu/). We downloaded Sentinel-2 images that coincided with the field data collection. For spring, we used a Sentinel-2 image acquired on 13 June 2017, while for summer we used a Sentinel-2 image acquired on 13 July 2017. For autumn, we used a Sentinel-2 image acquired on 26 September 2017. The multi-spectral instrument on board Sentinel-2 MSI data consists of 13 spectral bands spanning from the visible through the NIR to SWIR at a spatial resolution ranging from 10 to 60 m and a swath width of 290 km. Atmospheric correction was performed using Sen2Cor module in Sentinel Application Platform (SNAP). After atmospheric correction, we resampled the 20 m spatial resolution bands (bands 5, 6, 8A, 11 and 12) to 10 m using the nearest neighbour analysis. In this study, bands 1 (coastal aerosol), 9 (water vapour), and 10 (SWIR cirrus) designed for atmospheric analysis were not used for analysis. For the spring and autumn images, we used the output of the Sen2Cor's Scene Classification to mask out pixels classified as saturated or defective, cloud shadow, medium to high cloud probability and thin cirrus.

After pre-processing Sentinel-2 data for each season, we computed a number of vegetation indices as shown in Table 5.1. These vegetation indices were selected guided by their performance in estimating of leaf traits as reported in previous studies (Chemura *et al.*, 2018; Main *et al.*, 2011; Stagakis *et al.*, 2010). To harmonize spatial scales of canopy traits values measured in the field against satellite data, we extracted the reflectance of a plot as the average of nine (3 × 3) pixels centered on the plot centre.

Table 5.1 Vegetation indices evaluated in this study

Index	Formula	S2 bands	Reference
Normalized difference Vegetation Index (NDVI)	$(NIR - RE)/(NIR + RE)$	B5, B8	Gitelson and Merzlyak, (1994); Rouse *et al.*, (1973)
Red-edge Chlorophyll Index (CIrededge)	$\mathrm{NIR/RE3} - 1$	B7, B8	Gitelson *et al.*, (2005b)
Corrected Transformed Vegetation Index (CTVI)	$(\mathrm{NDVI} + 0.5) * \mathrm{NDVI} + 0.5$	B5, B8	Perry and Lautenschlager, (1984)
Renormalized NDVI (rNDVI)	$(\mathrm{NIR} - \mathrm{R})/(\sqrt{\mathrm{NIR} + \mathrm{R}}$	B4, B8	Gitelson and Merzlyak (1994)
Simplified Canopy Chlorophyll Index (SCCCI)	$(\mathrm{NDVI} * \mathrm{RE3})/\mathrm{NDVI}$	B5, B7, B8	Barnes *et al.*, (2000)
Sentinel-2 Red-edge Position (SREP)	$705 + 35 * \frac{\frac{\mathrm{NIR} + \mathrm{R}}{2} - \mathrm{RE}}{\mathrm{RE2} - \mathrm{RE1}}$	B4, B5, B6, B8	Frampton *et al.*, (2013)
Inverted Red-edge Chlorophyll Index (IRECI)	$(\mathrm{NIR} - \mathrm{R})/(\mathrm{RE2/RE1})$	B4, B5, B6, B8	Frampton *et al.*,(2013)
Modified Chlorophyll Absorption Ratio Index (MCARI)	$\left((\mathrm{RE1} - \mathrm{R}) - 0.2 * (\mathrm{B5} - \mathrm{B3})\right) * (\mathrm{B5/B4})$	B3, B4, B5	Daughtry *et al.*,(2000)
Transformed Chlorophyll Absorption in Reflectance Index/Optimized Soil-Adjusted Vegetation Index (TCARI/OSAVI)	$\frac{3[(\mathrm{RE1} - \mathrm{RE3}) - 0.2(\mathrm{RE1} - \mathrm{G})(\mathrm{RE1/R}]}{(1 + 0.16)(\mathrm{NIR} - \mathrm{R})/(\mathrm{NIR} + \mathrm{R} + 0.16)}$	B3, B4, B5, B7, B8	Daughtry *et al.*, (2000) Rondeaux *et al.*, (1996)
Global Environmental Monitoring Index (GEMI)	$\mathrm{n}(1 - 0.25\mathrm{n}) - (\mathrm{R} - 0.125)/(1 - \mathrm{R})$ Where n = $[2(\mathrm{NIR}^2 - \mathrm{R}^2) + 1.5\mathrm{NIR} + 0.5\mathrm{R}]/(\mathrm{NIR} + \mathrm{R} + 0.5)$	B4, B5, B8	Pinty and Verstraete, (1992)

5.2.6 Correlation analysis between Sentinel-2 bands and canopy traits

Prior to modelling canopy traits using the Random Forest algorithm, we used a Pearson's Correlation Coefficient to examine correlations between Sentinel-2 reflectance data and canopy traits estimated from the two canopy expressions. The correlation analysis explores how the canopy traits estimated from the two canopy expressions relate to the satellite data.

5.2.7 Modelling canopy traits using Sentinel-2 data

A machine learning algorithm, Random Forest (RF) validated using repeated *k-fold* cross-validation procedure was used to examine the effect of canopy traits expression on model performance and prediction accuracy. In this study we used the powerful machine learning RF algorithm because: i) it is more stable and equipped to handle collinear datasets such as satellite dataset (Shi *et al.*, 2018) ii) it generates an error matrix for internal validation and allow assessing the importance of each predictor variable (Breiman, 2001; Rodriguez-Galiano *et al.*, 2012) iii) it is computationally efficient and has been used widely in vegetation spectroscopy (Mutanga *et al.*, 2012; Ramoelo *et al.*, 2015b; Yan and de Beurs, 2016). RF employs an iterative bagging technique in which the number of trees (*ntree*) are independently constructed using a subset randomly selected from the training samples (Breiman, 2001). The respective nodes are partitioned based on the best performing input variables (*mtry*). To select the best *ntree* and *mtry* values that predicts canopy traits with the lowest RMSE, we optimized the RF models based on the cross-validated RMSE. We tested *ntree* from 500 to 2500 at 500 interval, while a *mtry* of 1-10 was assessed for models independently developed using vegetation indices and Sentinel 2 spectral bands as co-variates. For models that combined bands and vegetation indices as predictors variables, a *mtry* of 1-20 was evaluated.

The *k-fold* cross validation procedure was used to randomly partition the dataset into ten equal blocks. For each model run, *k-1* of the folds were used to calibrate the model while the other fold was reserved as 'out of bag' to estimate the prediction error and compute a variable importance vector. This procedure was repeated 10 times until all data partitions were exhaustively used for both calibration and validation data. To eliminate bias on the estimate based on the composition of each partition, we repeated the *k-fold* data resampling procedure 10 times. Therefore, 100 models (10-fold cross validation repeated 10 times) were simultaneously calibrated and validated using this procedure. The final model was thus a mean of the 100 models. The robust Mean Decrease Accuracy (%IncMSE) which estimates the increase in mean square error of prediction when a variable is permuted whilst other remain invariant was used to assess the importance of predictor variables (Breiman, 2001). The most important predictor variable yield high values of %IncMSE.

The generalized RF model was developed based on pooled data for the canopy traits and Sentinel data for all the three seasons. The pooled data dataset (n= 102) was randomly split into model calibration (65%) and external validation (35%) dataset. To ensure an even distribution of canopy traits in both the calibration and validation datasets, we sorted and randomly sampled data from each quartile for each season. Similar to seasonal models explained above the calibration dataset was internally validated using repeated *k-fold* cross validation and then the final model was externally validated on the external data that was never used in model calibration. Prior to Random Forest modeling the independent and dependent variable were all mean-centered.

The coefficient of determination (R^2), root mean square error (RMSE) and normalized root mean square error (NRMSE = RMSE/Range) were used to assess the performance of the Random Forest models in predicting the canopy traits using the Sentinel-2 reflectance data. The Random Forest modelling procedure was performed in R.3.5.1 for Windows using the classification and regression (caret) package.

5.3 Results

5.3.1 Seasonal variability in leaf traits across the vertical canopy profile

The trait content (LMA, Cab, N and carbon) for leaf samples collected from the upper canopy were significantly ($\alpha < 0.05$) higher compared with samples collected from the lower canopy throughout the three seasons (Fig 5.2). The variation in leaf traits content between upper canopy and lower canopy samples was more prominent in summer compared to the other seasons. This variation was more distinctive for the dry matter related leaf traits. Generally, the dry matter related leaf traits of the upper canopy demonstrated high seasonal variability compared to lower canopy. As expected, the mean leaf traits content for summer was significantly higher when compared to other seasons for all the leaf traits. Leaf chlorophyll content for summer showed high variability between upper and lower canopy compared to the other two seasons (Fig 5.2).

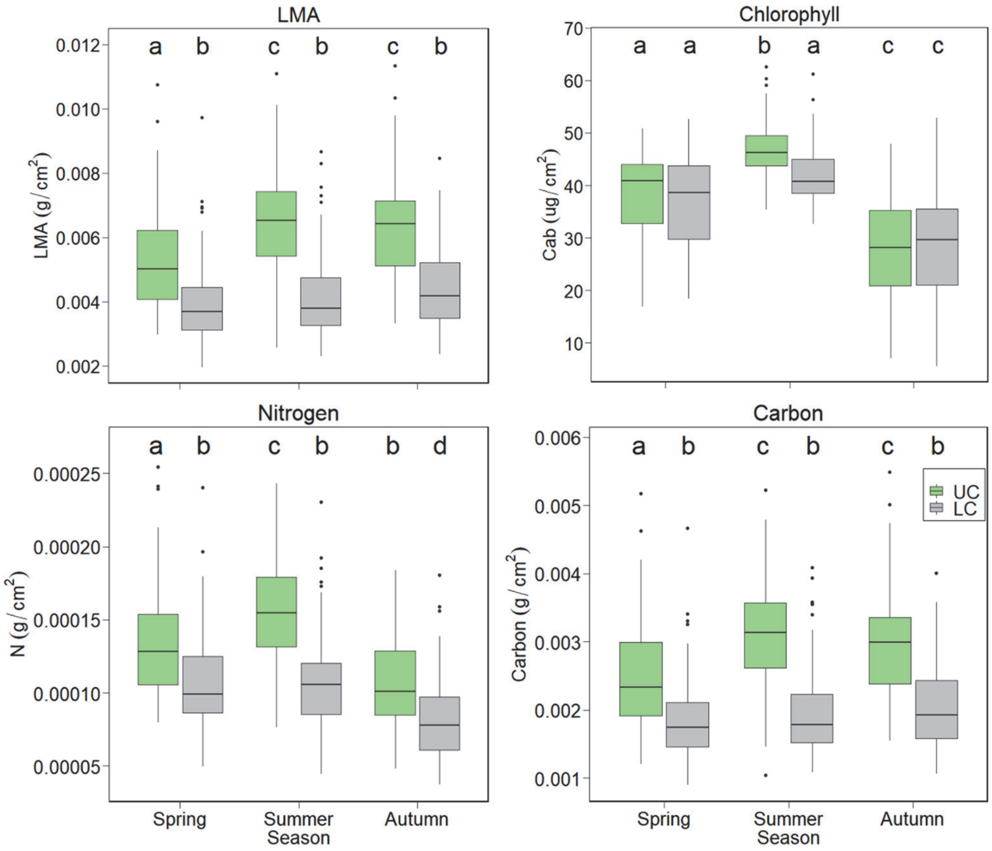

Figure 5.2 Seasonal variation in field measured leaf traits across the canopy vertical profile. Leaf traits with different letters indicate significant ($\alpha < 0.05$) difference based on *Tukey's* HSD test.

5.3.2 Correlation between Sentinel-2 spectral data and canopy traits

The strength of correlation between Sentinel-2 reflectance data and canopy traits varied between the two canopy traits expressions across seasons (Appendix Fig A4) as well as for the pooled dataset (Fig 5.3). Generally, canopy-level LMA, N and carbon estimated from the weighted canopy expression showed a stronger correlation with spectral reflectance of all Sentinel-2 bands compared to canopy traits estimated using the conventional top-of-canopy expression. The difference in correlation between canopy traits and Sentinel 2 spectral data in summer was wider from the red-edge 2 (RE2) band to the SWIR bands through the NIR bands. The SWIR bands and red-edge 1 yielded the highest correlations ($r > - 0.5$, $\alpha < 0.05$) with canopy LMA and carbon estimated using the weighted canopy expression. Canopy nitrogen demonstrated high correlation with the red band and red-edge 1 for the pooled dataset. Canopy N estimated from both canopy expressions demonstrated poor correlation ($-0.25 < r < 0.12$) to Sentinel-2 reflectance data in the summer compared to the two other seasons. LMA and carbon were strongly correlated ($r = 0.98$, $\alpha < 0.05$) and yielded almost similar result across seasons.

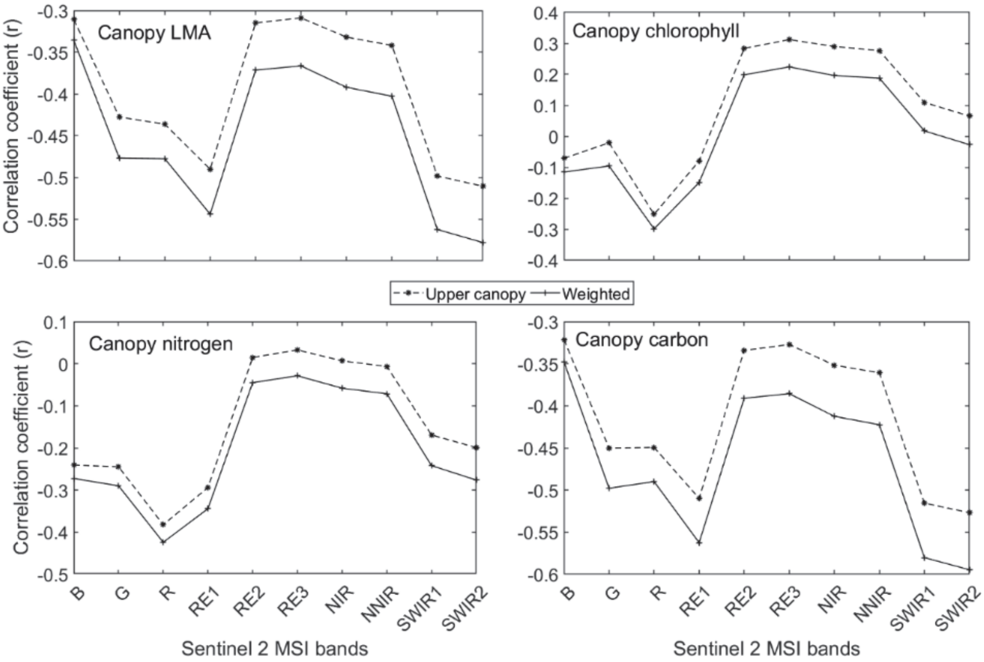

Figure 5.3 Correlation analysis between Sentinel-2 reflectance data and canopy traits for the pooled dataset.

In contrast, canopy chlorophyll estimated based on top-of-canopy expression exhibited a higher correlation with reflectance throughout all the Sentinel-2 bands for the pooled dataset. The difference in correlation was greater in the red-edge, NIR and SWIR bands. A similar observation is also evident for the seasonal correlations between Sentinel-2 spectral data and canopy chlorophyll especially in spring and summer (Appendix: Fig A4). In summer, canopy chlorophyll exhibited an increased correlation with Sentinel spectral data, especially with reflectance data from red edge bands and NIR ($r > 0.5$) compared to spring and autumn.

5.3.3 Effect of canopy trait expression on model performance

We compared the prediction accuracy of canopy traits estimated from the two canopy layer expression methods using RF models trained with reflectance data from Sentinel-2 spectral bands and vegetation indices. Overall, canopy traits estimated from the weighted expressions generated lower values of RMSEP for all models developed for canopy LMA, N and C throughout all the seasons. For example, canopy LMA was estimated with an error of 120.38 and 144.41 g/cm^2 for the weighted and top-of-canopy respectively for spring using the optimized model (Table 5.2). In summer, canopy N was estimated with an error of 1.47 and 1.77 g/cm^2 for weighted and top-of-canopy respectively for the optimized models (Table 5.3). Canopy carbon was also estimated with an error of 26.02 and 29.9 g/cm^2 for the weighted and top-of-canopy expressions for the optimized models (Table 5.4). All co-variates demonstrated a similar prediction pattern for the canopy traits estimated from the two canopy traits expressions.

Generally, the accuracy of estimation for all canopy traits increased in the order of spring, summer and autumn for all models across seasons. For example, canopy N was estimated with an error of 1.85, 1.47 and 1.03 g/cm^2 for spring, summer and autumn respectively. Canopy chlorophyll was estimated with an RMSEP of 0.48, 0.37 and 0.34 g/cm^2 for spring, summer and autumn respectively. A similar pattern was also observed for canopy LMA and carbon.

Table 5.2: Performance of the Random Forest model in modelling canopy traits for the spring season

		Based on sunlit canopy			Weighted canopy		
Trait	Co-variates	R^2 (SD)	RMSEP (SD)	NRMSE (SD)	R^2 (SD)	RMSEP (SD)	NRMSE (SD)
LMA_c	Raw bands	0.66 (0.36)	152.5 (90.62)	0.15 (0.089)	0.63 (0.35)	128.11 (74.37)	0.15 (0.089)
	VI	0.64 (0.32)	171.92 (89.57)	0.17 (0.089)	0.63 (0.35)	145.85 (70.75)	0.17 (0.084)
	Bands + VI	0.65 (0.34)	158.99 (89.64)	0.16 (0.089)	0.64 (0.34)	135.31 (67.35)	0.16 (0.08)
	Optimized	0.67 (0.34)	144.41 (90.69)	0.14 (0.09)	0.72 (0.33)	120.38 (74.45)	0.14 (0.08)
Cab_c	Raw bands	0.55 (0.38)	0.55 (0.22)	0.23 (0.092)	0.48 (0.38)	0.57 (0.25)	0.21 (0.091)
	VI	0.52 (0.37)	0.52 (0.21)	0.242 (0.088)	0.48 (0.36)	0.6 (0.26)	0.22 (0.094)
	Bands + VI	0.54 (0.37)	0.56 (0.22)	0.24 (0.09)	0.52 (0.35)	0.58 (0.25)	0.21 (0.091)
	Optimized	0.60 (0.36)	0.48 (0.22)	0.23 (0.093)	0.52 (0.36)	0.56 (0.26)	0.2 (0.093)
N_c	Raw bands	0.53 (0.36)	2.04 (0.93)	0.2 (0.09)	0.56 (0.34)	1.93 (1.04)	0.18 (0.098)
	VI	0.53 (0.35)	2.22 (0.91)	0.21 (0.088)	0.52 (0.38)	2.15 (1.03)	0.2 (0.097)
	Bands + VI	0.53 (0.35)	2.11 (0.91)	0.2 (0.087)	0.56 (0.38)	2.06 (0.95)	0.2 (0.09)
	Optimized	0.61 (0.32)	1.97 (0.96)	0.19 (0.093)	0.66 (0.32)	1.85 (1.09)	0.18 (0.103)
C_c	Raw bands	0.66 (0.35)	71.16 (41.51)	0.15 (0.088)	0.64 (0.35)	59.82 (35.5)	0.15(0.089)
	VI	0.63 (0.34)	80.12 (40.41)	0.17 (0.086)	0.64 (0.35)	68.7 (33.4)	0.17 (0.084)
	Bands + VI	0.64 (0.35)	74.43 (40.46)	0.16 (0.086)	0.65 (0.35)	63.46 (31.9)	1.16 (0.08)
	Optimized	0.62 (0.35)	67.11 (42.47)	0.14 (0.09)	0.66 (0.34)	57.97 (34.98)	0.15 (0.088)

Table 5.3 Performance of the Random Forest model in modelling canopy traits for the summer season

		Based on sunlit canopy			Weighted canopy		
Trait	Co-variates	R^2 (SD)	RMSEP (SD)	NRMSE (SD)	R^2 (SD)	RMSEP (SD)	NRMSE (SD)
LMA_c	Raw bands	0.55 (0.3)	103.47 (26.24)	0.202 (0.051)	0.64 (0.28)	84.89 (25.31)	0.21 (0.059)
	VI	0.52 (0.33)	103.63 (30.55)	0.202 (0.059)	0.62 (0.31)	86.12 (29.22)	0.21 (0.068)
	Bands + VI	0.53 (0.32)	103.27 (27.73)	0.201 (0.054)	0.62 (0.32)	85.72 (26.59)	0.2 (0.062)
	Optimized	0.57 (0.3)	98.01 (25.58)	0.191 (0.05)	0.64 (0.28)	82.97 (24.62)	0.19 (0.057)
Cab_c	Raw bands	0.49 (0.31)	0.46 (0.16)	0.234 (0.08)	0.44 (0.32)	0.45 (0.15)	0.24 (0.08)
	VI	0.60 (0.34)	0.4 (0.16)	0.2 (0.08)	0.56 (0.35)	0.39 (0.15)	0.21 (0.08)
	Bands + VI	0.59 (0.34)	0.42 (0.16)	0.21 (0.08)	0.5 (0.37)	0.4 (0.17)	0.21 (0.09)
	Optimized	0.62 (0.35)	0.37 (0.16)	0.19 (0.08)	0.56 (0.35)	0.38 (0.15)	0.21 (0.08)
N_c	Raw bands	0.32 (0.32)	1.97 (0.72)	0.21 (0.08)	0.40 (0.36)	1.55 (0.53)	0.21 (0.07)
	VI	0.37 (0.32)	1.83 (0.71)	0.2 (0.07)	0.38 (0.32)	1.52 (0.53)	0.21 (0.07)
	Bands + VI	0.36 (0.32)	1.86 (0.68)	0.2 (0.07)	0.42 (0.32)	1.52 (0.62)	0.2 (0.08)
	Optimized	0.41 (0.33)	1.77 (0.66)	0.19 (0.07)	0.48 (0.35)	1.47 (0.53)	0.19 (0.07)
C_c	Raw bands	0.54 (0.3)	51.02 (13.17)	0.21 (0.05)	0.63 (0.3)	41.32 (12.55)	0.2 (0.06)
	VI	0.51 (0.33)	51.18 (15.3)	0.21 (0.06)	0.63 (0.3)	41.62 (14.7)	0.19 (0.07)
	Bands + VI	0.52 (0.32)	50.95 (13.6)	0.21 (0.06)	0.65 (0.28)	41.68 (11.4)	0.2 (0.06)
	Optimized	0.57 (0.28)	49.67 (13.39)	0.2 (0.054)	0.65 (0.29)	40.4 (12.81)	0.19 (0.06)

VI: Vegetation indices

Table 5.4: Performance of Random Forest models in modelling canopy traits for the autumn season

		Based on sunlit canopy			Weighted canopy		
Trait	Co-variates	R^2 (SD)	RMSEP (SD)	NRMSE (SD)	R^2 (SD)	RMSEP (SD)	NRMSE (SD)
LMA_c	Raw bands	0.69 (0.31)	68.67 (30.4)	0.18 (0.08)	0.71 (0.3)	59.27 (25.69)	0.18 (0.077)
	VI	0.74 (0.28)	61.51 (28.72)	0.17 (0.08)	0.74 (0.26)	56.28 (21.35)	0.17 (0.064)
	Bands + VI	0.71 (0.33)	61.81 (30.4)	0.17 (0.08)	0.76 (0.3)	52.81 (26.16)	0.16 (0.079)
	Optimized	0.74 (0.28)	61.15 (28.57)	0.16 (0.08)	0.74 (0.29)	53.64 (24.18)	0.16 (0.073)
Cab_c	Raw bands	0.51 (0.34)	0.34 (0.11)	0.19 (0.06)	0.56 (0.33)	0.34 (0.11)	0.18 (0.061)
	VI	0.45 (0.36)	0.36 (0.12)	0.2 (0.06)	0.51 (0.32)	0.35 (0.13)	0.19 (0.068)
	Bands + VI	0.47 (0.33)	0.35 (0.11)	0.19 (0.06)	0.52 (0.33)	0.35 (0.13)	0.19 (0.07)
	Optimized	0.5 (0.34)	0.33 (0.1)	0.19 (0.06)	0.58 (0.32)	0.34 (0.11)	0.18 (0.06)
N_c	Raw bands	0.65 (0.3)	1.31 (0.72)	0.16 (0.09)	0.68 (0.32)	1.12(0.55)	0.16 (0.08)
	VI	0.69 (0.31)	1.23 (0.76)	0.15 (0.09)	0.69 (0.31)	1.06 (0.57)	0.15 (0.08)
	Bands + VI	0.7 (0.30)	1.22 (0.78)	0.15 (0.09)	0.69 (0.3)	1.04 (0.59)	0.15 (0.09)
	Optimized	0.71 (0.3)	1.21 (0.79)	0.14 (0.1)	0.72 (0.3)	1.03 (0.61)	0.15 (0.09)
C_c	Raw bands	0.7 (0.31)	33.51 (14.99)	0.18 (0.08)	0.72 (0.28)	28.69 (12.69)	0.18 (0.078)
	VI	0.74 (0.28)	30.41 (13.96)	0.16 (0.08)	0.74 (0.27)	27.81 (10.32)	0.17 (0.06)
	Bands + VI	0.71 (0.32)	30.15 (15.19)	0.16 (0.08)	0.73 (0.3)	26.44 (13.22)	0.16 (0.08)
	Optimized	0.74 (0.27)	29.9 (14.12)	0.16 (0.08)	0.74 (0.28)	26.02 (11.97)	0.16 (0.07)

VI: Vegetation indices

Analysis for the pooled dataset demonstrated that the weighted canopy expression consistently outperformed the top-of-canopy expression method using both the internal and the independent external validation procedure. Canopy LMA estimated from the weighted canopy expression yielded a RMSEP of 66.86 compared to 83.92 g/cm^2 obtained for the top-of-canopy expression. A similar pattern was also observed for canopy N (1.21 and 1.62 g/cm^2 for weighted and top-of-canopy expression respectively) and carbon (31.88 and 40.99 g/cm^2 for weighted and top-of-canopy expression respectively). Chlorophyll estimated based on top-of-canopy expression yielded higher prediction accuracy (0.38 g/cm^2) compared to canopy weighted expression (0.47 g/cm^2) for the pooled dataset. It is important to note that the generalized model based on the pooled dataset underestimated canopy chlorophyll content in high canopy chlorophyll content stands. This is reflected by the shift in the estimated canopy chlorophyll content values below the 1:1 line (Fig 5.4).

Table 5.5: Performance of generalized Random Forest models in modelling canopy traits across all the seasons

		Based on sunlit canopy					Weighted canopy				
		Internal validation		External validation			Internal validation		External validation		
Trait	Co-variates	R^2 (SD)	RMSEP (SD)	R^2	RMSEP	NRMSE	R^2 (SD)	RMSEP (SD)	R^2	RMSEP	NRMSE
LMA_c	Raw bands	0.48 (0.28)	104.44 (25.67)	0.54	82.33	0.173	0.52 (0.24)	90.15 (22.88)	0.68	68.84	0.17
	VI	0.45 (0.27)	107.68 (27.01)	0.49	87.75	0.184	0.5 (0.25)	93.89 (23.85)	0.55	76.87	0.19
	Bands + VI	0.49 (0.28)	103.38 (25.18)	0.56	82.43	0.173	0.52 (0.24)	90.5 (21.93)	0.7	61.97	0.15
	Optimized	50.21 (0.28)	101.39 (25.62)	0.54	83.92	0.176	**0.55 (0.23)**	**89.5** (21.6)	**0.67**	**65.9**	**0.158**
Cab_c	Raw bands	0.45 (0.24)	0.39 (0.087)	0.43	0.447	0.27	0.41 (0.24)	0.396 (0.07)	0.42	0.51	0.28
	VI	0.47 (0.27)	0.39 (0.11)	0.46	0.41	0.23	0.46 (0.28)	0.386 (0.09)	0.45	0.49	0.25
	Bands + VI	0.46 (0.25)	0.389 (0.0093)	0.46	0.42	0.25	0.44(0.26)	0.389 (0.08)	0.43	0.494	0.27
	Optimized	**0.49 (0.26)**	**0.37** (0.09)	**0.55**	**0.379**	**0.192**	0.46 (0.27)	0.386 (0.086)	0.47	0.472	0.24
N_c	Raw bands	0.41 (0.26)	1.78 (0.44)	0.25	1.67	0.19	0.39 (0.26)	1.52 (0.36)	0.46	1.23	0.16
	VI	0.41 (0.28)	1.81 (0.48)	0.34	1.56	0.18	0.42(0.27)	1.55 (0.42)	0.42	1.26	0.16
	Bands + VI	0.40(0.28)	1.8 (0.46)	0.32	1.55	0.18	0.4 (0.26)	1.53 (0.38)	0.51	1.17	0.15
	Optimized	0.42 (0.27)	1.75 (0.46)	0.32	1.62	**0.19**	**0.45 (0.26)**	**1.49** (0.37)	**0.53**	**1.132**	**0.144**
C_c	Raw bands	0.5 (0.28)	49.88 ()	0.55	40.69	0.18	0.55 (0.24)	43.37 (9.89)	0.68	31.33	0.158
	VI	0.48 (0.27)	51.73 ()	0.52	40.76	0.179	0.53 (0.24)	44.09 (11.52)	0.59	36.12	0.182
	Bands + VI	0.52 (0.28)	49.78 ()	0.56	39.84	0.175	0.54 (0.23)	42.66 (11.34)	0.71	30.74	0.155
	Optimized	0.53 (0.27)	49.17 ()	54.5	40.99	**0.18**	**57 (23.02)**	**41.83** (11.05)	**0.68**	**31.85**	**0.161**

VI: Vegetation indices

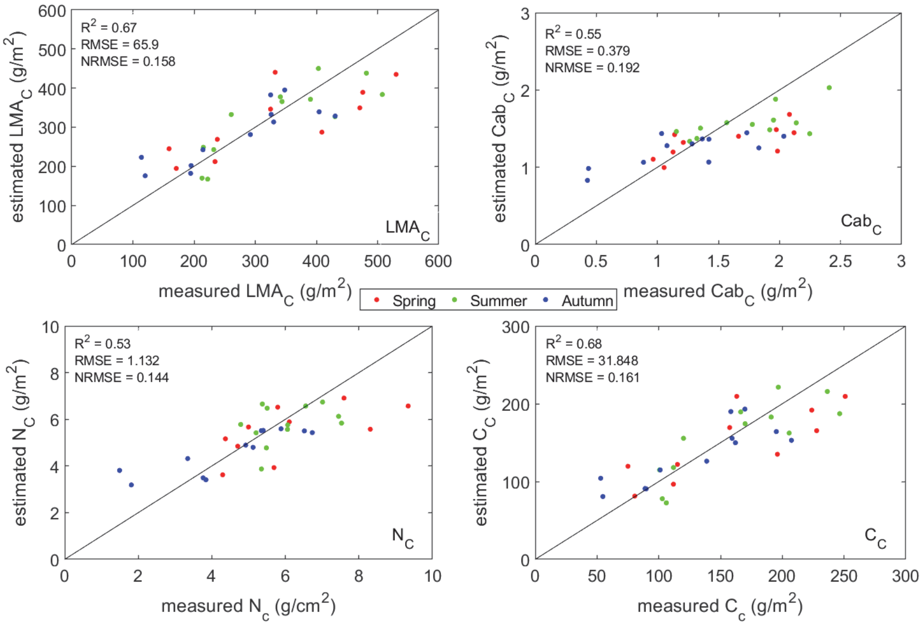

Figure 5.4: Independent validation for the pooled dataset based on the optimized model.

Fig 5.5 indicates the significance and ranking of each predictor variables in modelling canopy traits for each season and for the pooled data set using the RF technique. It is evident that SWIR bands outranked other spectral bands in modelling dry matter related canopy traits. IRECI consistently ranked higher compared to other vegetation indices. Generally, the blue reflectance band ranked lowest compared to other spectral bands for canopy LMA, N and carbon modelling. This result concur with correlation analysis observed between the canopy traits and Sentinel-2 bands in Fig 5.3. For canopy chlorophyll, the red edge bands ranked higher. Generally, vegetation indices outranked spectral bands in canopy chlorophyll modelling especially in summer and for the pooled dataset.

5.3.2 Mapping seasonal variation in canopy traits

Fig 5.6 and 5.7 show the spatial and temporal variation in canopy traits mapped using the best performing RF models across the three seasons. Variations in canopy chlorophyll for the three seasons were mapped based on top-of-canopy expression, while variations in LMA, N and carbon were based on canopy traits estimated using canopy-weighted expression. A visual inspection of the maps display seasonal shifts in canopy traits across the three seasons that confirm to our knowledge on plant phenological changes. For example, the seasonal changes in chlorophyll show high chlorophyll content in summer, followed by spring and then autumn (Fig 5.6). The seasonal shifts displayed in canopy chlorophyll maps and as well as for canopy LMA, N and carbon (Fig 5.6 and 5.7) corresponds to the seasonal variability in leaf traits content observed in Fig 5.2.

5.4 Discussion

5.4.1 Variability in *in-situ* leaf traits across the vertical canopy profile throughout the growing season

All leaf traits measured in the field demonstrated seasonal dynamics that also exhibited dependence on the canopy microclimate (Fig 5.2). These dynamics conform to previous studies (Gara *et al.*, 2018b; Yang *et al.*, 2016) and with our understanding of vegetation physiology across the canopy vertical profile (Hikosaka, 2005). The seasonal dynamics are mainly a result of phenological shifts due to changes in the photoperiod across the growing season. As expected, all the traits exhibited high content in summer, which coincides with an increase in diurnal temperature and maximum photoperiod (Behrman *et al.*, 2015). The wide difference in trait content between lower and upper canopy leaf samples in summer for all traits can be explained by the manifestation of the shade effect as foliage material of the upper canopy block and absorb most of the incoming PAR during peak vegetative season. Until now very few studies (Yang *et al.*, 2016; Zhang *et al.*, 2007) have reported phenological dynamics in leaf traits across the canopy vertical profile in temperate vegetation biomes.

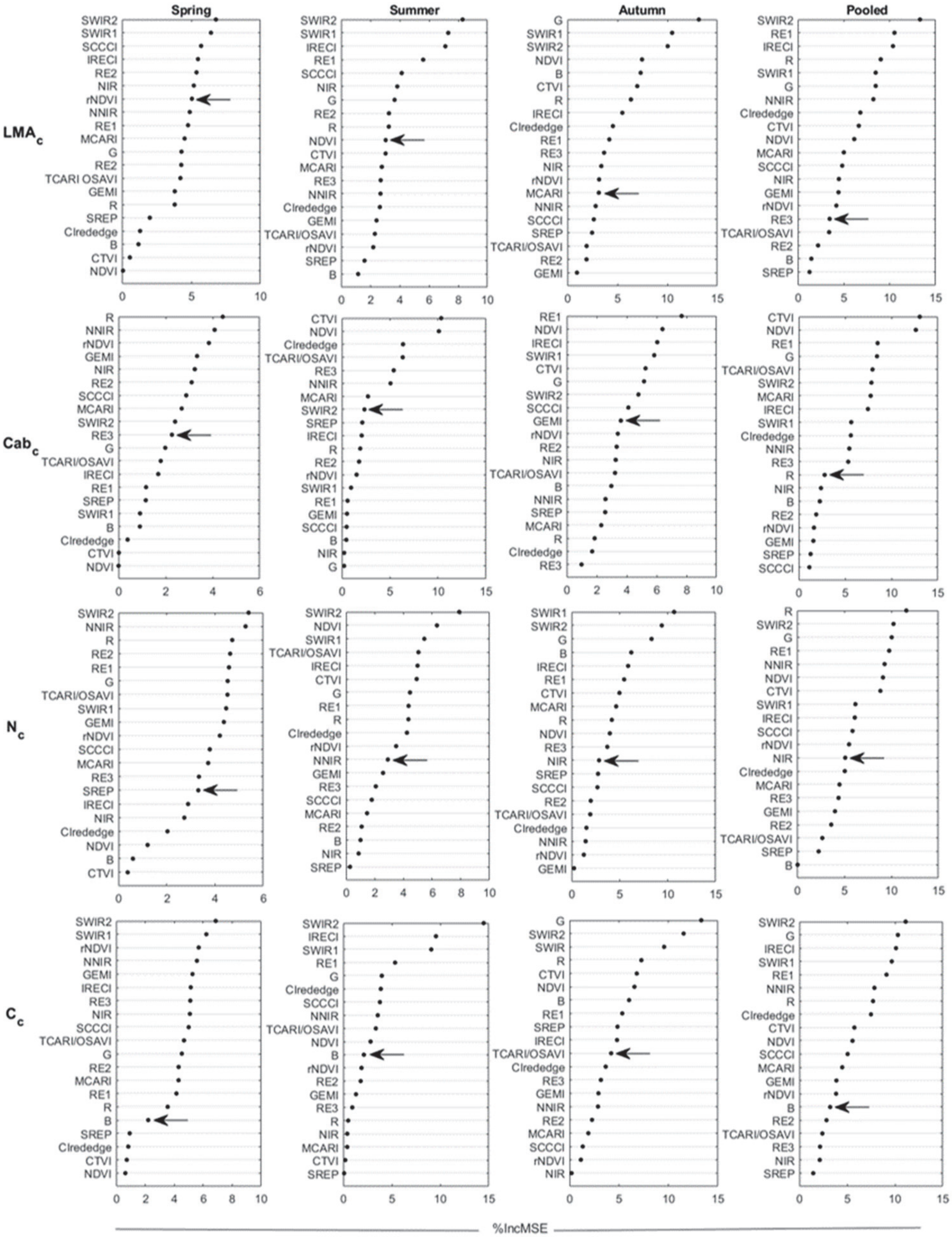

Figure 5.5: Variable ranking and optimization for the prediction of canopy traits across seasons and for the pooled dataset using Sentinel-2 bands and vegetation indices. The arrow indicate the threshold of the variable selected for the optimized model in descending order.

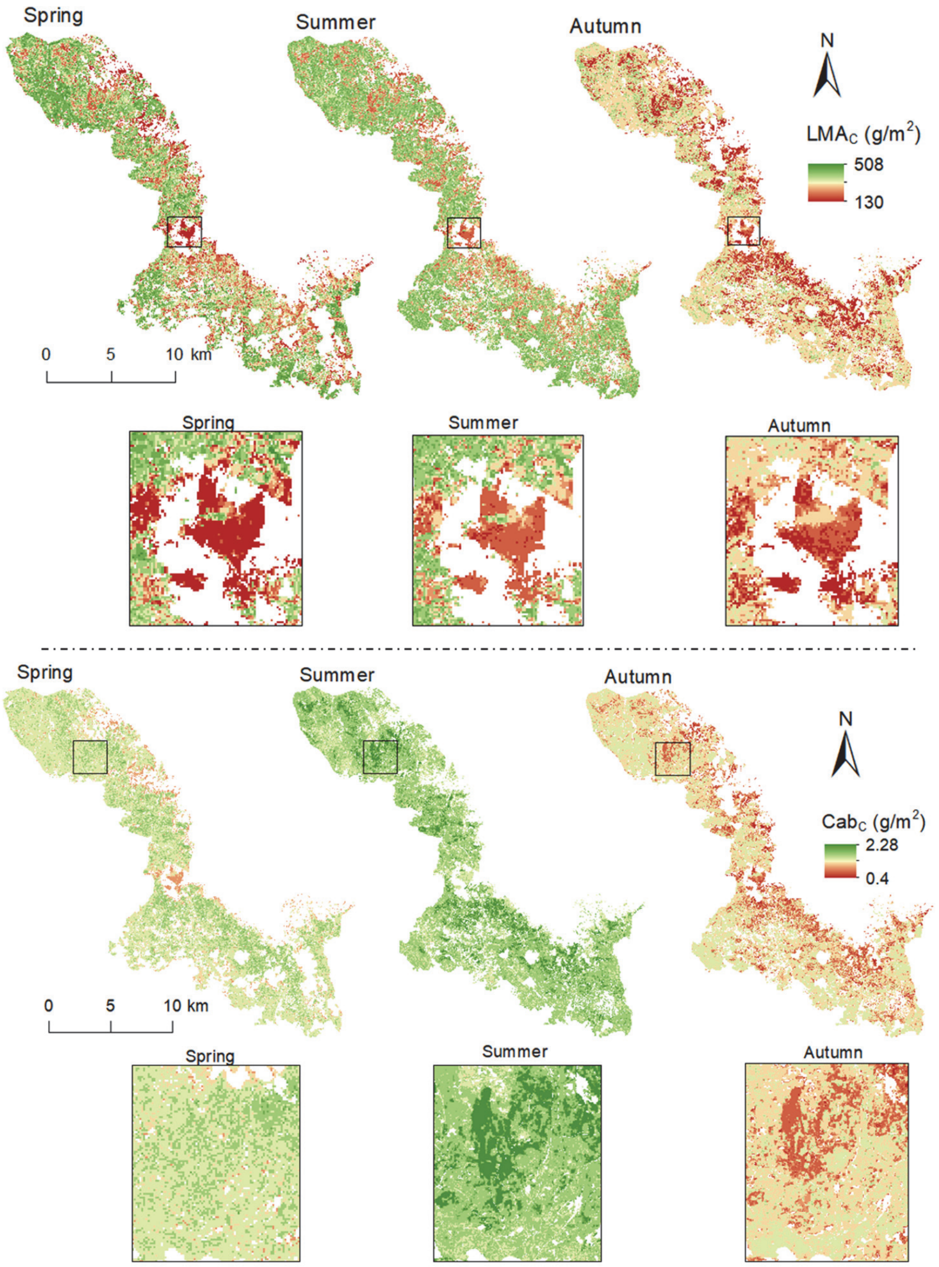

Figure 5.6: Spatial variation in canopy leaf mass per area and chlorophyll across seasons in Bavaria Forest National Park. The white parts of the map indicate pixels occupied by clouds and non-vegetative material such as rocks. The zoomed maps enhance visualization of seasonal dynamics in canopy LMA and chlorophyll.

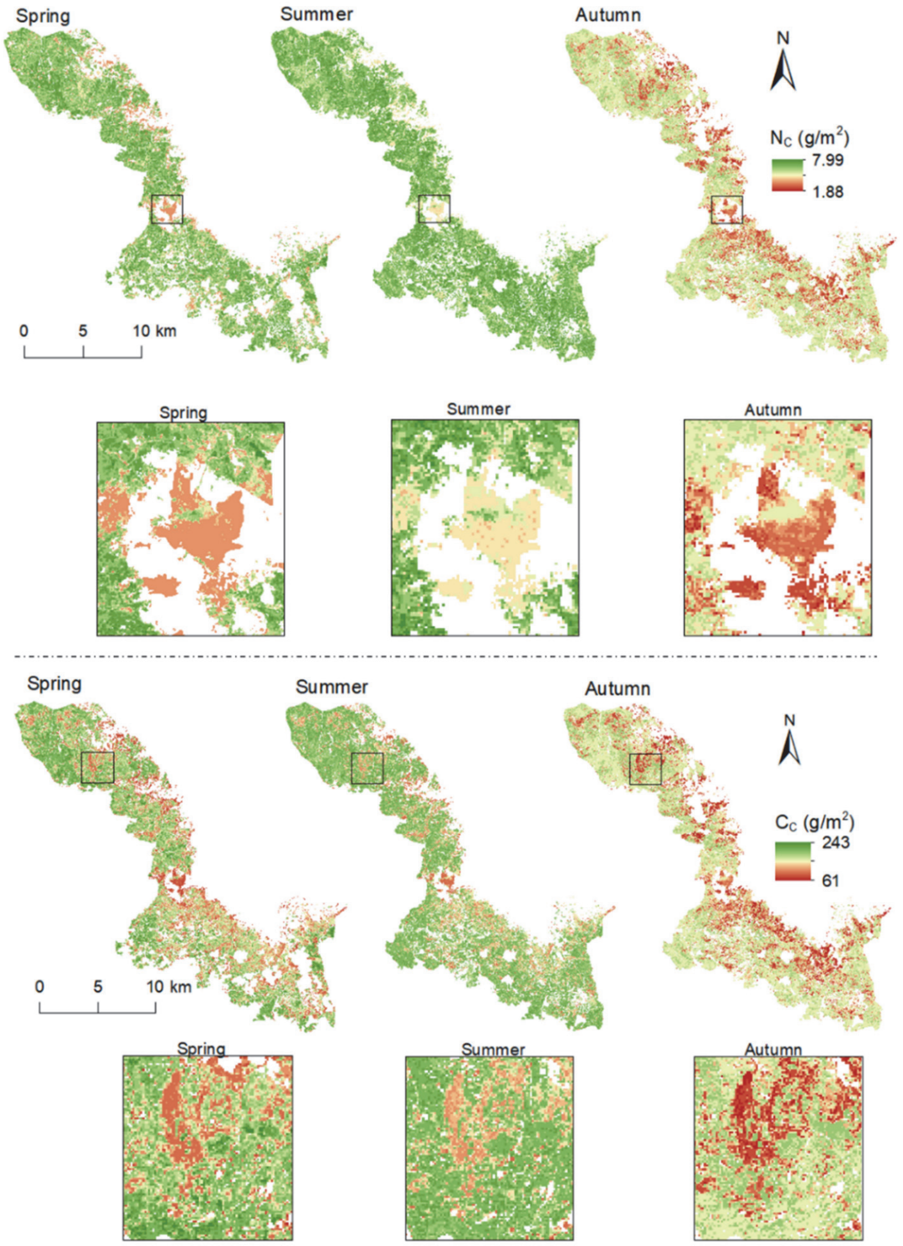

Figure 5.7: Spatial variation in canopy nitrogen and carbon across seasons in Bavaria Forest National Park. The white parts of the map indicate pixels occupied by clouds and non-vegetative material such as rocks. The zoomed maps enhance visualization of seasonal dynamics in canopy N and carbon.

5.4.2 Does canopy traits expression affect the correlation and estimation accuracy of canopy traits from Sentinel-2 data?

This study presented evidence that dry matter related canopy traits (LMA, N and carbon) computed from the weighted canopy expression, which exploits the vertical heterogeneity in leaf traits, correlate well with reflectance from all Sentinel-2 spectral bands compared to the conventional top-of-canopy expression throughout the growing season (Fig 5.3). Additionally, the weighted canopy expression generated a higher prediction accuracy compared to top-of-canopy expression using Sentinel-2 spectral data throughout the growing season (Table 5.2-4). These observations demonstrate that functional traits of the shaded layer significantly contribute to top of canopy reflectance measured by the Sentinel 2 multispectral instrument. Characterizing the canopy depth sensed by remote sensing instruments has remained an unsolved problem in vegetation spectroscopy (Ciganda *et al.*, 2012). Results presented in this study imply that Sentinel-2 multi-spectral instrument senses functional traits deep in the canopy beyond the exposed upper canopy. This observation confirms earlier results by Gara *et al.*, (2018b) who documented that dry matter related canopy traits (LMA, N and carbon) upscaled from the top two canopy layers yield higher accuracy using canopy reflectance measured with a field spectrometer. The current study extends this idea to a highly foliated forest ecosystem and presents results that demonstrate that canopy traits expression affects the correlation and estimation accuracy of canopy traits using satellite imagery data across multiple seasons.

The seasonal differences in the strength of correlation between reflectance of Sentinel-2 spectral bands and the two canopy traits expressions can be explained by changes in leaf traits heterogeneity between sunlit and shaded leaf samples across seasons. When the heterogeneity in leaf traits content between sunlit and shaded canopies is lower (i.e. spring and autumn Fig 5.2), the two canopy expressions naturally yield almost identical canopy trait values and subsequently display similar correlations patterns with Sentinel 2 data. However, as the heterogeneity in leaf traits between sunlit and shaded increase, the canopy traits show higher variation in the strength of correlation with Sentinel-2 data as evidenced in summer (Appendix Fig A4).

Generally, canopy LMA and carbon demonstrated higher correlation with red-edge 1 and SWIR bands, while canopy N was highly correlated with red, red-edge and SWIR spectral data. These bands also ranked higher in the variable importance ranking (Fig 5.5). The high relationship between SWIR and canopy LMA, N together with carbon concur with Kokaly *et al.*,(2001) who observed that the absorption feature centered at 2.1 μm broadens with increasing leaf N content. They report that the changes are a result of two absorption features at 2.055 and 2.172 μm that are positioned on the shoulders of the 2.1 μm absorption (Kokaly *et al.*, 2009). In this study, SWIR2 ranked higher in the variable importance and yielded a better correlation with canopy LMA and carbon compared to SWIR1. This can be explained by the Sentinel 2 spectral bands configuration. The SWIR2 is centered at 2190 nm and has a wider bandwidth (175 nm) compared to SWIR1, which is centered at 1610 nm and has a narrow bandwidth of 91 nm (European Space Agency, 2015). The SWIR2 band is also contained within the wavebands (2100-2300 nm) that Wang *et al*.,(2011) observed to be sensitive to LMA using hyperspectral measurements.

The high prediction accuracy obtained for all canopy traits for the autumn season can be explained by the distribution of nutrients within a given leaf volume during senescence. Experimental studies document that during senescence, chloroplasts degrade which results in the release of foliar nutrients like leaf protein and chlorophyll pigments in remobilizable form (Wada and Ishida, 2009). During this process these foliar nutrients become uniformly distributed across the leaf volume (Carrión *et al.*, 2014). The uniformly distributed nutrients freely interact with radiation and can be readily sensed by remote sensing instruments. Previous studies also demonstrated that spectral absorption features especially in the SWIR spectrum are obscured by water absorption (Fourty and Baret, 1998). We therefore speculate that the low leaf water content in autumn (results not shown) enhance leaf traits sensitivity and subsequently improved canopy traits prediction for this season (Ramoelo *et al.*, 2011).

The generalized models explained 52.57 - 67.82% variability in canopy traits across all seasons demonstrating the capability of Sentinel 2 data in capturing seasonal dynamics in leaf traits. Characterizing seasonal dynamics in leaf traits is essential in improving our understanding of ecosystem functions, processes and services. Dynamics in leaf traits displayed in Fig 5.2 matches seasonal fluctuations in canopy traits observed on the maps (Fig 5.6 and 5.7). For example, the high leaf chlorophyll content observed in summer in comparison to other seasons corresponds with the range of canopy chlorophyll observed for the summer map. A similar pattern can be observed for the other the canopy traits studied. The matching between leaf traits content and the mapped canopy traits highlights the capability of Sentinel 2 data in tracking canopy traits seasonality and ecosystem dynamics.

To the best of our knowledge, no study has explored the effect of canopy traits expression using a multispectral data across the entire growing season. Furthermore, in this study we mapped the spatial patterns of canopy traits repeatedly over space and time. Our study demonstrated for the first time the capability of Sentinel 2 data to estimate canopy LMA and carbon across vegetation phenophases. Previous efforts using Sentinel-2 data have mainly focused on foliar chlorophyll (Clevers *et al.*, 2017; Delloye *et al.*, 2018; Li *et al.*, 2018a; Vincini *et al.*, 2014) and nitrogen (Chemura *et al.*, 2018; Mutowo *et al.*, 2018) for single point in time typically at the peak growing season in agricultural systems. Our study, also demonstrated the development of a generalized model that captures phenological changes in leaf traits across multiple seasons. This result is important for monitoring ecosystem functions and processes in biodiversity studies and forest management. With the increasing use of multispectral imagery in estimating and mapping plants traits there is need to standardize field sampling protocols to ensure that studies are comparable. The general perception that field sampling is laborious and time consuming provides an escape route for limited sampling procedures. Therefore, sampling throughout the canopy requires more consideration, especially if the accuracy of estimation and mapping of plant traits is to be further improved.

5.5 Conclusion

In this study, we examined the effect of canopy traits expression in modelling canopy traits using Sentinel-2 multispectral satellite data across the growing season in a temperate forest. Based on results obtained in this study we conclude that:

i. Canopy traits estimated from the weighted canopy expression show higher correlation with Sentinel-2 bands across all seasons compared to canopy traits estimated from top-of-canopy expression.
ii. The weighted canopy expression that accounts for the heterogeneity in leaf traits between sunlit and shaded canopy yield a higher prediction accuracy using Sentinel-2 bands and vegetation indices across all seasons.
iii. A generalized model that captures dynamics in canopy traits across all seasons can be developed using Sentinel-2 spectral data.
iv. Sentinel-2 multispectral data can be successfully used to map variability in canopy traits over space and time.

Our work demonstrated that Sentinel-2 multispectral data can accurately monitor the seasonal dynamics of a suite of canopy traits. This study showed the importance of multispectral instruments in monitoring ecosystem dynamics across a range of spatial and temporal scales. However, further research should be performed in the other biomes to ascertain the validity of results obtained in this study.

Chapter 6

Synthesis: Remote sensing of foliar traits across the plant’s canopy

6.1 Introduction

Accurate and up-to-date information of leaf traits is critical in monitoring ecosystem function, processes and services (Lavorel *et al.*, 2011). Plant traits are critical in improving our understanding of ecosystem services and plant community productivity across biomes (Houborg *et al.*, 2015). Understanding the spatio-temporal variations in leaf traits is vital in tracking changes in the cycling of nutrients within the earth system. For example, leaf traits such as LMA and N_{mass} are inputs into models such as the Community Land Model (Wang *et al.*, 2014). The Community Land Model simulates past, present and future global climate states driven by components that include vegetation composition, structure, and phenology (Oleson, 2013). This, therefore, implies that ecosystem functioning and structure are key elements of our climate system (Barboni *et al.*, 2004; Soudzilovskaia *et al.*, 2013). Understanding foliar nutrient content in terrestrial ecosystem across a variety of spatial and temporal scales is therefore critical.

Foliar nutrients do not exclusively exhibit variations over space and time but also changes across the vertical domain of plant canopies (Chen *et al.*, 1993; Coble *et al.*, 2016b). The vertical heterogeneity in leaf traits across canopy is known to improve the photosynthetic capacity of the whole canopy as plants allocate higher nutrient amounts to the sunlit upper canopy to maximize high radiation flux density intercepted in the upper canopy layers (Ellsworth and Reich, 1993; Li *et al.*, 2013; Niinemets, 2007). This mechanism results in variation in leaf chemical, morphology and physiological properties and subsequently influence the optical properties of the whole canopy (Yang *et al.*, 2017). Previous studies demonstrate that the vertical heterogeneity in leaf chlorophyll, water and dry matter content have a significant effect on canopy reflectance measured by remote sensing instruments (Wang and Li, 2013). This therefore implies that capturing the vertical heterogeneity in leaf traits across canopy is important in reducing bias in canopy reflectance modelling and subsequent retrieval of plant biophysical and biochemical properties.

Remote sensing provides a cost-effective and practical means of estimating and mapping leaf traits from canopy spectra over large spatial extents. Basically, three approaches (empirical, physical and hybrid) are employed to quantify leaf traits from remote sensing data (Verrelst *et al.*, 2013; Verrelst *et al.*, 2015b). Empirical methods explore statistical relationships between spectral data or features and plant traits (Hill *et al.*, 2019). Common empirical methods in vegetation spectroscopy include partial least squares regression (Adjorlolo *et al.*, 2015; Alvarez-Guerra *et al.*, 2010; Martin *et al.*, 2008), stepwise multiple linear regression (Kokaly and Clark, 1999; Peterson *et al.*, 1988) and support vector machine regression (Axelsson *et al.*, 2013). Physical models, rigorously simulate light absorption and scattering inside vegetation canopies accounting for leaf traits composition, canopy structural properties and soil background based on radiation transfer theory (Féret *et al.*, 2011). Hybrid models integrate elements of empirical and physical methods. Hybrid models often entail calibrating statistical models especially machine learning algorithm using a LUT generated from physical models (Verrelst *et al.*, 2014). However, understanding the performance of these methods in the context of vertical heterogeneity of leaf traits across the canopy has received limited attention.

This thesis, therefore, seek to understand the role of canopy vertical heterogeneity on modelling leaf spectral properties and retrieval of leaf traits. In addition, the thesis examines the effect upscaling approaches on the estimation of canopy traits using *in-situ* hyperspectral measurements and Sentinel-2 multispectral data across multiple seasons. Specifically, the objectives of this thesis are to: (1) examine the effect of canopy vertical position on leaf spectral properties and traits across multiple species, (2) examine the effect of leaf position within a canopy on the performance of the PROSPECT model in modelling leaf optical properties and retrieval of leaf traits across the growing season, (3) evaluate the effect of leaf-to-canopy upscaling approaches on modelling canopy traits using *in-situ* hyperspectral and simulated Sentinel-2 measurements, (4) examine the effect of canopy traits expression on modelling canopy traits using Sentinel-2 MSI across the growing season. The thesis synthesizes results obtained in this study by initially focusing on results obtained at leaf level using empirical models and physical models. The thesis proceeds to discussed results obtained at canopy level using *in-situ* hyperspectral measurements in a laboratory environment. The relevance of this study to remote sensing of plants traits at the landscape level is discussed in Section 6.5. The thesis concludes by discussing possible future research avenues.

6.2 Leaf level

6.2.1 Do leaf spectral properties track variability in leaf traits across the canopy vertical profile?

Leaf trait content is known to vary across the canopy vertical domain (Hirose and Werger, 1987). The vertical heterogeneity in leaf traits across canopy improves the photosynthetic capacity of the whole plant (Li *et al.*, 2013). Sunlit upper canopy leaves exhibit high nutrient content to commensurate the high radiation amounts intercepted by foliage material of the upper canopy (Yang *et al.*, 2016). This mechanism consequently results in marked effects on leaf morphological, chemical and physiological properties of leaf samples across the canopy (Weerasinghe *et al.*, 2014). Although the vertical heterogeneity in leaf traits concept is well documented in plant physiological domain, the impact of vertical canopy position on leaf properties across the entire spectrum for multiple species remains scanty. We, therefore, examined the effect of canopy vertical position on leaf spectral properties across multiple species. We sought to identify spectral wavebands that are key in the discrimination of leaf samples into their respective canopy layers.

Leaf samples from the upper canopy exhibited higher traits content compared to samples collected from the lower canopy (Fig 2.6). Leaf spectral reflectance mirrored variation in traits content across the canopy. Leaf spectral reflectance shifted to longer wavelengths in the 'red edge' spectrum (685 - 701 nm) in the order of lower > middle > upper (Fig 2.2). The spectral shift in the red-edge spectrum reflected a trend in the increase of nitrogen and chlorophyll from lower canopy leaves to the upper canopy. The observation in the red edge concurs with Ma and Upadhyaya (2018) who observed that spectral reflectance of canopy leaves measured at 730 nm upper was significantly ($p < 0.05$) lower compared spectral reflectance of shaded leaves at 730 nm. Leaf samples were successfully discriminated into their respective canopy position groups with an overall accuracy of 64% using a bootstrapped PLS-DA (Table 2.3). Key wavebands (400 - 761, 1372 - 1407, 1902 -1989 and 2106 - 2170 nm [30.37% of wavebands]) that enhance leaf samples discrimination are documented to be sensitive to variation in chlorophyll, EWT, N, carbon and SLA (Curran, 1989). Our results demonstrated the capability of leaf spectra to track variability in leaf traits across the canopy vertical profile. Our results have strong implication on leaf sampling procedures and upscaling leaf traits to canopy level especially in vegetation communities of low LAI. We hypothesize that foliage material from the lower canopy significantly contributes to canopy optical properties especially in vegetation communities characterised by low LAI. This observation implies that failure to account the vertical heterogeneity in key traits across the vertical canopy profile can potentially lead to considerable inaccuracies in upscaling leaf traits to canopy level, canopy reflectance modelling and subsequent retrieval of leaf traits at canopy scale.

6.2.2 Does the position of a leaf within a canopy affect the performance of PROSPECT in modelling leaf optical properties and retrieval of leaf traits throughout the growing season

A number of studies demonstrate the capability of leaf radiative transfer models such as the widely used PROSPECT to simulate leaf optical properties and subsequently retrieve leaf traits such as C_{ab}, LMA and EWT through model inversion in different vegetation types (Féret *et al.*, 2017; Jacquemoud and Baret, 1990; Li and Wang, 2013b; Romero *et al.*, 2012; Wang *et al.*, 2015a). The PROSPECT model is often calibrated and validated using mature, sunlit leaves at peak vegetation season (Ali *et al.*, 2016; Atherton *et al.*, 2017).

However, the performance of the PROSPECT to model leaf optical properties and retrieve leaf traits across the canopy vertical profile remains rudimentary. In light of this background, we examined the effect of leaf position on the performance of the PROSPECT in modelling leaf optical properties and retrieval of C_{ab}, LMA and EWT. We collected 588 leaf samples from upper and lower canopies of deciduous stands over the growing season of 2017 in Bavaria Forest National Park. The performance of the PROSPECT model to model leaf optical properties and retrieve C_{ab}, LMA and EWT was tested by generating a LUT of 250 000 simulations. A look-up-table (LUT) model inversion approach was employed to retrieve C_{ab}, LMA and EWT for the lower canopy and upper canopy respectively.

Results obtained in this study demonstrated a strong agreement between measured and simulated reflectance spectra for leaf samples collected from the lower canopy compared to the upper canopy across all seasons (Fig 3.4). The variation in agreement between measured and simulated reflectance across canopy can be attributed to the difference in leaf morphological traits such as LMA and SLA. Our field data demonstrated that upper canopy leaves are thicker compared to lower canopy leaves. Leaf thickness is known to have an effect radiation transfer within a leaf as thicker leaves are associated with low leaf reflectance due to increase in path length and quantity of radiation intercepting tissue (Demarez, 1999; Li and Wang, 2011). The mismatch between measured and simulated reflectance between the lower canopy and upper canopy leaf samples was wider in spring and summer seasons compared to autumn. This observation reflects the slender variation in leaf traits across the canopy in autumn compared to the other seasons (Fig 3.2). C_{ab} and EWT for leaf samples collected from the lower canopy were retrieved with higher accuracy ($C_{ab:}$ NRMSE=0.103, EWT: =0.125) compared to leaf samples collected from the upper canopy (C_{ab}: NRMSE=0.122, EWT: =0.188) (Fig 3.6 and Fig 3.7). The higher retrieval accuracy of C_{ab} for leaf samples collected from the lower canopy can be explained by the distribution of chloroplast with the leaf volume. Chloroplasts in upper sunlit leaves are clumped in the palisade layer while for shaded leaves, the chloroplasts are evenly distributed between the palisade and spongy mesophyll layer (Adds *et al.*, 1997). The even distribution of chloroplasts within the leaf volume for the shaded lower canopy leaves enhance the interaction of radiation and pigments. The relatively high EWT retrieval accuracies obtained for the lower canopy leaf samples in comparison to sample collected from the upper canopy across the growing season, reflect on the variation in spectral matching between measured and simulated reflectance spectra in key water absorption wavebands [970, 1200 and 1400 nm] (Curran, 1989). The retrieval accuracy for LMA was higher for the upper canopy (NRMSE = 0.154) compared to lower canopy (NRMSE = 0.176) (Fig 3.8). This observation does not conform to the spectral matching observed for samples collected across the canopy. LMA consists of a number of leaf constituents, such as protein, lignin, cellulose, starch, sugar and lipids (Qiu *et al.*, 2018). The PROSPECT model use a weighted average specific absorption coefficient of the molecular absorption spectra of these numerous constitutes (Jacquemoud *et al.*, 1996). This approach has the potential of inducing increased bias and uncertainties, especially in wavelengths of high LMA absorption as the different composition of the constituents can yield different spectral behaviour. Our results imply that variation in leaf biochemistry and morphology through the canopy vertical profile potentially affects the performance of the PROSPECT model. Results obtained in this study have implications on retrieval of leaf biochemical traits at the canopy scale especially using multi-layer radiative transfer models.

6.3 Canopy and landscape level

6.3.1 Within canopy variation in leaf traits is essential for accurate modelling of canopy traits

Leaf traits are often upscaled to canopy level using leaf samples collected from the sunlit upper canopy (Gara *et al.*, 2019). The basis for this approach is that absorption of incident photosynthetically active radiation (PAR) follow a bell-shaped function skewed to the upper canopy (Kropff and Goudriaan, 1994). This infers that upper canopy foliage material controls canopy radiation dynamics especially with regard to the amount of reflected radiation measured by remote sensing instruments. On this basis, the contribution of biophysical and biochemical properties of shaded leaves from the lower canopy is often considered 'invalid' (Yang *et al.*, 2017). The validity of this theory to other leaf traits that control variation in spectral reflectance in other portions of the electromagnetic spectrum outside the visible wavebands remains unexplored. Establishing a canopy-level trait value that corresponds to the signal measured by the remote sensing instrument is critical in estimating and mapping foliar nutrients at both canopy and landscape scales with less uncertainties (Roelofsen *et al.*, 2013). The principal aim of this study is to examine the effect of different approaches of upscaling leaf traits to canopy level on model performance and estimation accuracy using spectral measurements (*in-situ* canopy hyperspectral and simulated Sentinel-2 data) in short woody vegetation in a laboratory setup. The study proceeded to upscale this setup to examine the effect of canopy traits expression on modelling canopy traits using Sentinel-2 multispectral data across the growing season in a temperate forest of Bavaria Forest National Park in Germany.

Results obtained from laboratory data showed that leaf-to-canopy upscaling approaches that consider the contribution of leaf traits from the exposed upper canopy layer together with the shaded middle canopy layer yield significantly ($p < 0.05$) lower error ($NRMSE_{cv} < 0.2$ for canopy N, LMA and carbon) as well as high explained variance ($R^2 > 0.71$) for both *in-situ* hyperspectral and simulated Sentinel-2 data (Fig 4.3). The traditional upscaling approach that considers leaf traits from the exposed top-of-canopy yielded an improved accuracy in estimating canopy chlorophyll content. As this observation was purely based on a laboratory experiment, we tested the validity of these results at canopy and landscape level using Sentinel-2 multispectral data acquired in a high foliated forest of Bavaria Forest National Park.

Using Sentinel-2 multispectral data at landscape level, our results demonstrated that dry matter related canopy traits (LMA, N and carbon) estimated based on the weighted canopy expression yield stronger correlations (Fig 5.3) and higher prediction accuracy (generally $NRMSE_{CV} < 0.19$) compared to the top-of-canopy traits expression across all seasons (Table 5.5). Similar to results obtained from laboratory data, canopy chlorophyll estimated from the top-of-canopy expression demonstrated strong fidelity with Sentinel-2 bands and vegetation indices (RMSE < 0.48 $\mu g/cm^2$) compared to weighted canopy chlorophyll (RMSE > 0.48 $\mu g/cm^2$) across all seasons. These results reveal that sampling protocol and upscaling approach have a profound effect on estimating and mapping plants traits at canopy level. Our results imply that remote sensing instruments sense leaf traits beyond the sunlit upper canopy both in a laboratory and based on satellite remote sensing system. These results have a strong implication in modelling leaf biochemical traits using remote sensing. An understanding of the depth of canopy sensed by multispectral instruments has remained elusive over the years. The traditional and widely accepted approach of sampling foliar material exclusively from the sunlit upper canopy for remote sensing canopy traits has lately been subjected to scrutiny. Recent studies have also demonstrated that the vertical heterogeneity in leaf traits is a source of variation in canopy reflectance measured by remote sensing instruments (Yang *et al.*, 2017; Zhao *et al.*, 2017). Canopy traits expression has a strong implication in earth system models such as the Community Land Model that require accurate characterization of key input parameters such as LMA and foliar nitrogen. In addition, our results are important in monitoring vegetation health for both cropping and forest system assessment. This is particularly demonstrated by the capability of the newly launched Sentinel-2 to map seasonal changes in leaf traits at the landscape level (Fig 5.6 and Fig 5.7).

6.4 Practical relevance

This thesis demonstrated the importance of vertical heterogeneity of leaf traits in estimating plants traits at leaf, canopy and landscape level. We showed that incorporating the leaf traits content of foliage material from the shaded canopy improves the estimation accuracy of plants traits at canopy and landscape level using *in-situ* hyperspectral measurements in the laboratory and Sentinel-2 multispectral data at the landscape level. This observation is particularly valid for dry matter related leaf traits, i.e. LMA, carbon and nitrogen. These results have implications on sampling protocols of leaf samples as the vegetation remote sensing community seek to establish a meaningful canopy trait value that matches canopy reflectance observed by remote sensing instruments.

Accurate estimation of leaf traits at both leaf and canopy level is important to further our understanding of ecological processes, functions and services. *In-situ* measured leaf traits and traits data archived in databases such as TRY have traditionally been used to understand the effect of environmental change on vegetation. However, challenges ranging from costs and huge spatial gaps have limited the use of these methods. For example, approximately 40% of traits entries archived in the TRY databases are georeferenced (Moreno-Martínez *et al.*, 2018). Augmenting *in-situ* trait measurements and remote sensing provides an opportunity to monitor ecosystem functions and structure towards the Aichi Biodiversity Targets. Repeated mapping of leaf traits across landscapes across the vegetation growing season using new multispectral instruments such as Sentinel-2 is important in monitoring key processes such as primary productivity and nutrient dynamics. The effect of global environmental change on the ecological system can be assessed by analyzing the changes in the quantitative relationship between plant traits and reflectance spectra. Moreover, changes in seasonal patterns of foliar traits provide an insight into environmental change or disturbances and assist in developing early warning systems of biodiversity change (Alcaraz-Segura *et al.*, 2017).

Results presented in this thesis also have a broader implication on the design and parameterization of multi-layer RTM that accounts for the vertical heterogeneity in leaf traits. Most RTMs used in quantitative remote sensing of vegetation such as PROSAIL and INFORM do not consider the vertical homogeneity in leaf traits content. However, the results presented in this thesis demonstrated significant variation in leaf traits across the canopy. Other studies also reported the vertical heterogeneity in biophysical and biochemical properties (Yang *et al.*, 2016). Variation in leaf traits across canopy is known to affect re-absorption and scattering of radiation inside vegetation canopies and subsequently top-of-canopy reflectance (Yang *et al.*, 2017). This observation implies that failure to account the vertical heterogeneity in leaf traits between sunlit upper and shaded lower leaf samples together with their optical properties might introduce significant uncertainties in modelling canopy reflectance and retrieval of canopy traits.

6.5 General conclusions

Leaf properties, *i.e.*, traits and optical are distinct across the canopy of multiple species. Essentially, significant variation in leaf properties between and across species across the canopy vertical profile was observed. Influential wavebands in the discrimination of leaf samples into their respective canopy position groups match absorption features of C_{ab}, EWT, SLA and N. Our results demonstrated the capability of leaf optical properties to track variability in leaf traits across the canopy. We therefore concluded that changes in foliar traits across the canopies as a result of canopy microclimate translates to variation in leaf spectral variation. These findings have implications on leaf sampling within vegetation canopies and subsequent upscaling of leaf traits to canopy level.

Although the PROSPECT model provides a reasonable simulation of leaf optical properties and subsequent retrieval of leaf traits, our results demonstrate that the performance of the PROSPECT model and retrieval of C_{ab}, EWT and LMA is likely to be affected by the leaf biochemistry and morphological changes through the vertical canopy profile over the growing season. This observation implies that the calibration and designing the PROPSECT model requires further development. This is particularly relevant for LMA which constitute a weighted specific absorption coefficients of a number of leaf constituents such as lignin, cellulose, protein, sugar and lipids. Observations made with regard to PROSPECT highlight potential source of uncertainties in leaf and canopy reflectance simulation.

This research demonstrated the effect of leaf-to-canopy upscaling approach on modelling leaf traits at canopy and landscape level using *in-situ* hyperspectral data and Sentinel-2 multispectral data, respectively. Based on results obtained in this study we conclude that leaf-to-canopy upscaling approach or canopy traits expressions that incorporate the contribution of both the exposed upper canopy leaves together with the shaded lower canopy leaves results in the improved prediction of canopy nitrogen, LMA and carbon both at canopy and landscape level. We also concluded that the new Sentinel-2 multispectral imagery is suitable in monitoring and mapping leaf traits at canopy level across multiple seasons.

6.6 Future research avenues

This thesis examined the role of leaf position on the heterogeneity of leaf traits across canopy and the retrieval of leaf traits using hyperspectral measurements and. We also examined the effect of leaf to canopy upscaling approach on the estimation of canopy traits using *in-situ* hyperspectral measurements and Sentinel-2 satellite imagery. Specifically, conclusions reached in the thesis are based on reflectance data measured in the optical domain (400-2500 nm). There is a need to explore whether other parts of the electromagnetic spectrum especially the thermal spectrum can improve results obtained in this study.

Considering that LiDAR has the capability of characterizing the 3D structure of vegetation canopies with increased accuracy. Future studies should aim integrating hyperspectral measurements and LiDAR data to improve our understanding of the 3D variation of leaf traits across vegetation canopies. Fusing LiDAR and hyperspectral measurements has the potential of improving our understanding of the spatial and vertical variability in leaf traits in ecosystem processes and functioning.

As a result of sampling challenges, we sampled foliage material specifically from sunlit and shaded canopies in Bavaria Forest National Park. However, sampling efforts performed at short intervals of a few meters across the canopy can provide an explicit understanding of the depth of the canopy that controls canopy reflectance observed by multispectral instruments such as Sentinel-2. There is need to explicitly understand the depth of canopy that influences the canopy reflectance dynamics.

This study used leaf trait data collected from plants grown in a greenhouse experiment as well as leaf samples collected from a temperate forest ecosystem. The Bavarian Forest National Park is dominated by Norway spruce (*Picea abies*) and deciduous European beech (*Fagus sylvatica*). Therefore, results obtained in this study require validation in other vegetation biomes using other multispectral and airborne hyperspectral sensors.

Appendices

Table A.1: Retrieval accuracies of leaf traits across canopy positions throughout the growing season for European beech only

		C_{ab}			LMA			EWT		
Category	n	R^2	RMSE	NRMSE	R^2	RMSE	NRMSE	R^2	RMSE	NRMSE
Pooled	546	0.83	5.78	0.115	0.78	0.00132	0.14	0.77	0.00121	0.14
Spring	156	0.76	5.61	0.157	0.68	0.00128	0.146	0.8	0.0011	0.128
Summer	194	0.59	6.68	0.287	0.85	0.00124	0.141	0.79	0.00129	0.172
Autumn	196	0.79	4.89	0.116	0.8	0.00143	0.159	0.78	0.00123	0.178
UC	273	0.83	6.42	0.131	0.63	0.00132	0.16	0.63	0.00145	0.185
LC	273	0.82	5.06	0.108	0.79	0.00133	0.171	0.8	0.00091	0.131
Spring UC	78	0.78	5.79	0.17	0.53	0.00136	0.182	0.71	0.00126	0.161
Spring LC	78	0.76	5.42	0.159	0.74	0.00119	0.154	0.84	0.00086	0.135
Summer UC	97	0.43	7.55	0.368	0.66	0.00119	0.149	0.61	0.00155	0.238
Summer LC	97	0.55	5.68	0.344	0.86	0.00129	0.2	0.79	0.00096	0.219
Autumn UC	98	0.75	5.64	0.138	0.66	0.00139	0.18	0.64	0.00149	0.25
Autumn LC	98	0.85	3.99	0.103	0.81	0.00147	0.24	0.78	0.00089	0.129

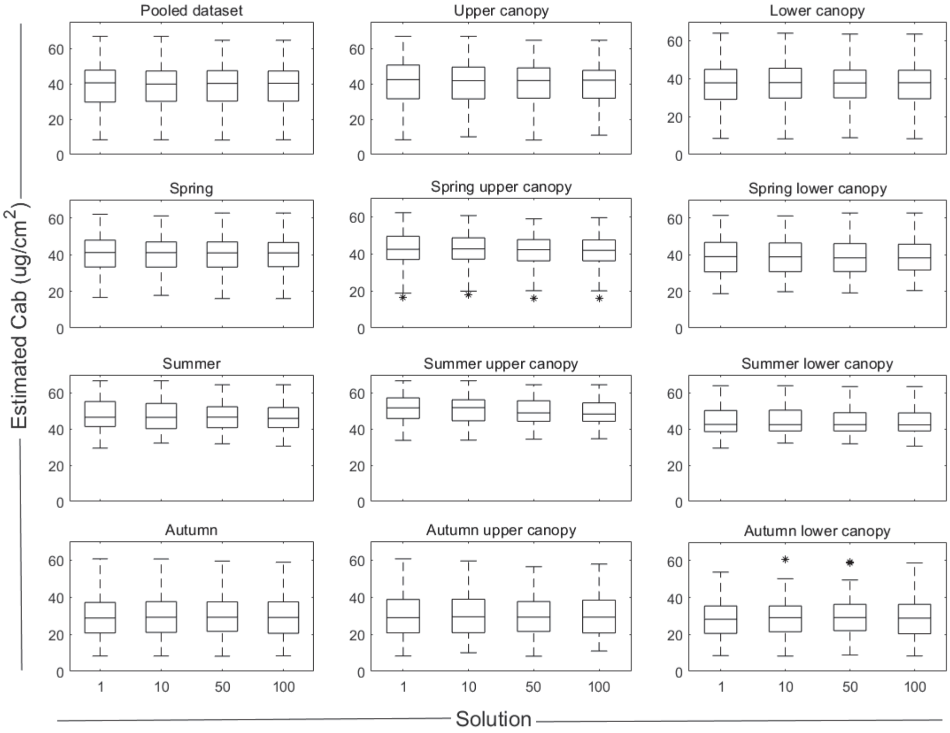

Figure A1: Distribution of retrieved C_{ab} based on different solutions across the canopy throughout the growing season

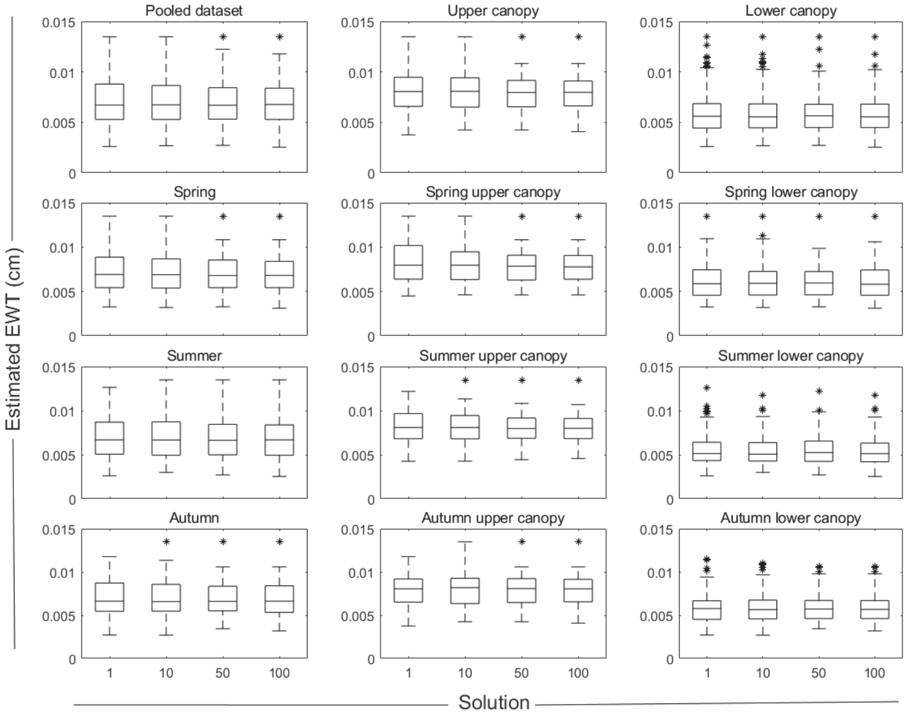

Figure A2: Distribution of retrieved EWT based on different solutions across the canopy throughout the growing season

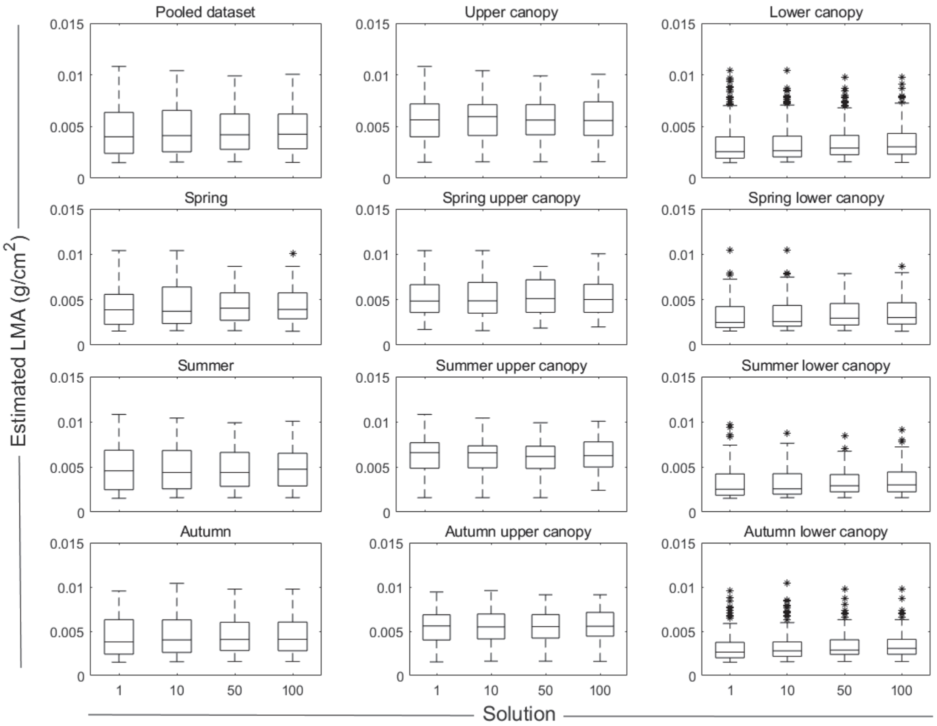

Figure A3: Distribution of retrieved LMA based on different solutions across the canopy throughout the growing season

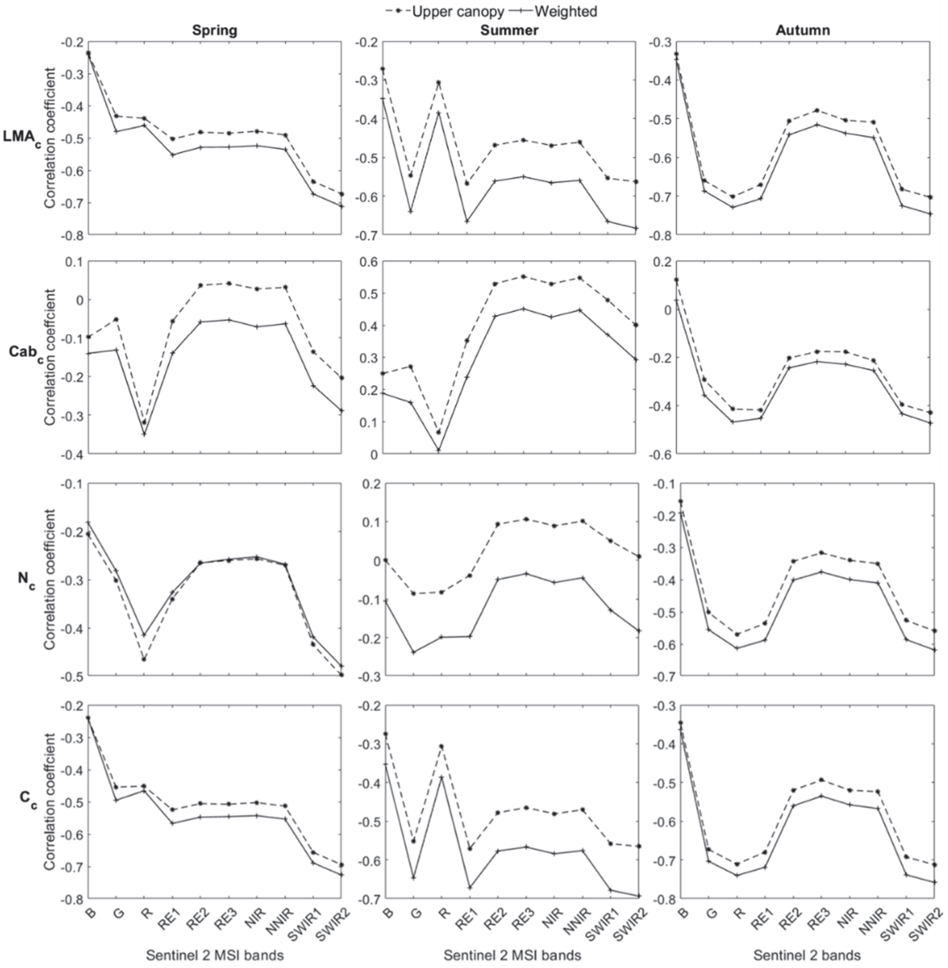

Figure A4: Seasonal correlation analysis between Sentinel-2 MSI bands and canopy traits

Bibliography

ADC-BioScientific, 2013. AM350 Portable Leaf Area Meter. ADC BioScientific Ltd, Hoddesdon.

Adds, J., Larkcom, E. and Miller, R.N., 1997. The Organism and the Environment. Nelson.

Adjorlolo, C., Mutanga, O. and Cho, M.A., 2015. Predicting C3 and C4 grass nutrient variability using in situ canopy reflectance and partial least squares regression. International Journal of Remote Sensing, 36(6): 1743-1761.

Agency, E.S., 2015. Sentinel-2 Radiometric Resolutions. In: E.S. Agency (Editor).

Alcaraz-Segura, D., Lomba, A., Sousa-Silva, R., Nieto-Lugilde, D., Alves, P., Georges, D., Vicente, J.R. and Honrado, J.P., 2017. Potential of satellite-derived ecosystem functional attributes to anticipate species range shifts. International Journal of Applied Earth Observation and Geoinformation, 57: 86-92.

Ali, A.M., Darvishzadeh, R., Skidmore, A.K., Duren, I.v., Heiden, U. and Heurich, M., 2016. Estimating leaf functional traits by inversion of PROSPECT: Assessing leaf dry matter content and specific leaf area in mixed mountainous forest. International Journal of Applied Earth Observation and Geoinformation, 45, Part A: 66-76.

Allen, W.A. and Richardson, A.J., 1968. Interaction of Light with a Plant Canopy*. Journal of the Optical Society of America, 58(8): 1023-1028.

Alvarez-Guerra, M., Ballabio, D., Amigo, J.M., Bro, R. and Viguri, J.R., 2010. Development of models for predicting toxicity from sediment chemistry by partial least squares-discriminant analysis and counter-propagation artificial neural networks. Environmental Pollution, 158(2): 607-614.

Anten, N.P.R. and Ackerly, D.D., 2001. Canopy-level photosynthetic compensation after defoliation in a tropical understorey palm. Functional Ecology, 15(2): 252-262.

Archontoulis, S.V., Vos, J., Yin, X., Bastiaans, L., Danalatos, N.G. and Struik, P.C., 2011. Temporal dynamics of light and nitrogen vertical distributions in canopies of sunflower, kenaf and cynara. Field Crops Research, 122(3): 186-198.

Arellano, P., Tansey, K., Balzter, H. and Boyd, D.S., 2017. Field spectroscopy and radiative transfer modelling to assess impacts of petroleum pollution on biophysical and biochemical parameters of the Amazon rainforest. Environmental Earth Sciences, 76(5): 217.

Asbjornsen, H., Goldsmith, G.R., Alvarado-Barrientos, M.S., Rebel, K., Van Osch, F.P., Rietkerk, M., Chen, J., Gotsch, S., Tobón, C., Geissert, D.R., Gómez-Tagle, A., Vache, K. and Dawson, T.E., 2011. Ecohydrological advances and applications in plant–water relations research: a review. Journal of Plant Ecology, 4(1-2): 3-22.

Aschbacher, J. and Milagro-Pérez, M.P., 2012. The European Earth monitoring (GMES) programme: Status and perspectives. Remote Sensing of Environment, 120(0): 3-8.

ASD, 2008. Integrating Sphere User Manual. Analytical Spectral Devices, Inc. (ASD), Boulder, CO.

Atherton, J., Olascoaga, B., Alonso, L. and Porcar-Castell, A., 2017. Spatial Variation of Leaf Optical Properties in a Boreal Forest Is Influenced by Species and Light Environment. Frontiers in Plant Science, 8(309).

Atzberger, C. and Richter, K., 2012. Spatially constrained inversion of radiative transfer models for improved LAI mapping from future Sentinel-2 imagery. Remote Sensing of Environment, 120(0): 208-218.

Axelsson, C., Skidmore, A.K., Schlerf, M., Fauzi, A. and Verhoef, W., 2013. Hyperspectral analysis of mangrove foliar chemistry using PLSR and support vector regression. International Journal of Remote Sensing, 34(5): 1724-1743.

Barboni, D., Harrison, S.P., Bartlein, P.J., Jalut, G., New, M., Prentice, I.C., Sanchez-Goñi, M.F., Spessa, A., Davis, B. and Stevenson, A.C., 2004. Relationships between plant traits and climate in the Mediterranean region: A pollen data analysis. Journal of Vegetation Science, 15(5): 635-646.

Baret, F. and Fourty, T., 1997. Estimation of leaf water content and specific leaf weight from reflectance and transmittance measurements. Agronomie, 17(9-10): 455-464.

Barnes, E.M., Clarke, T.R., Richards, S.E., Colaizzi, P.D., Haberland, J., Kostrzewski, M., Waller, P., Choi, C., Riley, E., Thompson, T., Lascano, R.J., Li, H. and Moran, M.S., 2000. Coincident detection of crop water stress, nitrogen status and canopy density using ground-based multispectral data. American Society of Agronomy, Madison, pp. 1-15.

Barry, K.M., Newnham, G.J. and Stone, C., 2009. Estimation of chlorophyll content in Eucalyptus globulus foliage with the leaf reflectance model PROSPECT. Agricultural and Forest Meteorology, 149(6–7): 1209-1213.

Bässler, C., Förster, B., Moning, C. and Müller, J., 2009. The BIOKLIM project: biodiversity research between climate change and wilding in a temperate montane forest : the conceptual framework. Waldökologie, Landschaftsforschung und Naturschutz(7): 21-34.

Behrman, E.L., Watson, S.S., O'Brien, K.R., Heschel, M.S. and Schmidt, P.S., 2015. Seasonal variation in life history traits in two Drosophila species. Journal of evolutionary biology, 28(9): 1691-1704.

Bian, M., Skidmore, A.K., Schlerf, M., Fei, T., Liu, Y. and Wang, T., 2010. Reflectance Spectroscopy of Biochemical Components as Indicators of Tea (Camellia Sinensis) Quality. Photogrammetric Engineering & Remote Sensing, 76(12): 1385-1392.

Bouzoubaâ, Z., El Mousadik, A. and Belahsen, Y., 2006. Variation in amounts of epicuticular wax on leaves of Argania spinosa (L). Skeels. Acta Botanica Gallica, 153(2): 167-177.

Breiman, L., 2001. Random Forests. Machine Learning, 45(1): 5-32.

Buddenbaum, H. and Hill, J., 2015. PROSPECT Inversions of Leaf Laboratory Imaging Spectroscopy – a Comparison of Spectral Range and Inversion Technique Influences. Photogrammetrie - Fernerkundung - Geoinformation, 2015(3): 231-240.

Cailleret, M., Heurich, M. and Bugmann, H., 2014. Reduction in browsing intensity may not compensate climate change effects on tree species composition in the Bavarian Forest National Park. Forest Ecology and Management, 328: 179-192.

Carrascal, L.M., Galván, I. and Gordo, O., 2009. Partial least squares regression as an alternative to current regression methods used in ecology. Oikos, 118(5): 681-690.

Carrión, C., Martínez, D., Costa, M. and Guiamet, J., 2014. Senescence-Associated Vacuoles, a Specific Lytic Compartment for Degradation of Chloroplast Proteins? Plants, 3(4): 498.

Carvalho, S., Schlerf, M., van der Putten, W.H. and Skidmore, A.K., 2013. Hyperspectral reflectance of leaves and flowers of an outbreak species discriminates season and successional stage of vegetation. International Journal of Applied Earth Observation and Geoinformation, 24: 32-41.

Casas, A., Riaño, D., Ustin, S.L., Dennison, P. and Salas, J., 2014. Estimation of water-related biochemical and biophysical vegetation properties using multitemporal airborne hyperspectral data and its comparison to MODIS spectral response. Remote Sensing of Environment, 148(0): 28-41.

Chazdon, R.L., 1986. Light Variation and Carbon Gain in Rain Forest Understorey Palms. Journal of Ecology, 74(4): 995-1012.

Chemura, A., Mutanga, O., Odindi, J. and Kutywayo, D., 2018. Mapping spatial variability of foliar nitrogen in coffee (Coffea arabica L.) plantations with multispectral Sentinel-2 MSI data. ISPRS Journal of Photogrammetry and Remote Sensing, 138: 1-11.

Chen, J.-L., Reynolds, J.F., Harley, P.C. and Tenhunen, J.D., 1993. Coordination theory of leaf nitrogen distribution in a canopy. Oecologia, 93(1): 63-69.

Chen Jing, M., Mo, G., Pisek, J., Liu, J., Deng, F., Ishizawa, M. and Chan, D., 2012. Effects of foliage clumping on the estimation of global terrestrial gross primary productivity. Global Biogeochemical Cycles, 26(1).

Chen, J.M., Liu, J., Cihlar, J. and Goulden, M.L., 1999. Daily canopy photosynthesis model through temporal and spatial scaling for remote sensing applications. Ecological Modelling, 124(2): 99-119.

Cho, M.A., Ramoelo, A., Debba, P., Mutanga, O., Mathieu, R., van Deventer, H. and Ndlovu, N., 2013. Assessing the effects of subtropical forest fragmentation on leaf nitrogen distribution using remote sensing data. Landscape Ecology, 28(8): 1479-1491.

Christensen, L.K., Bennedsen, B.S., Jørgensen, R.N. and Nielsen, H., 2004. Modelling Nitrogen and Phosphorus Content at Early Growth Stages in Spring Barley using Hyperspectral Line Scanning. Biosystems Engineering, 88(1): 19-24.

Ciganda, V.S., Gitelson, A.A. and Schepers, J., 2012. How deep does a remote sensor sense? Expression of chlorophyll content in a maize canopy. Remote Sensing of Environment, 126(0): 240-247.

Clevers, J. and Kooistra, L., 2012. Using Hyperspectral Remote Sensing Data for Retrieving Canopy Chlorophyll and Nitrogen Content. Ieee Journal of Selected Topics in Applied Earth Observations and Remote Sensing, 5(2): 574-583.

Clevers, J., Kooistra, L. and van den Brande, M., 2017. Using Sentinel-2 Data for Retrieving LAI and Leaf and Canopy Chlorophyll Content of a Potato Crop. Remote Sensing, 9(5): 405.

Clevers, J.G.P.W. and Gitelson, A.A., 2013. Remote estimation of crop and grass chlorophyll and nitrogen content using red-edge bands on Sentinel-2 and -3. International Journal of Applied Earth Observation and Geoinformation, 23(0): 344-351.

Coble, A.P., VanderWall, B., Mau, A. and Cavaleri, M.A., 2016a. How vertical patterns in leaf traits shift seasonally and the implications for modeling canopy photosynthesis in a temperate deciduous forest. Tree Physiology, 36(9): 1077-1091.

Coble, A.P., VanderWall, B., Mau, A. and Cavaleri, M.A., 2016b. How vertical patterns in leaf traits shift seasonally and the implications for modeling canopy photosynthesis in a temperate deciduous forest. Tree Physiology.

Combal, B., Baret, F., Weiss, M., Trubuil, A., Macé, D., Pragnère, A., Myneni, R., Knyazikhin, Y. and Wang, L., 2003. Retrieval of canopy biophysical variables from bidirectional reflectance: Using prior information to solve the ill-posed inverse problem. Remote Sensing of Environment, 84(1): 1-15.

Croft, H., Chen, J.M., Zhang, Y., Simic, A., Noland, T.L., Nesbitt, N. and Arabian, J., 2015. Evaluating leaf chlorophyll content prediction from multispectral remote sensing data within a physically-based modelling framework. ISPRS Journal of Photogrammetry and Remote Sensing, 102: 85-95.

Curran, P.J., 1989. Remote sensing of foliar chemistry. Remote Sensing of Environment, 30(3): 271-278.

Curran, P.J., Dungan, J.L. and Peterson, D.L., 2001. Estimating the foliar biochemical concentration of leaves with reflectance spectrometry:

Testing the Kokaly and Clark methodologies. Remote Sensing of Environment, 76(3): 349-359.

Darvishzadeh, R., Atzberger, C., Skidmore, A.K. and Abkar, A.A., 2009. Leaf Area Index derivation from hyperspectral vegetation indicesand the red edge position. International Journal of Remote Sensing, 30(23): 6199-6218.

Darvishzadeh, R., Matkan, A.A. and Ahangar, A.D., 2012. Inversion of a Radiative Transfer Model for Estimation of Rice Canopy Chlorophyll Content Using a Lookup-Table Approach. Ieee Journal of Selected Topics in Applied Earth Observations and Remote Sensing, 5(4): 1222-1230.

Darvishzadeh, R., Skidmore, A., Atzberger, C. and van Wieren, S., 2008a. Estimation of vegetation LAI from hyperspectral reflectance data: Effects of soil type and plant architecture. International Journal of Applied Earth Observation and Geoinformation, 10(3): 358-373.

Darvishzadeh, R., Skidmore, A., Schlerf, M. and Atzberger, C., 2008b. Inversion of a radiative transfer model for estimating vegetation LAI and chlorophyll in a heterogeneous grassland. Remote Sensing of Environment, 112(5): 2592-2604.

Darvishzadeh, R., Skidmore, A., Schlerf, M., Atzberger, C., Corsi, F. and Cho, M., 2008c. LAI and chlorophyll estimation for a heterogeneous grassland using hyperspectral measurements. ISPRS Journal of Photogrammetry and Remote Sensing, 63(4): 409-426.

Daughtry, C.S.T., Walthall, C.L., Kim, M.S., de Colstoun, E.B. and McMurtrey, J.E., 2000. Estimating Corn Leaf Chlorophyll Concentration from Leaf and Canopy Reflectance. Remote Sensing of Environment, 74(2): 229-239.

Dawson, T.P., Curran, P.J. and Plummer, S.E., 1998. LIBERTY—Modeling the Effects of Leaf Biochemical Concentration on Reflectance Spectra. Remote Sensing of Environment, 65(1): 50-60.

Delegido, J., Alonso, L., González, G. and Moreno, J., 2010. Estimating chlorophyll content of crops from hyperspectral data using a normalized area over reflectance curve (NAOC). International Journal of Applied Earth Observation and Geoinformation, 12(3): 165-174.

Delegido, J., Van Wittenberghe, S., Verrelst, J., Ortiz, V., Veroustraete, F., Valcke, R., Samson, R., Rivera, J.P., Tenjo, C. and Moreno, J., 2014. Chlorophyll content mapping of urban vegetation in the city of Valencia based on the hyperspectral NAOC index. Ecological Indicators, 40(0): 34-42.

Delloye, C., Weiss, M. and Defourny, P., 2018. Retrieval of the canopy chlorophyll content from Sentinel-2 spectral bands to estimate nitrogen uptake in intensive winter wheat cropping systems. Remote Sensing of Environment, 216: 245-261.

Demarez, V., 1999. Seasonal variation of leaf chlorophyll content of a temperate forest. Inversion of the PROSPECT model. International Journal of Remote Sensing, 20(5): 879-894.

Diaz, S., Hodgson, J.G., Thompson, K., Cabido, M., Cornelissen, J.H.C., Jalili, A., Montserrat-Martí, G., Grime, J.P., Zarrinkamar, F., Asri, Y., Band, S.R., Basconcelo, S., Castro-Díez, P., Funes, G., Hamzehee, B., Khoshnevi, M., Pérez-Harguindeguy, N., Pérez-Rontomé, M.C., Shirvany, F.A., Vendramini, F., Yazdani, S., Abbas-Azimi, R., Bogaard, A., Boustani, S., Charles, M., Dehghan, M., de Torres-Espuny, L., Falczuk, V., Guerrero-Campo, J., Hynd, A., Jones, G., Kowsary, E., Kazemi-Saeed, F., Maestro-Martínez, M., Romo-Díez, A., Shaw, S., Siavash, B., Villar-Salvador, P. and Zak, M.R., 2004. The plant traits that drive ecosystems: Evidence from three continents. Journal of Vegetation Science, 15(3): 295-304.

Dreccer, M.F., van Oijen, M., Schapendonk, A.H.C.M., Pot, C.S. and Rabbinge, R., 2000. Dynamics of Vertical Leaf Nitrogen Distribution in a Vegetative Wheat Canopy. Impact on Canopy Photosynthesis. Annals of Botany, 86(4): 821-831.

Dusseux, P., Hubert-Moy, L., Corpetti, T. and Vertès, F., 2015. Evaluation of SPOT imagery for the estimation of grassland biomass. International Journal of Applied Earth Observation and Geoinformation, 38(0): 72-77.

Dutta, D., Das, P.K., Bhunia, U.K., Singh, U., Singh, S., Sharma, J.R. and Dadhwal, V.K., 2015. Retrieval of tea polyphenol at leaf level using spectral transformation and multi-variate statistical approach. International Journal of Applied Earth Observation and Geoinformation, 36(0): 22-29.

Eitel, J.U.H., Vierling, L.A. and Long, D.S., 2010. Simultaneous measurements of plant structure and chlorophyll content in broadleaf saplings with a terrestrial laser scanner. Remote Sensing of Environment, 114(10): 2229-2237.

Ellsworth, D.S. and Reich, P.B., 1993. Canopy structure and vertical patterns of photosynthesis and related leaf traits in a deciduous forest. Oecologia, 96(2): 169-178.

European Space Agency, 2010. GMES Sentinel-2 Mission Requirements Document: Technical Report issue 2 revision 1. In: E.S. Agency (Editor).

Evans, J.R. and Poorter, H., 2001. Photosynthetic acclimation of plants to growth irradiance: the relative importance of specific leaf area and nitrogen partitioning in maximizing carbon gain. Plant, Cell & Environment, 24(8): 755-767.

Fang, H., Liu, W., Li, W. and Wei, S., 2018. Estimation of the directional and whole apparent clumping index (ACI) from indirect optical measurements. ISPRS Journal of Photogrammetry and Remote Sensing, 144: 1-13.

Feret, J.-B., François, C., Asner, G.P., Gitelson, A.A., Martin, R.E., Bidel, L.P.R., Ustin, S.L., le Maire, G. and Jacquemoud, S., 2008. PROSPECT-4 and 5: Advances in the leaf optical properties model separating photosynthetic pigments. Remote Sensing of Environment, 112(6): 3030-3043.

Féret, J.-B., François, C., Gitelson, A., Asner, G.P., Barry, K.M., Panigada, C., Richardson, A.D. and Jacquemoud, S., 2011. Optimizing spectral indices and chemometric analysis of leaf chemical properties using radiative transfer modeling. Remote Sensing of Environment, 115(10): 2742-2750.

Féret, J.B., Gitelson, A.A., Noble, S.D. and Jacquemoud, S., 2017. PROSPECT-D: Towards modeling leaf optical properties through a complete lifecycle. Remote Sensing of Environment, 193: 204-215.

Féret, J.B., le Maire, G., Jay, S., Berveiller, D., Bendoula, R., Hmimina, G., Cheraiet, A., Oliveira, J.C., Ponzoni, F.J., Solanki, T., de Boissieu, F., Chave, J., Nouvellon, Y., Porcar-Castell, A., Proisy, C., Soudani, K., Gastellu-Etchegorry, J.P. and Lefèvre-Fonollosa, M.J., 2018. Estimating leaf mass per area and equivalent water thickness based on leaf optical properties: Potential and limitations of physical modeling and machine learning. Remote Sensing of Environment.

Ferwerda, J.G. and Skidmore, A.K., 2007. Can nutrient status of four woody plant species be predicted using field spectrometry? ISPRS Journal of Photogrammetry and Remote Sensing, 62(6): 406-414.

Field, C., 1983. Allocating leaf nitrogen for the maximization of carbon gain: Leaf age as a control on the allocation program. Oecologia, 56(2-3): 341-347.

Fisher, J.B., Badgley, G. and Blyth, E., 2012. Global nutrient limitation in terrestrial vegetation. Global Biogeochemical Cycles, 26(3).

Fourty, T. and Baret, F., 1998. On spectral estimates of fresh leaf biochemistry. International Journal of Remote Sensing, 19(7): 1283-1297.

Frampton, W.J., Dash, J., Watmough, G. and Milton, E.J., 2013. Evaluating the capabilities of Sentinel-2 for quantitative estimation of biophysical variables in vegetation. ISPRS Journal of Photogrammetry and Remote Sensing, 82: 83-92.

Gara, T., Darvishzadeh, R., Skidmore, A. and Wang, T., 2018a. Impact of Vertical Canopy Position on Leaf Spectral Properties and Traits across Multiple Species. Remote Sensing, 10(2): 346.

Gara, T.W., Skidmore, A.K., Darvishzadeh, R. and Wang, T., 2018b. Leaf to canopy upscaling approach affects the estimation of canopy traits. GIScience & Remote Sensing: 1-22.

Gara, T.W., Skidmore, A.K., Darvishzadeh, R. and Wang, T., 2019. Leaf to canopy upscaling approach affects the estimation of canopy traits GIScience & Remote Sensing, 56(4): 554-575.

Geladi, P. and Kowalski, B.R., 1986. Partial least-squares regression: a tutorial. Analytica Chimica Acta, 185: 1-17.

Gibson, D.J., 2008. Grasses and Grassland Ecology. Oxford University Press, New York.

Gitelson, A. and Merzlyak, M.N., 1994. Quantitative estimation of chlorophyll-a using reflectance spectra: Experiments with autumn chestnut and maple leaves. Journal of Photochemistry and Photobiology B: Biology, 22(3): 247-252.

Gitelson, A.A., Viña, A., Ciganda, V., Rundquist, D.C. and Arkebauer, T.J., 2005a. Remote estimation of canopy chlorophyll content in crops. Geophysical Research Letters, 32(8): 1-4.

Gitelson, A.A., Viña, A., Ciganda, V., Rundquist, D.C. and Arkebauer, T.J., 2005b. Remote estimation of canopy chlorophyll in crops. Geophysical Research Letters, 32.

Govaerts, Y.M. and Verstraete, M.M., 1998. Raytran: a Monte Carlo ray-tracing model to compute light scattering in three-dimensional heterogeneous media. IEEE Transactions on Geoscience and Remote Sensing, 36(2): 493-505.

Haboudane, D., Miller, J.R., Pattey, E., Zarco-Tejada, P.J. and Strachan, I.B., 2004. Hyperspectral vegetation indices and novel algorithms for predicting green LAI of crop canopies: Modeling and validation in the context of precision agriculture. Remote Sensing of Environment, 90(3): 337-352.

Haboudane, D., Miller, J.R., Tremblay, N., Zarco-Tejada, P.J. and Dextraze, L., 2002. Integrated narrow-band vegetation indices for prediction of crop chlorophyll content for application to precision agriculture. Remote Sensing of Environment, 81(2–3): 416-426.

Hassall, M., Riddington, R. and Helden, A., 2001. Foraging behaviour of brent geese, Branta b. bernicla, on grasslands: effects of sward length and nitrogen content. Oecologia, 127(1): 97-104.

He, L., Zhang, H.-Y., Zhang, Y.-S., Song, X., Feng, W., Kang, G.-Z., Wang, C.-Y. and Guo, T.-C., 2016. Estimating canopy leaf nitrogen concentration in winter wheat based on multi-angular hyperspectral remote sensing. European Journal of Agronomy, 73: 170-185.

He, Y. and Mui, A., 2010a. Scaling up Semi-Arid Grassland Biochemical Content from the Leaf to the Canopy Level: Challenges and Opportunities. Sensors 10(12): 11072-11087.

He, Y. and Mui, A., 2010b. Scaling up Semi-Arid Grassland Biochemical Content from the Leaf to the Canopy Level: Challenges and Opportunities. Sensors (Basel, Switzerland), 10(12): 11072-11087.

Heurich, M., Beudert, B., Rall, H. and Křenová, Z., 2010a. National Parks as Model Regions for Interdisciplinary Long-Term Ecological Research: The Bavarian Forest and Šumavá National Parks Underway to Transboundary Ecosystem Research. In: F. Müller, C. Baessler, H. Schubert and S. Klotz (Editors), Long-Term Ecological Research: Between Theory and Application. Springer Netherlands, Dordrecht, pp. 327-344.

Heurich, M., Ochs, T., Andresen, T. and Schneider, T., 2010b. Object-orientated image analysis for the semi-automatic detection of dead trees following a spruce bark beetle (Ips typographus) outbreak. European Journal of Forest Research, 129(3): 313-324.

Hikosaka, K., 2005. Leaf Canopy as a Dynamic System: Ecophysiology and Optimality in Leaf Turnover. Annals of Botany, 95(3): 521-533.

Hikosaka, K. and Hirose, T., 2000. Photosynthetic nitrogen-use efficiency in evergreen broad-leaved woody species coexisting in a warm-temperate forest. Tree Physiology, 20(18): 1249-1254.

Hill, J., Buddenbaum, H. and Townsend, P.A., 2019. Imaging Spectroscopy of Forest Ecosystems: Perspectives for the Use of Space-borne Hyperspectral Earth Observation Systems. Surveys in Geophysics.

Hill, M.J., 2013. Vegetation index suites as indicators of vegetation state in grassland and savanna: An analysis with simulated SENTINEL 2 data for a North American transect. Remote Sensing of Environment, 137(0): 94-111.

Hirose, T. and Werger, M.J.A., 1987. Maximizing daily canopy photosynthesis with respect to the leaf nitrogen allocation pattern in the canopy. Oecologia, 72(4): 520-526.

Hirose, T., Werger, M.J.A. and Rheenen, J.W.A.v., 1989. Canopy Development and Leaf Nitrogen Distribution in a Stand of Carex Acutiformis. Ecology, 70(6): 1610-1618.

Homolová, L., Malenovský, Z., Clevers, J.G.P.W., García-Santos, G. and Schaepman, M.E., 2013. Review of optical-based remote sensing for plant trait mapping. Ecological Complexity, 15(0): 1-16.

Houborg, R., Fisher, J.B. and Skidmore, A.K., 2015. Advances in remote sensing of vegetation function and traits. International Journal of Applied Earth Observation and Geoinformation, 43: 1-6.

Huang, W., Wang, Z., Huang, L., Lamb, D., Ma, Z., Zhang, J., Wang, J. and Zhao, C., 2011. Estimation of vertical distribution of chlorophyll concentration by bi-directional canopy reflectance spectra in winter wheat. Precision Agriculture, 12(2): 165-178.

Huang, W., Yang, Q., Pu, R. and Yang, S., 2014. Estimation of Nitrogen Vertical Distribution by Bi-Directional Canopy Reflectance in Winter Wheat. Sensors, 14(11): 20347.

Jacoby, P.W., Ansley, R.J., Meadors, C.H. and Huffman, A.H., 1990. Epicuticular Wax in Honey Mesquite: Seasonal Accumulation and Intraspecific Variation. Journal of Range Management, 43(4): 347-350.

Jacquemoud, S. and Baret, F., 1990. PROSPECT: A model of leaf optical properties spectra. Remote Sensing of Environment, 34(2): 75-91.

Jacquemoud, S., Ustin, S.L., Verdebout, J., Schmuck, G., Andreoli, G. and Hosgood, B., 1996. Estimating leaf biochemistry using the PROSPECT leaf optical properties model. Remote Sensing of Environment, 56(3): 194-202.

Jacquemoud, S., Verhoef, W., Baret, F., Bacour, C., Zarco-Tejada, P.J., Asner, G.P., François, C. and Ustin, S.L., 2009. PROSPECT + SAIL models: A review of use for vegetation characterization. Remote Sensing of Environment, 113, Supplement 1(0): S56-S66.

Jiang, J., Comar, A., Burger, P., Bancal, P., Weiss, M. and Baret, F., 2018. Estimation of leaf traits from reflectance measurements: comparison between methods based on vegetation indices and several versions of the PROSPECT model. Plant Methods, 14(1): 23.

Kalacska, M., Lalonde, M. and Moore, T.R., 2015. Estimation of foliar chlorophyll and nitrogen content in an ombrotrophic bog from hyperspectral data: Scaling from leaf to image. Remote Sensing of Environment, 169: 270-279.

Kattge, J., DÍAz, S., Lavorel, S., Prentice I, C., Leadley, P., BÖNisch, G., Garnier, E., Westoby, M., Reich P, B., Wright I, J., Cornelissen J. H, C., Violle, C., Harrison S, P., Van, B.P.M., Reichstein, M., Enquist B, J., Soudzilovskaia N, A., Ackerly D, D., Anand, M., Atkin, O., Bahn, M., Baker T, R., Baldocchi, D., Bekker, R., Blanco C, C., Blonder, B., Bond W, J., Bradstock, R., Bunker D, E., Casanoves, F., Cavender-Bares, J., Chambers J, Q., Chapin Iii F, S., Chave, J., Coomes, D., Cornwell W, K., Craine J, M., Dobrin B, H., Duarte, L., Durka, W., Elser, J., Esser, G., Estiarte, M., Fagan W, F., Fang, J., FernÁNdez-MÉNdez, F., Fidelis, A., Finegan, B., Flores, O., Ford, H., Frank, D., Freschet G, T., Fyllas N, M., Gallagher R, V., Green W, A., Gutierrez A, G., Hickler, T., Higgins S, I., Hodgson J, G., Jalili, A., Jansen, S., Joly C, A., Kerkhoff A, J., Kirkup, D., Kitajima, K., Kleyer, M., Klotz, S., Knops J. M, H., Kramer, K., KÜHn, I., Kurokawa, H., Laughlin, D., Lee T, D., Leishman, M., Lens, F., Lenz, T., Lewis S, L., Lloyd, J., LlusiÀ, J., Louault, F., Ma, S., Mahecha M, D., Manning, P., Massad, T., Medlyn B, E., Messier, J., Moles A, T., MÜLler S, C., Nadrowski, K., Naeem, S., Niinemets, Ü., NÖLlert, S., NÜSke, A., Ogaya, R., Oleksyn, J., Onipchenko V, G., Onoda, Y., OrdoÑEz, J., Overbeck, G., Ozinga W, A., PatiÑO, S., Paula, S., Pausas J, G., PeÑUelas, J., Phillips O, L., Pillar, V., Poorter, H., Poorter, L., Poschlod, P., Prinzing, A., Proulx, R., Rammig, A., Reinsch, S., Reu, B., Sack, L., Salgado-Negret, B., Sardans, J., Shiodera, S., Shipley, B., Siefert, A., Sosinski, E., Soussana, J.F., Swaine, E., Swenson, N., Thompson, K., Thornton, P., Waldram, M., Weiher, E., White, M., White, S., Wright S, J., Yguel, B., Zaehle, S., Zanne A, E. and Wirth, C., 2011. TRY – a global database of plant traits. Global Change Biology, 17(9): 2905-2935.

Khavaninzadeh, A.R., Veroustraete, F., Van Wittenberghe, S., Verrelst, J. and Samson, R., 2015. Leaf reflectance variation along a vertical crown gradient of two deciduous tree species in a Belgian industrial habitat. Environmental Pollution, 204: 324-332.

Kimes, D.S., Knyazikhin, Y., Privette, J.L., Abuelgasim, A.A. and Gao, F., 2000. Inversion methods for physically-based models. Remote Sensing Reviews, 18(2-4): 381-439.

Kissling, W.D., Ahumada Jorge, A., Bowser, A., Fernandez, M., Fernández, N., García Enrique, A., Guralnick Robert, P., Isaac Nick, J.B., Kelling, S., Los, W., McRae, L., Mihoub, J.B., Obst, M., Santamaria, M., Skidmore Andrew, K., Williams Kristen, J., Agosti, D., Amariles, D., Arvanitidis, C., Bastin, L., De Leo, F., Egloff, W., Elith, J., Hobern, D., Martin, D., Pereira Henrique, M., Pesole, G., Peterseil, J., Saarenmaa, H., Schigel, D., Schmeller Dirk, S., Segata, N., Turak, E., Uhlir Paul, F., Wee, B. and Hardisty Alex, R., 2017. Building essential biodiversity variables (EBVs) of species distribution and abundance at a global scale. Biological Reviews, 93(1): 600-625.

Knox, N.M., Skidmore, A.K., Schlerf, M., de Boer, W.F., van Wieren, S.E., van der Waal, C., Prins, H.H.T. and Slotow, R., 2010. Nitrogen prediction in grasses: effect of bandwidth and plant material state on absorption feature selection. International Journal of Remote Sensing, 31(3): 691-704.

Knyazikhin, Y., Schull, M.A., Stenberg, P., Mõttus, M., Rautiainen, M., Yang, Y., Marshak, A., Latorre Carmona, P., Kaufmann, R.K., Lewis, P., Disney, M.I., Vanderbilt, V., Davis, A.B., Baret, F., Jacquemoud, S., Lyapustin, A. and Myneni, R.B., 2013. Hyperspectral remote sensing of foliar nitrogen content. Proceedings of the National Academy of Sciences, 110(3): E185–E192.

Kokaly, R.F., 2001. Investigating a Physical Basis for Spectroscopic Estimates of Leaf Nitrogen Concentration. Remote Sensing of Environment, 75(2): 153-161.

Kokaly, R.F., Asner, G.P., Ollinger, S.V., Martin, M.E. and Wessman, C.A., 2009. Characterizing canopy biochemistry from imaging spectroscopy and its application to ecosystem studies. Remote Sensing of Environment, 113, Supplement 1(0): S78-S91.

Kokaly, R.F. and Clark, R.N., 1999. Spectroscopic Determination of Leaf Biochemistry Using Band-Depth Analysis of Absorption Features and Stepwise Multiple Linear Regression. Remote Sensing of Environment, 67(3): 267-287.

Kropff, M.J. and Goudriaan, J., 1994. Competition for resource capture in agricultural crops, Resource capture by crops. Nottingham University Press.

Kuhn, M., 2008. Building Predictive Models in R Using the caret Package. 2008, 28(5): 26.

Kull, O. and Kruijt, B., 1999. Acclimation of photosynthesis to light: a mechanistic approach. Functional Ecology, 13(1): 24-36.

Kumar, L., Schmidt, K., Dury, S. and Skidmore, A., 2001. Imaging Spectrometry and Vegetation Science. In: F.D.d.v. Meer and S.M.D. Jong (Editors), Imaging Spectrometry: Basic Principles and Prospective Applications. Springer Netherlands, Dordrecht, pp. 111-155.

Kuusk, A., 2001. A two-layer canopy reflectance model. Journal of Quantitative Spectroscopy and Radiative Transfer, 71(1): 1-9.

Lavorel, S., Grigulis, K., Lamarque, P., Colace, M.-P., Garden, D., Girel, J., Pellet, G. and Douzet, R., 2011. Using plant functional traits to understand the landscape distribution of multiple ecosystem services. Journal of Ecology, 99(1): 135-147.

Li, C., Zhu, X., Wei, Y., Cao, S., Guo, X., Yu, X. and Chang, C., 2018a. Estimating apple tree canopy chlorophyll content based on Sentinel-2A remote sensing imaging. Scientific Reports, 8(1): 3756.

Li, F., Miao, Y., Feng, G., Yuan, F., Yue, S., Gao, X., Liu, Y., Liu, B., Ustin, S.L. and Chen, X., 2014. Improving estimation of summer maize nitrogen status with red edge-based spectral vegetation indices. Field Crops Research, 157: 111-123.

Li, H., Zhao, C., Huang, W. and Yang, G., 2013. Non-uniform vertical nitrogen distribution within plant canopy and its estimation by remote sensing: A review. Field Crops Research, 142(0): 75-84.

Li, L., Jákli, B., Lu, P., Ren, T., Ming, J., Liu, S., Wang, S. and Lu, J., 2018b. Assessing leaf nitrogen concentration of winter oilseed rape with canopy hyperspectral technique considering a non-uniform vertical nitrogen distribution. Industrial Crops and Products, 116: 1-14.

Li, P. and Wang, Q., 2011. Retrieval of Leaf Biochemical Parameters Using PROSPECT Inversion: A New Approach for Alleviating Ill-Posed Problems. IEEE Transactions on Geoscience and Remote Sensing, 49(7): 2499-2506.

Li, P. and Wang, Q., 2013a. Developing and validating novel hyperspectral indices for leaf area index estimation: Effect of canopy vertical heterogeneity. Ecological Indicators, 32(0): 123-130.

Li, P. and Wang, Q., 2013b. Retrieval of chlorophyll for assimilating branches of a typical desert plant through inversed radiative transfer models. International Journal of Remote Sensing, 34(7): 2402-2416.

Liang, L., Di, L., Zhang, L., Deng, M., Qin, Z., Zhao, S. and Lin, H., 2015. Estimation of crop LAI using hyperspectral vegetation indices and a hybrid inversion method. Remote Sensing of Environment, 165: 123-134.

Liang, S., 2007. Recent developments in estimating land surface biogeophysical variables from optical remote sensing. Progress in Physical Geography: Earth and Environment, 31(5): 501-516.

Liao, Q., Wang, J., Yang, G., Zhang, D., Li, H., Fu, Y. and Li, Z., 2013. Comparison of spectral indices and wavelet transform for estimating chlorophyll content of maize from hyperspectral reflectance. Journal of Applied Remote Sensing, 7(1): 0735751-07357511.

Lichtenthaler, H.K. and Buschmann, C., 2001. Chlorophylls and Carotenoids: Measurement and Characterization by UV-VIS Spectroscopy, Current Protocols in Food Analytical Chemistry. John Wiley & Sons, Inc.

Lichtenthaler, H.K., Lang, M., Sowinska, M., Heisel, F. and Miehé, J.A., 1996. Detection of Vegetation Stress Via a New High Resolution Fluorescence Imaging System. Journal of Plant Physiology, 148(5): 599-612.

Ling, B., Goodin, D., Mohler, R., Laws, A. and Joern, A., 2014. Estimating Canopy Nitrogen Content in a Heterogeneous Grassland with Varying Fire and Grazing Treatments: Konza Prairie, Kansas, USA. Remote Sensing, 6(5): 4430-4453.

Liu, S., Peng, Y., Du, W., Le, Y. and Li, L., 2015. Remote Estimation of Leaf and Canopy Water Content in Winter Wheat with Different Vertical Distribution of Water-Related Properties. Remote Sensing, 7(4): 4626.

LÖTscher, M., Stroh, K. and Schnyder, H., 2003. Vertical Leaf Nitrogen Distribution in Relation to Nitrogen Status in Grassland Plants. Annals of Botany, 92(5): 679-688.

Luo, J., Ma, R., Feng, H. and Li, X., 2016. Estimating the Total Nitrogen Concentration of Reed Canopy with Hyperspectral Measurements Considering a Non-Uniform Vertical Nitrogen Distribution. Remote Sensing, 8(10): 789.

Ma, L. and Upadhyaya, M.K., 2018. Effects of leaf position on reflectance, transmittance and absorption of red and far-red light in tomato, Chenopodium album and Amaranthus retroflexus leaves. Weed Research, 58(1): 17-24.

Maier, S.W., Lüdeker, W. and Günther, K.P., 1999. SLOP: A Revised Version of the Stochastic Model for Leaf Optical Properties. Remote Sensing of Environment, 68(3): 273-280.

Maillard, A., Diquélou, S., Billard, V., Laîné, P., Garnica, M., Prudent, M., Garcia-Mina, J.-M., Yvin, J.-C. and Ourry, A., 2015. Leaf mineral nutrient remobilization during leaf senescence and modulation by nutrient deficiency. Frontiers in Plant Science, 6(317).

Main, R., Cho, M.A., Mathieu, R., O'Kennedy, M.M., Ramoelo, A. and Koch, S., 2011. An investigation into robust spectral indices for leaf chlorophyll estimation. ISPRS Journal of Photogrammetry and Remote Sensing, 66(6): 751-761.

Makvandi, S., Ghasemzadeh-Barvarz, M., Beaudoin, G., Grunsky, E.C., McClenaghan, M.B., Duchesne, C. and Boutroy, E., 2016. Partial least squares-discriminant analysis of trace element compositions of magnetite from various VMS deposit subtypes: Application to mineral exploration. Ore Geology Reviews, 78: 388-408.

Malenovský, Z., Albrechtová, J., Lhotáková, Z., Zurita-Milla, R., Clevers, J.G.P.W., Schaepman, M.E. and Cudlín, P., 2006. Applicability of the PROSPECT model for Norway spruce needles. International Journal of Remote Sensing, 27(24): 5315-5340.

Malenovsky, Z., Homolova, L., Zurita-Milla, R., Lukes, P., Kaplan, V., Hanus, J., Gastellu-Etchegorry, J.-P. and Schaepman, M.E., 2013. Retrieval of spruce leaf chlorophyll content from airborne image data using continuum removal and radiative transfer. Remote Sensing of Environment, 131: 85-102.

Malenovský, Z., Homolová, L., Zurita-Milla, R., Lukeš, P., Kaplan, V., Hanuš, J., Gastellu-Etchegorry, J.-P. and Schaepman, M.E., 2013. Retrieval of spruce leaf chlorophyll content from airborne image data using continuum removal and radiative transfer. Remote Sensing of Environment, 131(0): 85-102.

Marcoulides, G.A. and Saunders, C., 2006. Editor's Comments: PLS: A Silver Bullet? MIS Quarterly, 30(2): iii-ix.

Mariey, L., Signolle, J.P., Amiel, C. and Travert, J., 2001. Discrimination, classification, identification of microorganisms using FTIR spectroscopy and chemometrics. Vibrational Spectroscopy, 26(2): 151-159.

Martin, A.R. and Thomas, S.C., 2011. A Reassessment of Carbon Content in Tropical Trees. PLOS ONE, 6(8): e23533.

Martin, M.E., Plourde, L.C., Ollinger, S.V., Smith, M.L. and McNeil, B.E., 2008. A generalizable method for remote sensing of canopy nitrogen across a wide range of forest ecosystems. Remote Sensing of Environment, 112(9): 3511-3519.

Meerdink, S.K., Roberts, D.A., King, J.Y., Roth, K.L., Dennison, P.E., Amaral, C.H. and Hook, S.J., 2016. Linking seasonal foliar traits to VSWIR-TIR spectroscopy across California ecosystems. Remote Sensing of Environment, 186: 322-338.

Mercado, L., Lloyd, J., Carswell, F., Malhi, Y., Meir, P. and Nobre, A.D., 2006. Modelling Amazonian forest eddy covariance data: a comparison of big leaf versus sun/shade models for the C-14 tower at Manaus I. Canopy photosynthesis. Acta Amazonica, 36: 69-82.

Moreno-Martínez, Á., Camps-Valls, G., Kattge, J., Robinson, N., Reichstein, M., van Bodegom, P., Kramer, K., Cornelissen, J.H.C., Reich, P., Bahn, M., Niinemets, Ü., Peñuelas, J., Craine, J.M., Cerabolini, B.E.L., Minden, V., Laughlin, D.C., Sack, L., Allred, B., Baraloto, C., Byun, C., Soudzilovskaia, N.A. and Running, S.W., 2018. A methodology to derive global maps of leaf traits using remote sensing and climate data. Remote Sensing of Environment, 218: 69-88.

Mutanga, O., Adam, E. and Cho, M.A., 2012. High density biomass estimation for wetland vegetation using WorldView-2 imagery and random forest regression algorithm. International Journal of Applied Earth Observation and Geoinformation, 18: 399-406.

Mutanga, O. and Skidmore, A.K., 2004. Narrow band vegetation indices overcome the saturation problem in biomass estimation. International Journal of Remote Sensing, 25(19): 3999-4014.

Mutanga, O. and Skidmore, A.K., 2007. Red edge shift and biochemical content in grass canopies. ISPRS Journal of Photogrammetry and Remote Sensing, 62(1): 34-42.

Mutanga, O., Skidmore, A.K., Kumar, L. and Ferwerda, J., 2005. Estimating tropical pasture quality at canopy level using band depth analysis with continuum removal in the visible domain. International Journal of Remote Sensing, 26(6): 1093-1108.

Mutowo, G., Mutanga, O. and Masocha, M., 2018. Evaluating the Applications of the Near-Infrared Region in Mapping Foliar N in the Miombo Woodlands. Remote Sensing, 10(4): 505.

Neinavaz, E., Skidmore, A.K., Darvishzadeh, R. and Groen, T.A., 2016. Retrieval of leaf area index in different plant species using thermal hyperspectral data. ISPRS Journal of Photogrammetry and Remote Sensing, 119: 390-401.

Niinemets, Ü., 2007. Photosynthesis and resource distribution through plant canopies. Plant, Cell & Environment, 30(9): 1052-1071.

Niinemets, Ü., Kull, O. and Tenhunen, J.D., 1999. Variability in Leaf Morphology and Chemical Composition as a Function of Canopy Light Environment in Coexisting Deciduous Trees. International Journal of Plant Sciences, 160(5): 837-848.

Oleson, K., 2013. Technical description of version 4.5 of the Community Land Model (CLM).

Opti-Sciences, 2011. CCM-300 Chlorophyll Content Meter. Opti-Sciences, Inc., Hudson.

Pasolli, L., Asam, S., Castelli, M., Bruzzone, L., Wohlfahrt, G., Zebisch, M. and Notarnicola, C., 2015. Retrieval of Leaf Area Index in mountain grasslands in the Alps from MODIS satellite imagery. Remote Sensing of Environment, 165: 159-174.

Peng, Y., Nguy-Robertson, A., Arkebauer, T. and Gitelson, A., 2017. Assessment of Canopy Chlorophyll Content Retrieval in Maize and Soybean: Implications of Hysteresis on the Development of Generic Algorithms. Remote Sensing, 9(3): 226.

Pereira, H.M., Ferrier, S., Walters, M., Geller, G.N., Jongman, R.H.G., Scholes, R.J., Bruford, M.W., Brummitt, N., Butchart, S.H.M., Cardoso, A.C., Coops, N.C., Dulloo, E., Faith, D.P., Freyhof, J., Gregory, R.D., Heip, C., Höft, R., Hurtt, G., Jetz, W., Karp, D.S., McGeoch, M.A., Obura, D., Onoda, Y., Pettorelli, N., Reyers, B., Sayre, R., Scharlemann, J.P.W., Stuart, S.N., Turak, E., Walpole, M. and Wegmann, M., 2013. Essential Biodiversity Variables. Science, 339(6117): 277.

Pereira, H.V., Amador, V.S., Sena, M.M., Augusti, R. and Piccin, E., 2016. Paper spray mass spectrometry and PLS-DA improved by variable selection for the forensic discrimination of beers. Analytica Chimica Acta, 940: 104-112.

Perkin-Elmer, 2005. 2400 Series II CHNS/O Elemental Analysis. Perkin Elmer, Inc, Waltham.

Perry, C.R. and Lautenschlager, L.F., 1984. Functional equivalence of spectral vegetation indices. Remote Sensing of Environment, 14(1): 169-182.

Peterson, D.L., Aber, J.D., Matson, P.A., Card, D.H., Swanberg, N., Wessman, C. and Spanner, M., 1988. Remote sensing of forest canopy and leaf biochemical contents. Remote Sensing of Environment, 24(1): 85-108.

Pettorelli, N., Wegmann, M., Skidmore, A., Mücher, S., Dawson, T.P., Fernandez, M., Lucas, R., Schaepman, M.E., Wang, T., O'Connor, B., Jongman, R.H.G., Kempeneers, P., Sonnenschein, R., Leidner, A.K., Böhm, M., He, K.S., Nagendra, H., Dubois, G., Fatoyinbo, T., Hansen, M.C., Paganini, M., de Klerk, H.M., Asner, G.P., Kerr, J.T., Estes, A.B., Schmeller, D.S., Heiden, U., Rocchini, D., Pereira, H.M., Turak, E., Fernandez, N., Lausch, A., Cho, M.A., Alcaraz-Segura, D., McGeoch, M.A., Turner, W., Mueller, A., St-Louis, V., Penner, J., Vihervaara, P., Belward, A., Reyers, B. and Geller, G.N., 2016. Framing the concept of satellite remote sensing essential biodiversity variables: challenges and future directions. Remote Sensing in Ecology and Conservation, 2(3): 122-131.

Pinty, B. and Verstraete, M.M., 1992. GEMI: a non-linear index to monitor global vegetation from satellites. Vegetatio, 101(1): 15-20.

Poorter, H., Niinemets, Ü., Poorter, L., Wright, I.J. and Villar, R., 2009. Causes and consequences of variation in leaf mass per area (LMA): a meta-analysis. New Phytologist, 182(3): 565-588.

Poschlod, P., Kleyer, M., Jackel, A.-K., Dannemann, A. and Tackenberg, O., 2003. BIOPOP — A database of plant traits and internet application for nature conservation. Folia Geobotanica, 38(3): 263-271.

Prabhakara, K., Hively, W.D. and McCarty, G.W., 2015. Evaluating the relationship between biomass, percent groundcover and remote sensing indices across six winter cover crop fields in Maryland, United States. International Journal of Applied Earth Observation and Geoinformation, 39: 88-102.

Preidl, S. and Doktor, D., 2011. Comparison of radiative transfer model inversions to estimate vegetation physiological status based on hyperspectral data, 2011 3rd Workshop on Hyperspectral Image and Signal Processing: Evolution in Remote Sensing (WHISPERS), pp. 1-4.

Qiu, F., Chen, J.M., Ju, W., Wang, J., Zhang, Q. and Fang, M., 2018. Improving the PROSPECT Model to Consider Anisotropic Scattering of Leaf Internal Materials and Its Use for Retrieving Leaf Biomass in Fresh Leaves. IEEE Transactions on Geoscience and Remote Sensing, 56(6): 3119-3136.

Quanzhou, Y., Shaoqiang, W., Hao, S., Kun, H. and Lei, Z., 2014. An Evaluation of Spaceborne Imaging Spectrometry for Estimation of Forest Canopy Nitrogen Concentration in a Subtropical Conifer Plantation of Southern China. Journal of Resources and Ecology, 5(1): 1-10.

Quinn, G.P. and Keough, M.J., 2002. Experimental design and data analysis for biologists. Cambridge University Press, UK.

Ramoelo, A., Cho, M., Mathieu, R. and Skidmore, A.K., 2015a. Potential of Sentinel-2 spectral configuration to assess rangeland quality. Journal of Applied Remote Sensing, 9(1): 094096-094096.

Ramoelo, A., Cho, M.A., Mathieu, R., Madonsela, S., van de Kerchove, R., Kaszta, Z. and Wolff, E., Monitoring grass nutrients and biomass as indicators of rangeland quality and quantity using random forest modelling and WorldView-2 data. International Journal of Applied Earth Observation and Geoinformation(0).

Ramoelo, A., Cho, M.A., Mathieu, R., Madonsela, S., van de Kerchove, R., Kaszta, Z. and Wolff, E., 2015b. Monitoring grass nutrients and biomass as indicators of rangeland quality and quantity using random forest modelling and WorldView-2 data. International Journal of Applied Earth Observation and Geoinformation, 43: 43-54.

Ramoelo, A., Skidmore, A.K., Cho, M.A., Mathieu, R., Heitkönig, I.M.A., Dudeni-Tlhone, N., Schlerf, M. and Prins, H.H.T., 2013. Non-linear partial least square regression increases the estimation accuracy of grass nitrogen and phosphorus using in situ hyperspectral and environmental data. ISPRS Journal of Photogrammetry and Remote Sensing, 82(0): 27-40.

Ramoelo, A., Skidmore, A.K., Schlerf, M., Mathieu, R. and Heitkönig, I.M.A., 2011. Water-removed spectra increase the retrieval accuracy when estimating savanna grass nitrogen and phosphorus concentrations. ISPRS Journal of Photogrammetry and Remote Sensing, 66(4): 408-417.

Rapaport, T., Hochberg, U., Shoshany, M., Karnieli, A. and Rachmilevitch, S., 2015. Combining leaf physiology, hyperspectral imaging and partial least squares-regression (PLS-R) for grapevine water status assessment. ISPRS Journal of Photogrammetry and Remote Sensing, 109: 88-97.

Reich, P.B., Wright, I.J., Cavender-Bares, J., Craine, J.M., Oleksyn, J., Westoby, M. and Walters, M.B., 2003. The Evolution of plant functional variation : traits, spectra, and strategies. International Journal of Plant Sciences, 164: S143-S164.

Renzullo, L.J., Blanchfield, A.L., Guillermin, R., Powell, K.S. and Held, A.A., 2006. Comparison of PROSPECT and HPLC estimates of leaf chlorophyll contents in a grapevine stress study. International Journal of Remote Sensing, 27(4): 817-823.

Riano, D., Vaughan, P., Chuvieco, E., Zarco-Tejada, P.J. and Ustin, S.L., 2005. Estimation of fuel moisture content by inversion of radiative transfer models to simulate equivalent water thickness and dry matter content: analysis at leaf and canopy level. IEEE Transactions on Geoscience and Remote Sensing, 43(4): 819-826.

Richter, K., Atzberger, C., Vuolo, F., Weihs, P. and D'Urso, G., 2009. Experimental assessment of the Sentinel-2 band setting for RTM-based LAI retrieval of sugar beet and maize. Canadian Journal of Remote Sensing, 35(3): 230-247.

Rivera, J., Verrelst, J., Leonenko, G. and Moreno, J., 2013. Multiple Cost Functions and Regularization Options for Improved Retrieval of Leaf Chlorophyll Content and LAI through Inversion of the PROSAIL Model. Remote Sensing, 5(7): 3280.

Rodriguez-Galiano, V.F., Ghimire, B., Rogan, J., Chica-Olmo, M. and Rigol-Sanchez, J.P., 2012. An assessment of the effectiveness of a random forest classifier for land-cover classification. ISPRS Journal of Photogrammetry and Remote Sensing, 67: 93-104.

Roelofsen, H., van Bodegom, P., Kooistra, L. and Witte, J.-P., 2013. Trait Estimation in Herbaceous Plant Assemblages from in situ Canopy Spectra. Remote Sensing, 5(12): 6323.

Romero, A., Aguado, I. and Yebra, M., 2012. Estimation of dry matter content in leaves using normalized indexes and PROSPECT model inversion. International Journal of Remote Sensing, 33(2): 396-414.

Rondeaux, G., Steven, M. and Baret, F., 1996. Optimization of soil-adjusted vegetation indices. Remote Sensing of Environment, 55(2): 95-107.

Rouse, J.W., Haas, R.H., Schell, J.A. and Deering, D.W., 1973. {Monitoring vegetation systems in the Great Plains with ERTS.}, Proceedings of the Third ERTS Symposium, Washington DC, pp. 309-317.

Savitzky, A. and Golay, M.J.E., 1964. Smoothing and Differentiation of Data by Simplified Least Squares Procedures. Analytical Chemistry, 36(8): 1627-1639.

Scheiter, S., Langan, L. and Higgins, S.I., 2013. Next-generation dynamic global vegetation models: learning from community ecology. New Phytologist, 198(3): 957-969.

Schlemmer, M., Gitelson, A., Schepers, J., Ferguson, R., Peng, Y., Shanahan, J. and Rundquist, D., 2013. Remote estimation of nitrogen and chlorophyll contents in maize at leaf and canopy levels. International Journal of Applied Earth Observation and Geoinformation, 25(0): 47-54.

Schlerf, M. and Atzberger, C., 2006. Inversion of a forest reflectance model to estimate structural canopy variables from hyperspectral remote sensing data. Remote Sensing of Environment, 100(3): 281-294.

Schmidt, K.S. and Skidmore, A.K., 2003. Spectral discrimination of vegetation types in a coastal wetland. Remote Sensing of Environment, 85(1): 92-108.

Schweiger, A.K., Schütz, M., Anderwald, P., Schaepman, M.E., Kneubühler, M., Haller, R. and Risch, A.C., 2015. Foraging ecology of three sympatric ungulate species – Behavioural and resource maps indicate differences between chamois, ibex and red deer. Movement Ecology, 3(1): 6.

Sehgal, V.K., Chakraborty, D. and Sahoo, R.N., 2016. Inversion of radiative transfer model for retrieval of wheat biophysical parameters from broadband reflectance measurements. Information Processing in Agriculture, 3(2): 107-118.

Serbin, S.P., Singh, A., McNeil, B.E., Kingdon, C.C. and Townsend, P.A., 2014. Spectroscopic determination of leaf morphological and biochemical traits for northern temperate and boreal tree species. Ecological Applications, 24(7): 1651-1669.

Shengyan, D., Jidong, G. and Lexiang, Q., 2002. Assessment of biochemical concentrations of vegetation using remote sensing technology. Journal of Geographical Sciences, 12(3): 321-330.

Shi, Y., Wang, T., Skidmore, A.K. and Heurich, M., 2018. Important LiDAR metrics for discriminating forest tree species in Central Europe. ISPRS Journal of Photogrammetry and Remote Sensing, 137: 163-174.

Shiklomanov, A.N., Dietze, M.C., Viskari, T., Townsend, P.A. and Serbin, S.P., 2016. Quantifying the influences of spectral resolution on uncertainty in leaf trait estimates through a Bayesian approach to RTM inversion. Remote Sensing of Environment, 183: 226-238.

Si, Y., Schlerf, M., Zurita-Milla, R., Skidmore, A. and Wang, T., 2012. Mapping spatio-temporal variation of grassland quantity and quality using MERIS data and the PROSAIL model. Remote Sensing of Environment, 121(0): 415-425.

Silveyra Gonzalez, R., Latifi, H., Weinacker, H., Dees, M., Koch, B. and Heurich, M., 2018. Integrating LiDAR and high-resolution imagery for object-based mapping of forest habitats in a heterogeneous temperate forest landscape. International Journal of Remote Sensing: 1-26.

Skidmore, A.K., Pettorelli, N., Coops, N.C., Geller, G.N., Hansen, M., Lucas, R., Mücher, C.A., O'Connor, B., Paganini, M., Pereira, H.M., Schaepman, M.E., Turner, W., Wang, T. and Wegmann, M., 2015. Environmental science: Agree on biodiversity metrics to track from space. Nature, 523(7561): 403-405.

Soudzilovskaia, N.A., Elumeeva, T.G., Onipchenko, V.G., Shidakov, I.I., Salpagarova, F.S., Khubiev, A.B., Tekeev, D.K. and Cornelissen, J.H.C., 2013. Functional traits predict relationship between plant abundance dynamic and long-term climate warming. Proceedings of the National Academy of Sciences of the United States of America, 110(45): 18180-18184.

Sprintsin, M., Chen, J.M., Desai, A. and Gough, C.M., 2012. Evaluation of leaf-to-canopy upscaling methodologies against carbon flux data in North America. Journal of Geophysical Research: Biogeosciences, 117(G01023): 1-17.

Stagakis, S., Markos, N., Sykioti, O. and Kyparissis, A., 2010. Monitoring canopy biophysical and biochemical parameters in ecosystem scale using satellite hyperspectral imagery: An application on a Phlomis fruticosa Mediterranean ecosystem using multiangular CHRIS/PROBA observations. Remote Sensing of Environment, 114(5): 977-994.

Sun, J., Shi, S., Yang, J., Du, L., Gong, W., Chen, B. and Song, S., 2018. Analyzing the performance of PROSPECT model inversion based on different spectral information for leaf biochemical properties retrieval. ISPRS Journal of Photogrammetry and Remote Sensing, 135: 74-83.

Tang, S., Chen, J.M., Zhu, Q., Li, X., Chen, M., Sun, R., Zhou, Y., Deng, F. and Xie, D., 2007. LAI inversion algorithm based on directional reflectance kernels. Journal of Environmental Management, 85(3): 638-648.

Thenkabail, P.S., Smith, R.B. and De Pauw, E., 2000. Hyperspectral Vegetation Indices and Their Relationships with Agricultural Crop Characteristics. Remote Sensing of Environment, 71(2): 158-182.

Thomas, V., Treitz, P., McCaughey, J.H., Noland, T. and Rich, L., 2008. Canopy chlorophyll concentration estimation using hyperspectral and lidar data for a boreal mixedwood forest in northern Ontario, Canada. International Journal of Remote Sensing, 29(4): 1029-1052.

Tissue, D.T., Lewis, J.D., Wullschleger, S.D., Amthor, J.S., Griffin, K.L. and Anderson, O.R., 2002. Leaf respiration at different canopy positions in sweetgum (Liquidambar styraciflua) grown in ambient and elevated concentrations of carbon dioxide in the field. Tree Physiology, 22(15-16): 1157-1166.

Tripathi, R., Sahoo, R.N., Sehgal, V.K., Tomar, R.K., Chakraborty, D. and Nagarajan, S., 2012. Inversion of PROSAIL Model for Retrieval of Plant Biophysical Parameters. Journal of the Indian Society of Remote Sensing, 40(1): 19-28.

Tukey, J.W., 1949. Comparing Individual Means in the Analysis of Variance. Biometrics, 5(2): 99-114.

Ullah, S., Skidmore, A.K., Ramoelo, A., Groen, T.A., Naeem, M. and Ali, A., 2014. Retrieval of leaf water content spanning the visible to thermal infrared spectra. ISPRS Journal of Photogrammetry and Remote Sensing, 93(0): 56-64.

van Deventer, H., Cho, M.A., Mutanga, O. and Ramoelo, A., 2015. Capability of models to predict leaf N and P across four seasons for six subtropical forest evergreen trees. ISPRS Journal of Photogrammetry and Remote Sensing, 101(0): 209-220.

Van Wittenberghe, S., Alonso, L., Verrelst, J., Hermans, I., Valcke, R., Veroustraete, F., Moreno, J. and Samson, R., 2014. A field study on solar-induced chlorophyll fluorescence and pigment parameters along a vertical canopy gradient of four tree species in an urban environment. Science of The Total Environment, 466-467: 185-194.

Verhoef, W., 1984. Light scattering by leaf layers with application to canopy reflectance modeling: The SAIL model. Remote Sensing of Environment, 16(2): 125-141.

Verhoef, W. and Bach, H., 2007. Coupled soil–leaf-canopy and atmosphere radiative transfer modeling to simulate hyperspectral multi-angular surface reflectance and TOA radiance data. Remote Sensing of Environment, 109(2): 166-182.

Verrelst, J., Camps-Valls, G., Muñoz-Marí, J., Rivera, J.P., Veroustraete, F., Clevers, J.G.P.W. and Moreno, J., 2015a. Optical remote sensing and the retrieval of terrestrial vegetation bio-geophysical properties – A review. ISPRS Journal of Photogrammetry and Remote Sensing, 108: 273-290.

Verrelst, J., Rivera, J.P., Leonenko, G., Alonso, L. and Moreno, J., 2014. Optimizing LUT-Based RTM Inversion for Semiautomatic Mapping of Crop Biophysical Parameters from Sentinel-2 and -3 Data: Role of Cost Functions. IEEE Transactions on Geoscience and Remote Sensing, 52(1): 257-269.

Verrelst, J., Rivera, J.P., Moreno, J. and Camps-Valls, G., 2013. Gaussian processes uncertainty estimates in experimental Sentinel-2 LAI and leaf chlorophyll content retrieval. ISPRS Journal of Photogrammetry and Remote Sensing, 86(0): 157-167.

Verrelst, J., Rivera, J.P., Veroustraete, F., Muñoz-Marí, J., Clevers, J.G.P.W., Camps-Valls, G. and Moreno, J., 2015b. Experimental Sentinel-2 LAI estimation using parametric, non-parametric and physical retrieval methods – A comparison. ISPRS Journal of Photogrammetry and Remote Sensing(0).

Verrelst, J., Schaepman, M.E., Malenovský, Z. and Clevers, J.G.P.W., 2010. Effects of woody elements on simulated canopy reflectance: Implications for forest chlorophyll content retrieval. Remote Sensing of Environment, 114(3): 647-656.

Vincini, M., Amaducci, S. and Frazzi, E., 2014. Empirical Estimation of Leaf Chlorophyll Density in Winter Wheat Canopies Using Sentinel-2 Spectral Resolution. IEEE Transactions on Geoscience and Remote Sensing, 52(6): 3220-3235.

Wada, S. and Ishida, H., 2009. Chloroplasts autophagy during senescence of individually darkened leaves. Plant Signaling & Behavior, 4(6): 565-567.

Wakeling, I.N. and Morris, J.J., 1993. A test of significance for partial least squares regression. Journal of Chemometrics, 7(4): 291-304.

Wang, D., Schuchart, J., Janjusic, T., Winkler, F., Xu, Y. and Kartsaklis, C., 2014. Toward Better Understanding of the Community Land Model within the Earth System Modeling Framework. Procedia Computer Science, 29: 1515-1524.

Wang, L., Qu, J.J., Hao, X. and Hunt, E.R., 2011. Estimating dry matter content from spectral reflectance for green leaves of different species. International Journal of Remote Sensing, 32(22): 7097-7109.

Wang, Q. and Li, P., 2013. Canopy vertical heterogeneity plays a critical role in reflectance simulation. Agricultural and Forest Meteorology, 169(0): 111-121.

Wang, Z., Skidmore, A.K., Darvishzadeh, R., Heiden, U., Heurich, M. and Wang, T., 2015a. Leaf Nitrogen Content Indirectly Estimated by Leaf Traits Derived From the PROSPECT Model. IEEE Journal of Selected Topics in Applied Earth Observations and Remote Sensing, 8(6): 3172-3180.

Wang, Z., Skidmore, A.K., Wang, T., Darvishzadeh, R. and Hearne, J., 2015b. Applicability of the PROSPECT model for estimating protein and cellulose + lignin in fresh leaves. Remote Sensing of Environment, 168: 205-218.

Wang, Z., Skidmore, A.K., Wang, T., Darvishzadeh, R., Heiden, U., Heurich, M., Latifi, H. and Hearne, J., 2017. Canopy foliar nitrogen retrieved from airborne hyperspectral imagery by correcting for canopy structure effects. International Journal of Applied Earth Observation and Geoinformation, 54: 84-94.

Wang, Z., Wang, J., Zhao, C., Zhao, M., Huang, W. and Wang, C., 2005. Vertical Distribution of Nitrogen in Different Layers of Leaf and Stem and Their Relationship with Grain Quality of Winter Wheat. Journal of Plant Nutrition, 28(1): 73-91.

Waring, R.H. and Landsberg, J.J., 2011. Generalizing plant–water relations to landscapes. Journal of Plant Ecology, 4(1-2): 101-113.

Weerasinghe, L.K., Creek, D., Crous, K.Y., Xiang, S., Liddell, M.J., Turnbull, M.H. and Atkin, O.K., 2014. Canopy position affects the relationships between leaf respiration and associated traits in a tropical rainforest in Far North Queensland. Tree Physiology, 34(6): 564-584.

Weiss, M., Baret, F., Myneni, R.B., Pragnère, A. and Knyazikhin, Y., 2000. Investigation of a model inversion technique to estimate canopy biophysical variables from spectral and directional reflectance data. Agronomie, 20(1): 3-22.

Whitehurst, A., Swatantran, A., Blair, J., Hofton, M. and Dubayah, R., 2013. Characterization of Canopy Layering in Forested Ecosystems Using Full Waveform Lidar. Remote Sensing, 5(4): 2014.

Widlowski, J.L., Verstraete, M., Pinty, B. and Gobron, N., 2003. Allometric Relationships of Selected European Tree Species: Parametrizations of Tree Architecture for the Purpose of 3-D Canopy Reflectance Models Used in the Interpretation of Remote Sensing Data Office for Official Publications of the European Communities.

Wilkes, P., Jones, S.D., Suarez, L., Haywood, A., Mellor, A., Woodgate, W., Soto-Berelov, M. and Skidmore, A.K., 2016. Using discrete-return airborne laser scanning to quantify number of canopy strata across diverse forest types. Methods in Ecology and Evolution, 7(6): 700-712.

Winemiller, K.O., Fitzgerald, D.B., Bower, L.M. and Pianka, E.R., 2015. Functional traits, convergent evolution, and periodic tables of niches. Ecology Letters, 18(8): 737-751.

Wold, S., Sjöström, M. and Eriksson, L., 2001. PLS-regression: a basic tool of chemometrics. Chemometrics and Intelligent Laboratory Systems, 58(2): 109-130.

Workie, T.G. and Debella, H.J., 2018. Climate change and its effects on vegetation phenology across ecoregions of Ethiopia. Global Ecology and Conservation, 13: e00366.

Wu, J., Serbin, S.P., Xu, X., Albert, L.P., Chen, M., Meng, R., Saleska, S.R. and Rogers, A., 2017. The phenology of leaf quality and its within-canopy variation is essential for accurate modeling of photosynthesis in tropical evergreen forests. Global Change Biology, 23(11): 4814-4827.

Yan, D. and de Beurs, K.M., 2016. Mapping the distributions of C3 and C4 grasses in the mixed-grass prairies of southwest Oklahoma using the Random Forest classification algorithm. International Journal of Applied Earth Observation and Geoinformation, 47: 125-138.

Yang, P., Verhoef, W. and van der Tol, C., 2017. The mSCOPE model: A simple adaptation to the SCOPE model to describe reflectance, fluorescence and photosynthesis of vertically heterogeneous canopies. Remote Sensing of Environment, 201: 1-11.

Yang, X., Tang, J., Mustard, J.F., Wu, J., Zhao, K., Serbin, S. and Lee, J.-E., 2016. Seasonal variability of multiple leaf traits captured by leaf spectroscopy at two temperate deciduous forests. Remote Sensing of Environment, 179: 1-12.

Yao, X., Jia, W., Si, H., Guo, Z., Tian, Y., Liu, X., Cao, W. and Zhu, Y., 2014. Exploring Novel Bands and Key Index for Evaluating Leaf Equivalent Water Thickness in Wheat Using Hyperspectra Influenced by Nitrogen. PLoS ONE, 9(6): e96352.

Yi, Q., Wang, F., Bao, A. and Jiapaer, G., 2014. Leaf and canopy water content estimation in cotton using hyperspectral indices and radiative transfer models. International Journal of Applied Earth Observation and Geoinformation, 33: 67-75.

Yoder, B.J. and Pettigrew-Crosby, R.E., 1995. Predicting nitrogen and chlorophyll content and concentrations from reflectance spectra (400–

2500 nm) at leaf and canopy scales. Remote Sensing of Environment, 53(3): 199-211.

Yu, K.-Q., Zhao, Y.-R., Li, X.-L., Shao, Y.-N., Liu, F. and He, Y., 2015. Hyperspectral Imaging for Mapping of Total Nitrogen Spatial Distribution in Pepper Plant. PLoS ONE, 9(12): e116205.

Zhang, S. and Wang, Q., 2015. Inverse Retrieval of Chlorophyll From Reflected Spectra for Assimilating Branches of Drought-Tolerant <italic>Tamarix ramosissima</italic>. IEEE Journal of Selected Topics in Applied Earth Observations and Remote Sensing, 8(4): 1498-1505.

Zhang, Y., Chen, J.M. and Thomas, S.C., 2007. Retrieving seasonal variation in chlorophyll content of overstory and understory sugar maple leaves from leaf-level hyperspectral data. Canadian Journal of Remote Sensing, 33(5): 406-415.

Zhao, C., Li, H., Li, P., Yang, G., Gu, X. and Lan, Y., 2017. Effect of Vertical Distribution of Crop Structure and Biochemical Parameters of Winter Wheat on Canopy Reflectance Characteristics and Spectral Indices. IEEE Transactions on Geoscience and Remote Sensing, 55(1): 236-247.

Zhu, X., Wang, T., Skidmore, A.K., Darvishzadeh, R., Niemann, K.O. and Liu, J., 2017. Canopy leaf water content estimated using terrestrial LiDAR. Agricultural and Forest Meteorology, 232: 152-162.

Summary

Understanding spatial and temporal dimension of leaf traits is key in monitoring ecosystem function, processes and services. Plant traits provides an insight in improved understanding of ecosystem services across biomes. Tracking changes in foliar nutrient content within the earth system is vital in assessing the effects and adaptation capacity of vegetation communities to climate change. Remote sensing provides a cost effective and practical means of charactering plants traits from spectra over large spatial extents.

We sought out to understand the role of vertical heterogeneity in leaf traits across canopy in estimating foliar traits using *in-situ* hyperspectral measurements and Sentinel-2. Results presented in this thesis demonstrated that leaf spectral reflectance mirror variation in trait content across canopy. Leaf spectral reflectance shifted to longer wavelengths in the 'red edge' spectrum (685 - 701 nm) in the order of lower > middle > upper canopy positions. Key wavebands that enhance leaf samples discrimination have been reported to be sensitive to variation in chlorophyll, EWT, N, carbon and SLA. These leaf traits exhibited significant variation across the canopy vertical profile.

Our results at field level showed that reflectance spectra of leaf samples collected from the lower canopy matched PROSPECT simulated reflectance spectra better compared to reflectance spectra measured from upper canopy across the growing season. Leaf chlorophyll and Equivalent Water Thickness for leaf samples collected from the lower canopy were retrieved with higher accuracy compared to leaf samples collected from the upper canopy. This observation imply that variation in leaf biochemistry and morphology through the canopy vertical profile potentially affects the performance of the PROSPECT model.

Results obtained using *in-situ* canopy hyperspectral measurements and simulated Sentinel-2 data showed that leaf-to-canopy upscaling approaches that consider the contribution of leaf traits from the exposed upper canopy layer together with the shaded middle canopy layer yield significantly ($p < 0.05$) lower error as well as high explained variance ($R^2 > 0.71$) in the estimation of canopy leaf mass per area, nitrogen and carbon. At landscape level, canopy leaf mass per area, nitrogen and carbon estimated based on the weighted canopy expression yielded stronger correlations and higher prediction accuracy from Sentinel-2 MSI data compared to the top-of-canopy traits expression across all seasons. This observation imply that remote sensing instruments sense leaf traits beyond the sunlit upper canopy. These results have a strong implication in modelling leaf traits using remote sensing. We also

demonstrated the capability of the newly launched Sentinel-2 to map seasonal changes in leaf traits at landscape level.

This thesis demonstrated the importance of vertical heterogeneity of leaf traits in estimating plants traits at leaf, canopy and landscape level. We showed that incorporating the leaf traits content of foliage material from the shaded canopy improves the estimation accuracy of plants traits at canopy and landscape level using *in-situ* hyperspectral measurements in the laboratory and Sentinel-2 multispectral data at field level. We also demonstrate that the performance of the PROSPECT model and retrieval of chlorophyll, equivalent water thickness and leaf mass per area is likely to be affected by the leaf biochemistry and morphological changes through the vertical canopy profile over the growing season. These results are important in canopy reflectance modelling and retrieval of canopy traits for various application ranging from forestry to agriculture.

Samenvatting

Het begrijpen van de ruimtelijke en temporele dimensie van bladkenmerken is essentieel bij het bewaken van de ecosysteemfunctie, -processen en -services. Plantaardige eigenschappen bieden inzicht in een beter begrip van ecosysteemdiensten in alle bomen. Het volgen van veranderingen in het nutriëntengehalte van de bladeren in het aardsysteem is essentieel voor het beoordelen van de effecten en aanpassingscapaciteit van vegetatiegemeenschappen op de klimaatverandering. Remote sensing biedt een kosteneffectieve en praktische manier om plantentrekken uit spectra over grote ruimtelijke gebieden te kenmerken.

We hebben geprobeerd de rol van verticale heterogeniteit in bladkenmerken door de kruin te begrijpen bij het schatten van bladkenmerken met behulp van in-situ hyperspectrale metingen en Sentinel-2. De resultaten die in dit proefschrift worden gepresenteerd, toonden aan dat variatie in de spectrale reflectie van het bladspectrum in de eigenschappen van de bladeren over de kruin varieert. Bladspectraalreflectie verschoven naar langere golflengten in het 'rode rand'-spectrum (685 - 701 nm) in de volgorde van lagere> middelste> bovenste kapposities. Sleutelgordels die de bladstaafdiscriminatie verbeteren, zijn naar verluidt gevoelig voor variatie in chlorofyl, EWT, N, koolstof en SLA. Deze bladkenmerken vertoonden aanzienlijke variatie over het verticale profiel van de luifel.

Onze resultaten op veldniveau toonden aan dat reflectiespectra van bladmonsters verzameld van de onderste canopy overeenkwamen met PROSPECT gesimuleerde reflectiespectra beter vergeleken met reflectiespectra gemeten vanaf de bovenkap gedurende het groeiseizoen. Bladchlorofyl en equivalente waterdikte voor bladmonsters verzameld uit de onderste kap werden met hogere nauwkeurigheid teruggewonnen vergeleken met bladmonsters verzameld uit de bovenste kap. Deze waarneming impliceert dat de variatie in bladbiochemie en -morfologie via het verticale profiel van de luifel mogelijk de prestaties van het PROSPECT-model beïnvloedt.

Resultaten verkregen met hyperspectrale metingen in situ en gesimuleerde Sentinel-2 gegevens toonden aan dat blad-naar-canopy opschaling benaderingen die de bijdrage van bladkenmerken van de blootgestelde bovenste luifellaag tezamen met de gearceerde middelste luifellaag significant opbrengen ($p < 0{,}05$)) lagere fout en sterk verklaarde variantie ($R2 > 0{,}71$) bij de schatting van de bladmassa van de kruin per gebied, stikstof en koolstof. Op landschapsniveau leverden bladluikmassa per oppervlakte, stikstof en koolstof geschat op basis van de gewogen canopy-expressie betere correlaties en hogere voorspellingsnauwkeurigheid op van Sentinel-2 MSI-gegevens vergeleken met de top-van-canopy-eigenschappen in alle seizoenen. Deze waarneming impliceert dat teledetectie-instrumenten bladkenmerken buiten de zonovergoten bovenkap waarnemen. Deze resultaten hebben een sterke implicatie voor het modelleren van biochemische eigenschappen van bladeren met behulp van teledetectie. We hebben ook aangetoond dat de nieuw gelanceerde Sentinel-2 seizoensveranderingen in bladkenmerken op landschapsniveau in kaart kan brengen.

Dit proefschrift heeft het belang aangetoond van verticale heterogeniteit van bladkenmerken bij het schatten van plantkarakteristieken op blad-, kruin- en landschapsniveau. We toonden aan dat het opnemen van de eigenschappen van bladkenmerken van bladmateriaal uit de schaduwrijke luifel de schattingsnauwkeurigheid van plantentrekken op luifel- en landschapsniveau verbetert met behulp van in-situ hyperspectrale metingen in het laboratorium en Sentinel-2 multispectrale gegevens op veldniveau. We tonen ook aan dat de prestaties van het PROSPECT-model en het ophalen van chlorofyl, equivalente waterdikte en bladmassa per gebied waarschijnlijk worden beïnvloed door de bladbiochemie en morfologische veranderingen door het verticale luifelprofiel gedurende het groeiseizoen. Deze resultaten zijn belangrijk bij het modelleren van de reflecties van de kruin en het terugvinden van de eigenschappen van de overkapping voor verschillende toepassingen, variërend van bosbouw tot landbouw.

Biography

Tawanda Winmore Gara was born in Kariba, Zimbabwe on the 1st of August 1983. He received a Hon degree in Geography and Environmental Science (2008) and a Master of Philosophy in Geography (2012) from the University of Zimbabwe. In 2014, he earned an MSc (*cum laude*) in Geo-Information Science and Earth Observation for Natural Resources Management, from ITC, University of Twente. In February 2015, he was awarded a four-year *AiO* position to study for his PhD in the Faculty of Geoinformation Science and Earth Observation (ITC), University of Twente, which has resulted in this thesis and the following publications.

ISI journal articles

Gara, T. W., Darvishzadeh, R., Skidmore, A. & Wang, T. 2018. Impact of Vertical Canopy Position on Leaf Spectral Properties and Traits across Multiple Species. *Remote Sensing*, 10, 346.

Gara, T. W., Skidmore, A. K., Darvishzadeh, R. & Wang, T. 2019. Leaf to canopy upscaling approach affects the estimation of canopy traits *GIScience & Remote Sensing,* 56**,** 554-575

Gara, T.W., Darvishzadeh, R., Skidmore, A. K., Wang, T and Huerich, M. 2019 Evaluating the performance of PROSPECT in retrieval of leaf traits throughout the growing season. *International Journal of Applied Earth Observation and Geoinformation* 83: 101919.

Under review

Gara, T.W., Skidmore, A. K., Darvishzadeh, R., Wang, T and Huerich, M. (*Under review after first revision*) Knowledge on the vertical heterogeneity in leaf traits is essential for accurate modelling of canopy trait content using seasonal Sentinel-2 imagery. *ISPRS Journal of Photogrammetry and Remote Sensing.*

International Conferences

Gara, T. W., Darvishzadeh, R., Skidmore, A. K., & Wang, T.*Leaf spectral proporties track variability in leaf traits across the canopy vertical profile :* Poster presented at 10th EARSeL SIG Imaging Spectroscopy Workshop 19-21 April 2017, Zurich, Switzerland

Gara, T. W., Darvishzadeh, R., Skidmore, A. K., & Wang, T. Seasonal modelling leaf optical properties and retrieval of leaf traits across the canopy using PROSPECT : Poster *presented at 11th EARSel SIG imaging spectroscopy Workshop 6-8 February 2019, Brno, Czech Republic.*

Other Publications

Gara, T. W., Murwira, A., Chivhenge, E., Dube, T., & Bangira, T. (2014). Estimating wood volume from canopy area in deciduous woodlands of Zimbabwe. *Southern Forests: a Journal of Forest Science*, 76(4), 237-244. doi:10.2989/20702620.2014.965981

Gara, T. W., Murwira, A., Ndaimani, H., Chivhenge, E., & Hatendi, C. M. (2015). Indigenous forest wood volume estimation in a dry savanna, Zimbabwe: exploring the performance of high-and-medium spatial resolution multispectral sensors. *Transactions of the Royal Society of South Africa*, 70(3), 285-293. doi:10.1080/0035919x.2015.1057269

Gara, T. W., Murwira, A., & Ndaimani, H. (2016). Predicting forest carbon stocks from high resolution satellite data in dry forests of Zimbabwe: exploring the effect of the red-edge band in forest carbon stocks estimation. *Geocarto International*, 31(2), 176-192. doi:10.1080/10106049.2015.1041563

Gara, T. W., Murwira, A., Dube, T., Sibanda, M., Rwasoka, D. T., Ndaimani, H., Hatendi, C. M. (2017). Estimating forest carbon stocks in tropical dry forests of Zimbabwe: exploring the performance of high and medium spatial-resolution multispectral sensors. *Southern Forests: a Journal of Forest Science*, 79(1), 31-40. doi:10.2989/20702620.2016.1233751

Gara, T. W., Wang, T., Skidmore, A. K., Ngene, S. M., Dube, T., & Sibanda, M. (2017). Elephants move faster in small fragments of low productivity in Amboseli ecosystems: Kenya. *Geocarto International*, 32(11), 1243-1253. doi:10.1080/10106049.2016.1206625

Gara, T. W., Wang, T., Skidmore, A. K., Zengeya, F. M., Ngene, S. M., Murwira, A., & Ndaimani, H. (2017). Understanding the effect of landscape fragmentation and vegetation productivity on elephant habitat utilization in Amboseli ecosystem, Kenya. *African Journal of Ecology*, 55(3), 259-269. doi:10.1111/aje.12346

Ndaimani, H., Murwira, A., Masocha, M., **Gara, T. W**., & Zengeya, F. M. (2017). Evaluating performance of aerial survey data in elephant habitat modelling. *African Journal of Ecology*, 55(3), 270-281. doi:10.1111/aje.12348

Mpakairi, K. S., Ndaimani, H., Tagwireyi, P., **Gara, T. W**., Zvidzai, M., & Madhlamoto, D. (2017). Missing in action: Species competition is a neglected predictor variable in species distribution modelling*.* *PLoS ONE*, 12(7), e0181088. doi:10.1371/journal.pone.0181088

Mareya, H. T., Tagwireyi, P., Ndaimani, H., **Gara, T. W**., & Gwenzi, D. (2018). Estimating Tree Crown Area and Aboveground Biomass in Miombo Woodlands From High-Resolution RGB-Only Imagery. *IEEE Journal of Selected Topics in Applied Earth Observations and Remote Sensing*, 11(3), 868-875. doi:10.1109/JSTARS.2018.2799386

Dube, T., **Gara, T. W**., Sibanda, M., Shoko, C., Murwira, A., Ndaimani, H., & Hatendi, C. (2018). Estimating forest standing biomass in savanna woodlands as an indicator of forest productivity using the new generation WorldView-2 sensor. *Geocarto International*, *33(2), 178-188. doi:10.1080/10106049.2016.1240717*

Darvishzadeh, R., Wang, T., Skidmore, A., Vrieling, A., O'Connor, B., **Gara, T. W**., Paganini, M. (2019). Analysis of Sentinel-2 and RapidEye for Retrieval of Leaf Area Index in a Saltmarsh Using a Radiative Transfer Model. *Remote Sensing*, 11(6), 671.